R-10-09

High-resolution hydrodynamic modelling of the marine environment at Forsmark between 6500 BC and 9000 AD

Anna Karlsson, Christin Eriksson,
Charlotta Borell Lövstedt, Olof Liungman
DHI Sverige AB

Anders Engqvist, Division of Water Resources Engineering, KTH

February 2010

Svensk Kärnbränslehantering AB
Swedish Nuclear Fuel
and Waste Management Co

Box 250, SE-101 24 Stockholm
Phone +46 8 459 84 00

ISSN 1402-3091
SKB Rapport R-10-09

High-resolution hydrodynamic modelling of the marine environment at Forsmark between 6500 BC and 9000 AD

Anna Karlsson, Christin Eriksson,
Charlotta Borell Lövstedt, Olof Liungman
DHI Sverige AB

Anders Engqvist, Division of Water Resources
Engineering, KTH

February 2010

Contents

Summary

The hydrodynamic conditions of the Forsmark marine area, present-day Öregrundsgrepen, have been modelled for 13 selected years between 6500 BC and 9000 AD. By using three-dimensional models of high complexity the mechanisms that force the water exchange in the area have been examined. In order to accurately describe past and future conditions the model bathymetry has been modified according to simulated land uplift.

For present-day conditions, it is found that the water exchange is greater in the deeper eastern parts of the area while it is more limited in the shallower western parts. There is also a net through-flow as long as Öregrundsgrepen is open-ended. During the period before 0 AD the area is situated in the open sea. Conditions are fairly homogeneous and the water exchange is at its maximum. In the future, conditions change and show the typical characteristics of estuarine circulation in an enclosed bay, as land uplift closes the southern boundary to the Baltic Sea.

Water exchange has also been examined in terms of flows between the predefined marine basins in Öregrundsgrepen. The interior conditions are shown to depend on the large water exchange with the Baltic Sea. The flows between basins computed in this study are found to be comparable to previous estimates.

The local high-resolution model agrees well with both observed temperature and sea level. Salinity, on the other hand, is overestimated even though the temporal development matches that which has been observed. This discrepancy is likely due to the boundary conditions but this remains to be thoroughly investigated.

A measure of the residence time – and thus the water exchange – called the Average Age (AvA) has also been calculated. It is found that the highest values of AvA are found in basins far from the boundaries and in the shallower parts of Öregrundsgrepen. AvA calculations have also been used to illuminate the importance of various forcing mechanisms in a sensitivity analysis. This analysis points out the importance of the local wind in determining the AvA, particularly in the shallower parts, and also indicates how the water exchange is likely to be influenced by changing climate and changes in bathymetry due to land uplift.

It is concluded that the modelling presented serves as a robust base for other modelling activities.

Sammanfattning

De hydrodynamiska förhållandena i Forsmarksområdet, nuvarande Öregrundsgrepen, har modellerats för 13 utvalda år mellan 6500 BC och 9000 AD. Med hjälp av avancerade tredimensionella modeller har de mekanismer som driver vattenutbytet i området studerats. För att på ett korrekt sätt beskriva dåtida och framtida förhållanden har modellernas batymetrier justerats utifrån beräknad landhöjning.

För nuvarande förhållanden visar modellresultaten att vattenutbytet är större i de djupare östra delarna av området än i de grundare västra delarna. Där finns dessutom ett nettoflöde genom Öregrundsgrepen så länge både den norra och södra änden är öppna mot Östersjön. Under perioden före 0 AD ligger Forsmarksområdet i öppna havet. Förhållandena är horisontellt i stort sett homogena och vattenutbytet är maximalt. Framåt i tiden förändras situationen i och med att landhöjningen stänger den södra öppna randen. Öregrundsgrepen blir en instängd vik med estuarin cirkulation.

Vattenutbytet har också analyserats utifrån flödena mellan enskilda fördefinierade bassänger. Förhållandena inne i Öregrundsgrepen visar sig till stor del bero på utbytet med Östersjön över de öppna ränderna. De beräknade bassängflödena visar god överensstämmelse med de som beräknats i en tidigare modellstudie.

En validering mot observationer visar att den lokala högupplösta modellen överensstämmer väl med uppmätta havsnivåer och temperaturer. Däremot överskattar modellen salthalten, även om den observerade tidsutvecklingen återspeglas i modellresultaten. Denna avvikelse beror troligen på de drivande randvillkoren, men detta återstår att undersökas ordentligt.

Ett mått på utbytestiden – och därmed vattenutbytet – som bygger på en beräkning av vattnets ålder har också tagits fram. Resultaten visar att vattnets medelålder ökar med avståndet från de öppna ränderna samt är generellt lägre i de grunda delarna av Öregrundsgrepen. Detta mått på utbytet har använts för att illustrera hur modellresultaten beror på de olika drivande mekanismerna, genom en typ av känslighetsanalys. Denna analys pekar ut den lokala vinden som en viktig faktor för utbytet, särskilt i de grundare områdena, men visar också hur utbytet kan tänkas påverkas av ett förändrat klimat och förändringar orsakade av landhöjningen.

Sammanfattningsvis bedöms den genomförda modelleringen utgöra en robust bas för andra modelleringsaktiviteter.

1 Introduction

This technical report describes the three-dimensional hydrodynamic modelling that has been performed for the Forsmark marine area, an area which currently consists of a coastal estuary named Öregrundsgrepen. In addition to describing the technical details regarding methods and input data, this report also presents the model results together with a discussion of the hydrodynamic properties of the area. Finally, it is investigated how dominating forcing and governing processes change over long time scales.

1.1 Background

The modelling study presented here is part of the ongoing assessment of Forsmark as a site for a long-term subterranean repository for spent nuclear fuel, carried out by the Swedish Nuclear Fuel and Waste Management Co. (SKB). Mathematical modelling studies are carried out within several subareas of the site assessment. The present study is only concerned with the marine environment at Forsmark and builds on earlier oceanographic modelling studies /Engqvist and Andrejev 1999, 2000, 2008/.

1.2 Purpose

The purpose of the hydrodynamic modelling effort presented here is to provide the physical forcing for other models, namely:

1. estimates of the water exchange in the marine environment for the period 7000 BC to 9000 AD to be used by the landscape dose model (e.g. /SKB 2006/),
2. detailed hydrodynamic flow fields for 2020 AD to be used by the high-resolution ecosystem and radionuclide models also developed by DHI /Erichsen et al. 2010/.

In addition, the model results are used to characterize the hydrodynamics of Öregrundsgrepen – past, present and future – in particular different measures of the water exchange and how these vary in time.

1.3 Deliverables

The Forsmark area is divided into a number of basins based on present elevation data as well as models of past and future elevations /Brydsten 2006/. The delineations follow the borders of future drainage basins (see Figure 2-2). These basins constitute the objects which form the basis of the landscape dose model. Hence, the primary deliverables of the hydrodynamic modelling are the following:

- Mean annual volume flows between neighbouring basins, including a division according to flow direction (positive or negative).
- A measure of the mean residence time for water in Öregrundsgrepen, including the spatial distribution over all basins.
- Detailed flow fields to be used as forcing in the high-resolution ecosystem and radionuclide models in /Erichsen et al. 2010/.

1.4 Contents

This report is structured as follows. Chapter two presents a description of the area and its evolution over time. Chapter three describes the methods used. This includes the mathematical definition of the deliverables, the overall solution strategy and descriptions of the numerical models used. The two following chapters present the input data and the results of the model computations, the latter from the viewpoint of the defined deliverables. The sixth chapter addresses the issue of model vali-

dation, presenting comparisons between model results and observations. The report is concluded by a chapter on model sensitivity – where the reliability of the model results is investigated together with implications of an altered climate – and a final chapter where the main conclusions are summarized. References and two appendices can be found at the end of the report.

This report deals with the hydrodynamics of the Forsmark marine area on a basin scale level, i.e. the overall mean circulation and the mean exchange between basins. The aim is to describe the important hydrodynamic characteristics of the Forsmark marine area as well as estimating the quantitative changes in inter-basin exchange due to shoreline evolution during an interglacial period. Changes in other factors, such as meteorological conditions, are only considered implicitly by investigating the relative importance of different factors influencing the circulation and basin exchange. This is what makes up the sensitivity analysis.

2 The Baltic Sea and Öregrundsgrepen

2.1 Description of Öregrundsgrepen

Öregrundsgrepen is a semi-enclosed coastal area located on the east coast of Sweden in the Gulf of Bothnia of the Baltic Sea (see Figure 2-1). The Baltic Sea is a large brackish estuary which is connected to the North Sea via narrow and shallow straits and the intermediate seas Kattegat and Skagerrak. There is a substantial input of fresh water to the Baltic Sea via land runoff whereas inflow of saline water from the Skagerrak and Kattegat is restricted. Tides in the Baltic Sea are very weak and may be neglected.

Öregrundsgrepen is funnel-shaped and open-ended with a northern and southern open boundary to the Baltic Sea (see Figure 2-2). The northern opening is wide, approximately 15 km, and relatively deep. Öregrundsgrepen then narrows towards the south-southeast to a long and narrow strait called Öregrundssund, about 15 km long and in several places less than a kilometre wide, which eventually opens out into the Baltic Sea. To the east the island of Gräsö separates the estuary from the Baltic Sea. There are two main discharges of freshwater in the area, the rivers Olandsån and Forsmarksån.

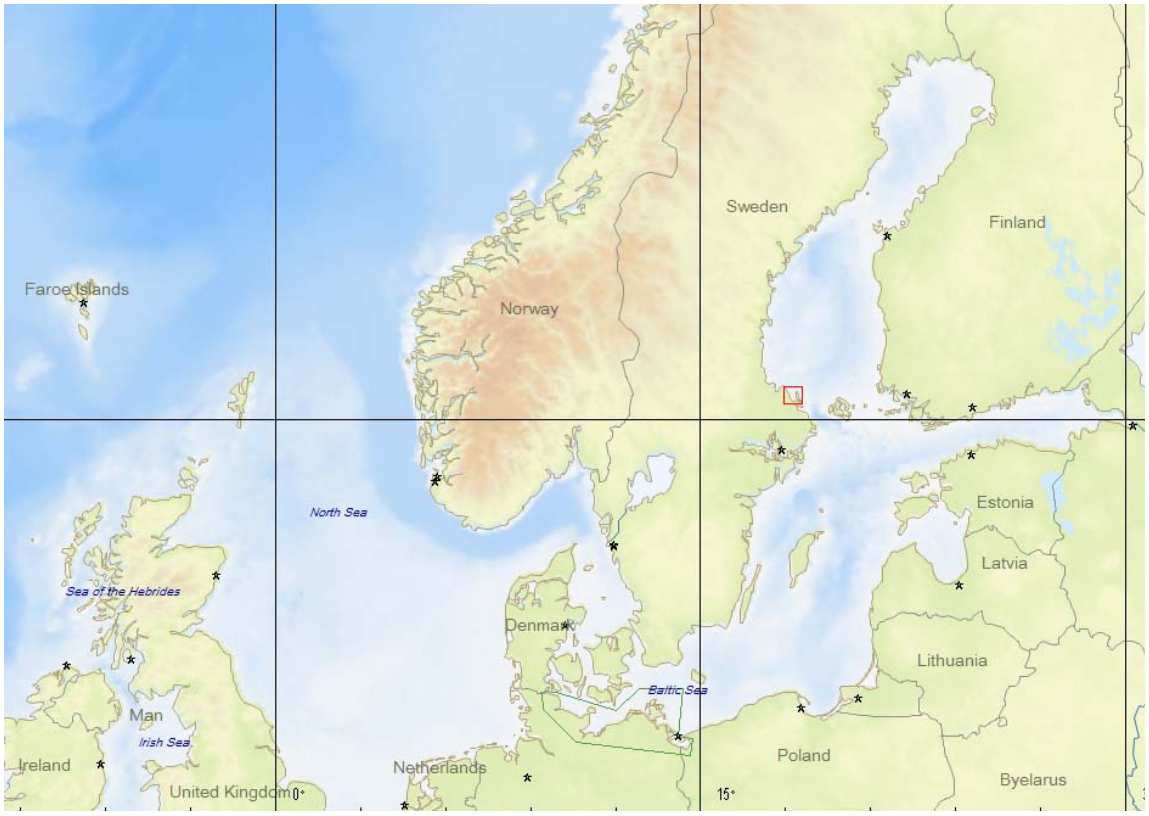

Figure 2-1. *Map of the North Sea and the Baltic Sea showing the location of Öregrundsgrepen (red rectangle).*

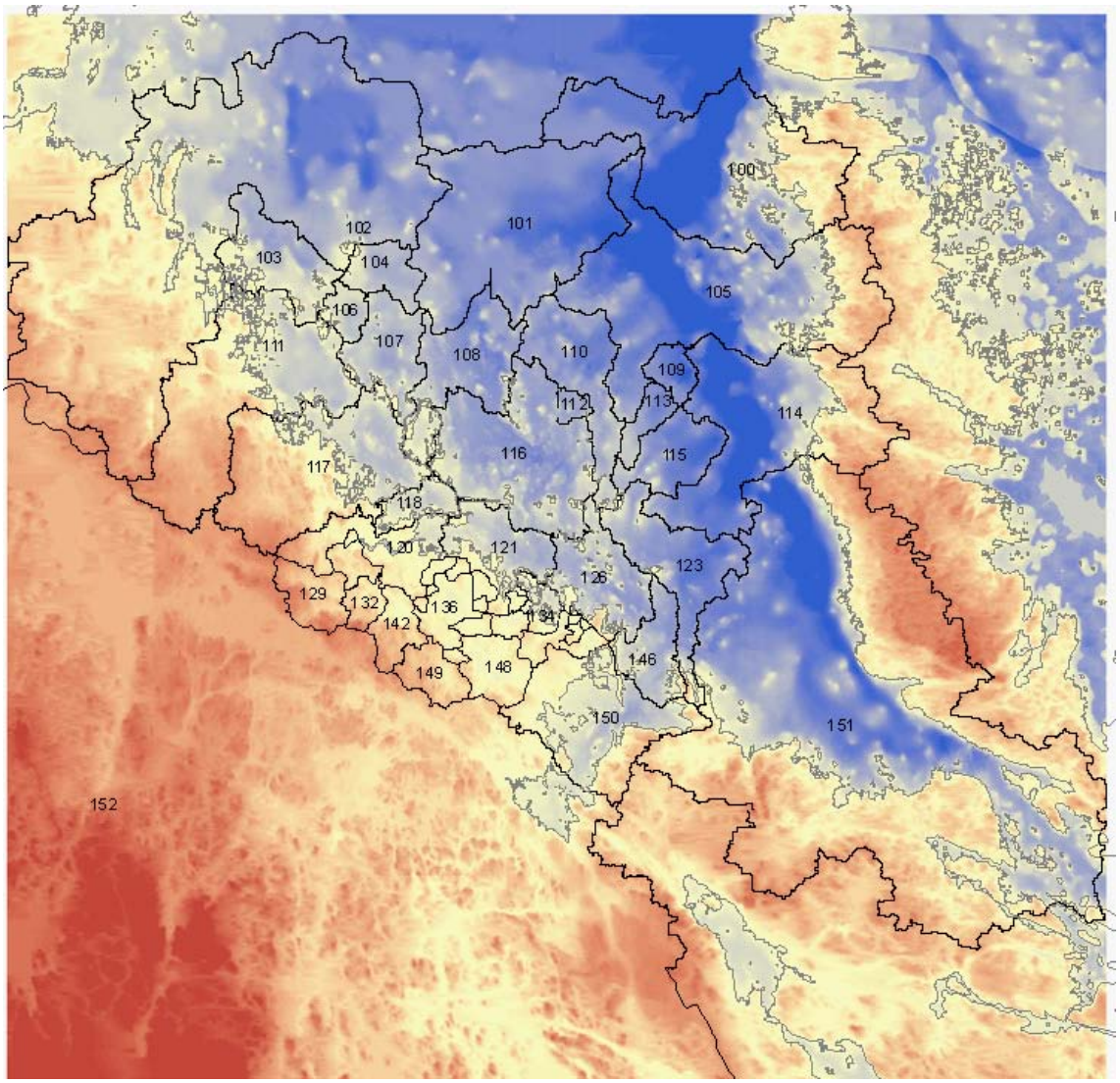

Figure 2-2. *Map of Öregrundsgrepen showing heights and the defined basins.*

2.2 Evolution

The Holocene history of the Baltic Sea, i.e. the present interglacial beginning at approximately 9500 BC, can be described by four major stages with altering freshwater and brackish water /Westman et al. 1999/: the fresh Baltic Ice Lake, the brackish Yoldia Sea, the fresh Ancylus Lake and the brackish Litorina Sea *sensu lato* ("in a wide sense"; cf. Litorina Sea proper below). The first three stages cover the period from about 9500 BC to about 7000 BC. The Litorina Sea *sensu lato* stage thus stretches from about 7000 BC to the present day. The evolution of the Baltic Sea and Öregrundsgrepen during this stage can be summarized in the following time line /Westman et al. 1999, Brydsten 2006/:

1. 7000 BC – 5500 BC (the Mastogloia Sea)
   The Baltic sills have opened and saline water may enter. The salinity gradually increases from 0 to about 4–5 psu. The area of Öregrundsgrepen is located in open sea, more than 10 km from coast.
2. 5500 BC – 3000 BC (the Litorina Sea proper)
   Sea level increase has been greater than land rise. The Baltic sills reach their maximum depth by the end of this period, and thus the salinity peaks at between 10 and 15 psu. The area of Öregrundsgrepen is still located in open sea, more than 10 km from coast.

3. 3000 BC – 500 AD (the Limnea Sea)
   Land rise is greater than sea level rise and the Baltic sills gradually become shallower. The sea salinity gradually decreases down to about 8–10 psu. The coastline is now within 10 km of the Öregrundsgrepen area but none of the defined basins intersect land.
4. 500 AD – present day (the Baltic Sea)
   Land rise continues. Sea salinities continue to decrease slowly towards current levels at just below 8 psu. An archipelago gradually forms in the Öregrundsgrepen area as the coastline advances eastward due to land rise.

Though it is difficult to predict what will happen in the future, based on shore displacement modelling /Brydsten 2006/ we can form some idea about how the future Baltic Sea will evolve. Thus we can continue the time line as follows:

5. 3000 AD
   Continued shallowing of the Baltic Sea, except for the southern part where land rise is approximately zero or perhaps slightly negative. Gradual closing of Öregrundssund.
6. 4000 AD
   The entrance to Bothnian Bay begins to close. Öregrundssund closes, changing Öregrundsgrepen into a bay. Gradual shallowing moves the coastline eastward.
7. 5000 AD
   As the coastline moves eastward in Öregrundsgrepen near-shore marine basins gradually turn into lakes.
8. 6000 AD
   The Bothnian Bay becomes a lake and the Åland Sea narrows and shallows. Öregrundsgrepen continues to narrow as the coastline advances eastward towards the deep channel.
9. 7000 AD – 9000 AD
   Öregrundsgrepen is now a narrow estuary, consisting of what formerly was the deep channel. Gradual isolation of marine basins from the south and northward, forming lakes.
10. 10,000 AD
    The marine environment of Öregrundsgrepen has now completely disappeared, with only lakes remaining.

Obviously we know more about the past than the future. It is also clear that overall very little is known about the hydrography, the hydrology or the meteorology, past or future. Basically, there exists a reasonable picture of the shoreline displacement but little else, except for proxy data that give some idea about, e.g., past salinities /Westman et al. 1999/.

Based on the time line above 13 years have been identified that may be thought to represent different significant periods during the existence of Öregrundsgrepen as a marine area, from the Mastogloia Sea period to when the last marine basin has become a lake due to shoreline advance. These 13 years are shown in Tabel 2-1. Note that there are only three years for the time period before 0 AD, namely 6500 BC, 3000 BC and 1000 BC. These represent the low saline Mastogloia Sea stage, the salinity maximum at the end of the Litorina Sea stage and the Limnea Sea stage before the formation of a recognizable Öregrundsgrepen. The reason for only choosing three years is that since the Öregrundsgrepen area is located in open sea until about 0 AD, no large differences in circulation and water exchange are expected.

The period from 0 AD to 9000 AD has been divided into 1000-year intervals, producing ten model years. This is judged the minimum time resolution required to resolve the gradual modification and eventual disappearance of the different marine basins as a result of shoreline advance.

2.3 Overview of present hydrodynamic conditions

The factors that determine the hydrodynamic conditions of the Baltic Sea may be summarized as follows. On long time scales the local mean sea level is determined by land rise and changes in oceanic mean sea level. The short-term relative sea level variations, which force the hydrodynam-

Table 2-1. The time period 7000 BC to 9000 AD and modeled years (S=salinity).

Calendar year	7000 BC	6500 BC	6000 BC	5500 BC	5000 BC	4500 BC	4000 BC	3500 BC	3000 BC	2500 BC	2000 BC	1500 BC	1000 BC	500 BC	0	500 AD	1000 AD	1500 AD	2000 AD	2500 AD	3000 AD	3500 AD	4000 AD	4500 AD	5000 AD	5500 AD	6000 AD	6500 AD	7000 AD	7500 AD	8000 AD	8500 AD	9000 AD	9500 AD
Baltic Sea phase	*Masto-gloia Sea*			*Litorina Sea*									*Limnea Sea*						*Baltic Sea*					*Baltic Sea with "current" land rise*											*Baltic Sea without Bothnian Bay*										
State of Baltic sea	sills open; lake -> brackish sea; low S			Deepening sills; increasing S. Maximum of ca 10-15 PSU at about 5000-2500 BC									Uplift exceeds sea level rise; decreasing S											Gradual closing off of Bottenviken, shallowing of Ålands hav and deepening of sills											Bottenviken a lake; Ålands hav a narrowing sound and gradually deepening sills										
State of Öregrun dsgrepen	*Open sea (> 10 km to coast)*														*Gradu-ally forming archi-pelago*		*Grepen exists*		*Öregrunds-sund gradually closing*					*Narrowing; lakes forming from west until only deep channel remains*											*Lakes forming northward until Öregrunds-grepen consists of only lakes*										
Model time steps	*6500 BC*			*3000 BC*									*1000 BC*		*0 AD*		*1000 AD*		*2020 AD*		*3000 AD*		*4000 AD*		*5000 AD*		*6000 AD*		*7000 AD*		*8000 AD*		*9000 AD*	

ics, are dominated by the wind and air pressure fields over Scandinavia. The sea temperature is dominated by the meteorological forcing, both on short and long time scales. The short-term salinity variations depend on short-term variations in runoff and wind conditions over the Baltic Sea (and to some degree over the Skagerrak, Kattegat and North Sea as well). The long-term salinity depends on long-term variations in runoff and the mean sea level /Gustafsson and Westman 2002/. The latter determines the Baltic Sea sill depth which in turn affects the exchange with the Kattegat and Skagerrak .

As for Öregrundsgrepen, this estuary is mostly relatively shallow – less than 20 m deep – but with a deeper channel in the east with depths exceeding 40 m that runs approximately in a north-south direction. Since the depth of the halocline in the Baltic Sea is about 60–70 m, the salinity stratification is generally weak in Öregrundsgrepen. Local fresh water runoff produces slightly lower salinities in Öregrundsgrepen compared to the Gulf of Bothnia /Wijnbladh et al. 2008/.

Through the large northern opening the area is highly influenced by Baltic Sea conditions. Variations in sea level and stratification will easily penetrate into the estuary from the north, but less so from the south due to the long and narrow strait. However, because of the limited high-frequency sea level variations in the Baltic Sea – tides are virtually nonexistent – and the weak stratification, the external forcing does not necessarily dominate the circulation. Of course, extreme events such as storm surges may temporarily give rise to large sea level changes.

There are three major types of forcing mechanisms that drive the water exchange: sea level differences (barotropic forcing), horizontal density differences (baroclinic forcing) and local wind.

Due to the limited sea level variations the magnitude of the barotropically forced water exchange would be small for a closed estuary. Since Öregrundsgrepen is open in both ends, a through-flow is possible. A small sea level difference between the northern and southern boundaries is enough to drive a flow through Öregrundsgrepen producing a noticeable water exchange. As a result of the freshwater supply to the Baltic Sea and the rotation of the earth, there is a net flow of water towards the south along the Swedish coast /Fonselius 1996/. This is forced by a sea level gradient along the coast, which in turn drives a net flow through Öregrundsgrepen from north to south. The direction of this through-flow varies from time to time, but should on average be directed in the southward direction.

The baroclinic water exchange has two forcing mechanisms: the freshwater discharge due to land runoff and the existence of more saline, and thus dense, Baltic Sea water at the open boundaries. Classic estuarine circulation relies on these two factors. The less dense freshwater flows towards the open sea at the surface, mixing with underlying water along the way to produce an increasing

volume flow. The underlying water that is mixed into the freshwater is replaced by an inflow at greater depths of denser water from outside. However, this mode of circulation does not appear to dominate the conditions in Öregrundsgrepen. The land runoff is not sufficiently large in relation to the volume of the estuary and the cross-sectional area of the northern boundary. Also, the open-ended nature of Öregrundsgrepen complicates the picture. Nevertheless, variations in stratification in the Gulf of Bothnia, particularly at the large northern boundary, do cause large flows across the boundaries. Particularly in the deeper parts of Öregrundsgrepen, regional upwelling events will force denser water from outside into the deeper parts of Öregrundsgrepen, flushing out the resident water and causing fairly large exchanges. In short, the stratification inside Öregrundsgrepen is dominated by the stratification outside the estuary.

The local wind is most likely an important factor influencing the circulation and exchange in Öregrundsgrepen. Because Öregrundsgrepen is relatively shallow with a large surface area, the local wind will not only generate surface currents but also extensive vertical mixing, reducing vertical gradients in temperature and salinity. Because the estuary is semi-enclosed, local wind setup may result in a two-layer circulation, i.e. a surface flow in the direction of the wind and a compensating counter-flow along the bottom.

3 Methods

The overall methodology was as follows. For each of the 13 years during the period from 6500 BC to 9000 AD a hydrodynamic model was run for one year using the same external forcing from the atmosphere, the surrounding sea and land runoff. The difference between the models lies in the bathymetry – depths and shoreline location – which was determined from a digital elevation model /Brydsten 2006/.

During the BC years – 6500 BC, 3000 BC and 1000 BC – Öregrundsgrepen is not a semi-enclosed well-defined area as it is during the AD years (see section 2). Instead, the basins shown in Figure 2-2 are located in an open coastal sea area. Thus, the hydrodynamics of this area is not governed by local conditions and well-defined boundary forcing, but is instead dependent on the large-scale circulation in the Mastogloia, Litorina and Limnea Seas. In fact, the basins are more or less arbitrary volumes of water. The flow field is likely to vary over spatial scales in the order of or larger than the size of the individual basins. As the area rises and land forms, variations on smaller scales become increasingly important.

For this reason, two different model approaches have been used for the three BC years and the ten AD years:

1. For the BC years a large-scale hydrodynamic model for the entire Baltic Sea has been used to produce flow fields which then have been interpolated to determine the basin exchange.
2. For the AD years a local high-resolution hydrodynamic model of Öregrundsgrepen has been used, which in turn has been forced on its lateral boundaries by results from the Baltic Sea model of the present time.

Both modelling approaches, i.e. for BC and AD years respectively, produce one-year time series of all hydrodynamic variables. The output time resolution is one hour. Using these results the water exchange for individual basins is calculated.

3.1 Basin flows

The basin flow is defined as the total volume flow between two neighbouring basins at a given instance of time. As the time resolution of the hydrodynamic model output was set at one hour, the basin flows are also hourly time series, i.e. each time series consists of 8,784 values.

Depending on the year different numbers or parts of basins are active, i.e. located within the marine environment. For example, for the BC years all 52 basins are active, yielding over 200 connections between neighbouring basins, and thus an equal number of time series of volume flows.

From these time series three annual means are calculated to describe the average exchange between basins:

1. the mean of the entire time series (net flow),
2. the mean of all occasions with positive flow, and
3. the mean of all occasions with negative flow.

The mean annual flows constitute a low estimate of the exchange. This is because they are based on the net exchange at each instance of time and therefore simultaneous inflows and outflows over the same boundary (e.g. at different depths) are not resolved. The annual means of negative and positive volume flows indicate whether the net mean is the result of large flows in both directions or primarily a flow in one direction only.

3.2 Average Age

One measure of residence time, and thus of the water exchange, is the so-called Average Age (AvA). This describes the average time that water parcels have spent within a given volume (see, e.g., /Engqvist et al. 2006/). To calculate this for the basins in Öregrundsgrepen an age tracer is used. Outside Öregrundsgrepen the tracer concentration is set to zero, i.e. water from outside the modelled basins is assumed to have age zero and is termed exogenous. In each point the concentration increases linearly with time, i.e. for a closed basin the concentration will increase monotonously at the same rate as the passing of time. This age tracer is transported and mixed in the model just as any other substance, e.g. salinity. Thus the concentration of the age tracer represents the age of the water, relative the water outside Öregrundsgrepen, at that particular point in space and time.

After an initial increase (the spin-up period) a balance will be reached between aging and mixing with exogenous water. Thus the age tracer concentration will eventually fluctuate around some long-term mean value. Taking this mean value – defined as the temporal average over the simulated period excluding the spin-up period – and averaging over each basin volume, yields the AvA for each basin relative the exogenous water. Note that this measure is the same as that termed "collective AvA" in chapter 5 of /Wijnbladh et al. 2008/. The AvA results in this study are thus not comparable to the "individual AvA" computed for the basins in chapter 5 of /Wijnbladh et al. 2008/, where water outside each basin is defined as exogenous.

3.3 Hydraulic residence time

An alternative measure of residence time is the hydraulic residence time (HRT). The hydraulic residence time is simply the time needed to replace all the water in a given volume with water from outside said volume, calculated by dividing the volume by the gross inflow (or outflow assuming conservation of volume).

Compared to the AvA above this is a cruder calculation of the residence time for three reasons. Firstly, the HRT is a step back in resolution as it does not resolve variations on the scale of the computational mesh. The HRT is defined on a basin level whereas the model actually resolves each basin using a number of computational cells. Secondly, the HRT calculation implicitly assumes that the inflowing water replaces the resident water completely without mixing, by simply pushing out the resident water. In reality mixing between inflowing and resident water will result in a more gradual exchange. Finally, the HRT does not include diffusive exchange processes such as turbulent mixing, as only purely advective transport is considered.

3.4 Description of models

3.4.1 BC years

To determine the basin water exchange for the BC years, i.e. the open sea phase, the AS3D Baltic Sea model /Engqvist and Andrejev 1999, 2000, 2008/ was used. This modelling work was carried out by Anders Engqvist (see Appendix B). The bathymetry and shoreline location in the hydrodynamic model was determined for each year from a 500-by-500 m digital elevation model /Brydsten 2006/. The resolution of the hydrodynamic model is 2-by-2 nautical miles, implying that the Öregrundsgrepen area is covered by 9-by-10 grid points (see Figure 3-1). The forcing is the same as for the Baltic Sea model for 2004 /Engqvist and Andrejev 2008/, except for river runoff which has been adjusted according to the results of /Gustafsson and Westman 2002/. The initial salinity conditions in the Baltic Sea have been determined from /Gustafsson and Westman 2002/ and /SKB 2006/. The model was spun up for half a year and then run for one year. For more details see Appendix B.

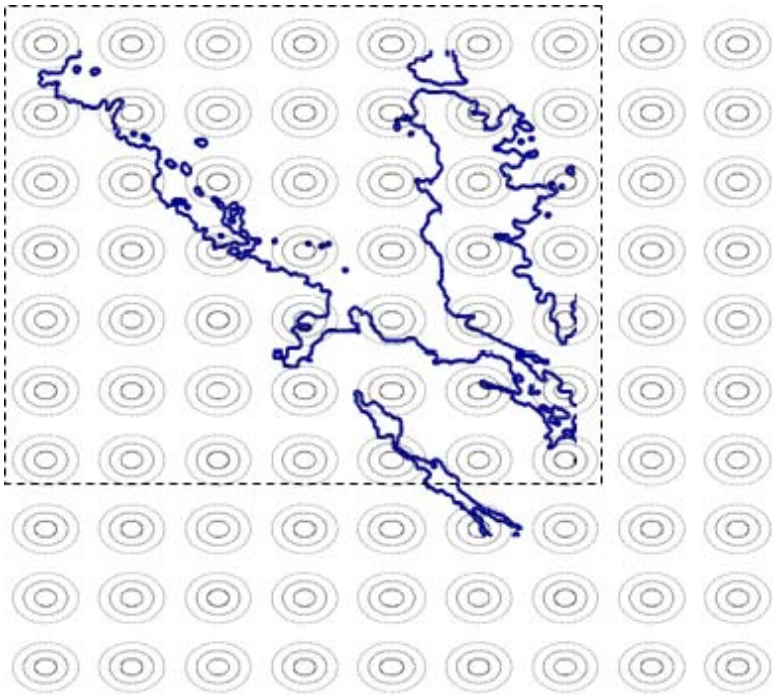

Figure 3-1. *The locations of velocity grid points in the Öregrundsgrepen area relative the present-day shoreline.*

To determine the flows through each cross-section between neighbouring basins from the model output, the following steps were carried out:

1. The modelled hourly 3-D time series of horizontal current components (east-west and north-south) for the Öregrundsgrepen area were interpolated horizontally to the midpoints of all cross-sections connecting neighbouring basins, using nearest neighbour interpolation. The result is two time series of vertical profiles of the horizontal current components for each connection. The Baltic Sea model consists of 40 layers in the vertical direction, with a resolution varying between 2.5 and 20 m with the highest resolution near the surface. The horizontal current components are assumed to represent the mean current in each layer.
2. Based on high-resolution 20×20 m digital elevation models (DEM, see section 4.1) of the Öregrundsgrepen area, the corresponding depth profiles for each inter-basin connection were determined. Each connection, defined as a straight line in the horizontal plane, was split into nine equal segments. At the resulting ten equally spaced points along each connection the depth was determined by two-dimensional linear interpolation of the depths in the DEM for that particular year. These depth profiles can then be integrated to produce the cross-sectional area of each connection (see Figure 3-2).
3. Next the normal components of the interpolated current vectors at each cross-section's midpoint were calculated, based on the normal unit vector for each connection.
4. Finally, these time series of vertical profiles of normal current components were integrated vertically using the previously determined depth profiles for each connection to produce time series of total volume flow for each cross-section.

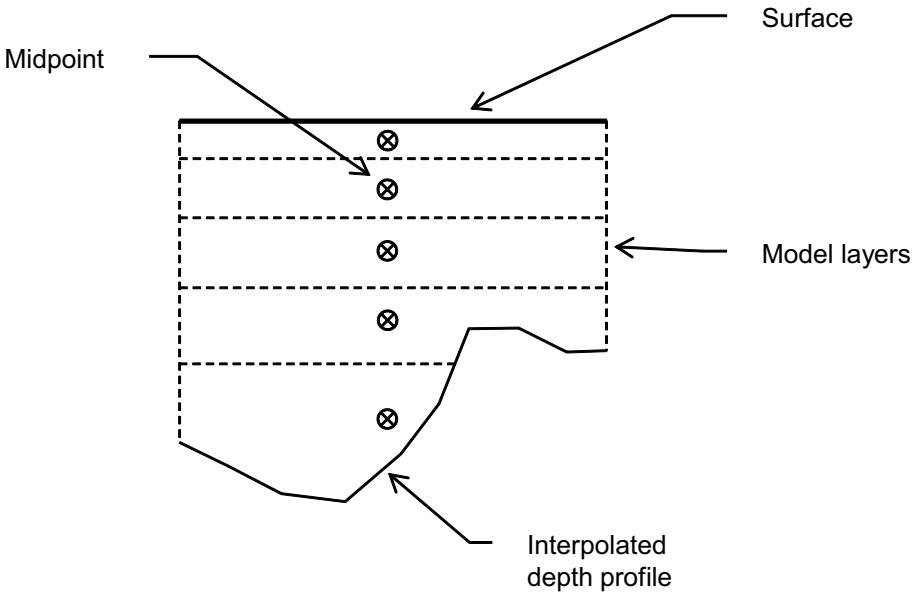

Figure 3-2. *Definition sketch for cross-sections connecting neighbouring basins.*

To calculate the AvA, a simple model describing the time evolution of the concentration of an age tracer has been set up for the 52 interconnected basins 100 to 151. For each basin i the time evolution of age tracer concentration C_i is given by

$$\frac{dC_i}{dt} = 1 + \frac{1}{V_i}\left(\sum_j Q_j^{in} C_j - C_i \sum_j Q_j^{out}\right)$$

where V_i is the volume of basin i, Q_j^{in} is the inflow from neighbouring basin j to basin i, C_j is the tracer concentration in neighbouring basin j and Q_j^{out} is the outflow from basin i to neighbouring basin j. The first term gives the aging, i.e. a source for the age tracer concentration equal to the passing of time, whereas the second term describes the exchange with the surrounding basins. If there is no exchange with neighbouring basins then the age tracer concentration increases linearly with time.

All together this constitutes a set of 52 ordinary differential equations. This has been solved in Matlab using the Runge-Kutta solver ode45. The previously calculated time series of volume flow, divided into positive (inflow) and negative (outflow) flows, constitute the forcing. The ode45 solver uses an adaptive step size technique and hence linear interpolation is used to determine the flows at times between the hourly values available in the time series. The age tracer concentration is fixed at zero exterior to the 52 basins. Basin 152 is also considered as part of the exterior area. The initial value is zero for all basins and the basin volumes are assumed constant.

The resulting one-year time series of the age tracer concentration in each basin have been output with a time resolution of one hour. At first there is a spin-up time during which the age tracer concentrations increase until a quasi-steady balance between exchange and aging is reached. The spin-up time is always less than one month. Thus, the annual mean average age of each basin has been calculated as the mean for the period February-December.

3.4.2 AD years

For the years where the Öregrundsgrepen is more or less enclosed (0 AD to 9000 AD; see Figure 3-3), a high-resolution flexible mesh model, MIKE 3 FM – developed for applications within oceanographic, coastal and estuarine environments – has been applied to calculate the circulation and exchange of water.

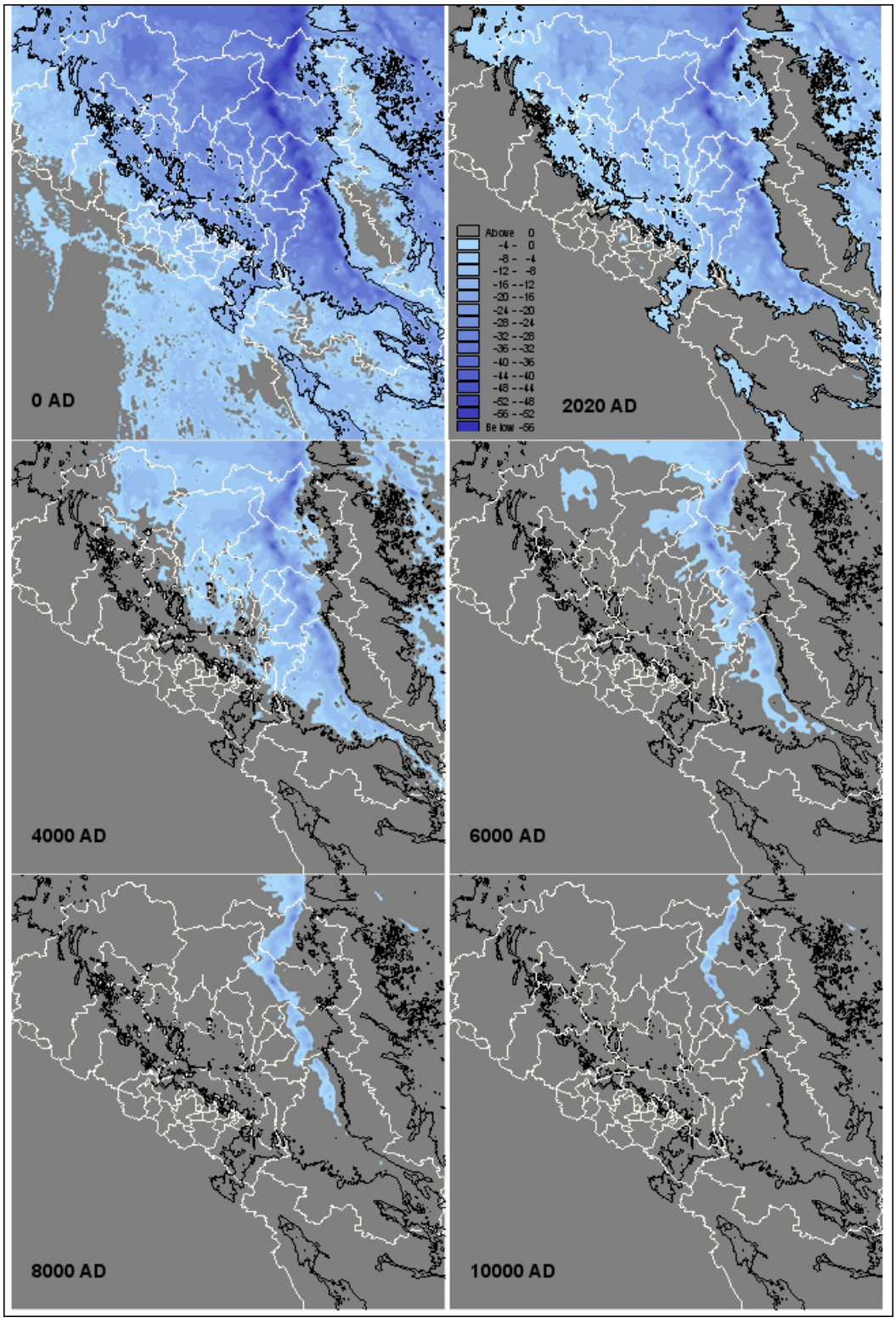

Figure 3-3. *Selected stages in the development of the Öregrundsgrepen from 0 AD to 10 000 AD. The present-day shoreline is given by the black line and the basin borders are shown in white. By the year 10 000 AD only lakes exists.*

The MIKE 3 system consists of several modules. The basic module, HD, simulates the hydrodynamic processes, describing the water movements based on the driving forces. The HD module is based on the numerical solution of the three-dimensional, incompressible, Reynolds-averaged Navier-Stokes equations invoking the assumptions of Boussinesq and of hydrostatic pressure. Thus,

the model consists of equations for the continuity of mass, momentum, temperature, salinity and an equation of state. The set of equations is closed by a turbulent closure scheme. The free surface is taken into account using a sigma-coordinate transformation approach /DHI 2007/.

MIKE 3 FM accounts for all the important hydrodynamic processes, i.e.:

- Density stratification due to temperature and salinity variations
- Transport of salt and heat
- Density driven currents
- Bottom friction
- Wind forcing on the surface
- Currents driven by sea level variations
- Fresh water runoff and cooling water discharge
- Heat exchange with the atmosphere
- Turbulence
- Coriolis force

The water volume in the area of interest is divided into a number of computational cells (a mesh), using a cell-centred finite volume method, in which sea level, currents, salinity, temperature, density and turbulence are calculated. In the horizontal plane an unstructured mesh is used while in the vertical the mesh is structured. The mesh elements (cells) can be prisms whose horizontal faces are triangles. The mesh is tailored to accurately describe the bathymetry and shoreline.

The model domain for Öregrundsgrepen has been chosen such that the model has one boundary to the Baltic in the north, between present day Örskär and Klungsten (approx. N 60º 31’ 46”) and one boundary in the south, between present day Vässarön and Storskäret. The model resolution (i.e. the size of the triangular cells) varies and has been tailored to represent the topography and pre-defined basins in the area as accurately as possible while retaining a reasonable run time. Resolution is higher in straights and shallow areas and coarser in the deeper more open water areas (see example of mesh at 2020 AD in Figure 3-4). The main focus when constructing meshes for different years has been to describe basin volumes and basin connections to adjacent basins adequately without producing unreasonable simulation times.

The MIKE 3 FM model has a built-in tool for calculating the net volume flow through a cross-section defined by a straight line in the horizontal plane. Using this facility hourly time series of volume flow for each connection between neighbouring basins have been stored.

To calculate the AvA, the so-called ECOLab module /DHI 2008/ has been used. This is an add-on module in which arbitrary internal processes can be defined for arbitrary substances, which is coupled to the hydrodynamics and the advection of these substances in the flow field. Hence, an age tracer C has been defined with an additional internal source described by (cf. section 3.4.1):

$$\frac{\delta C}{\delta t} = 1.$$

The dynamic development of the concentration, C, in each computational cell is then calculated as a result of advection, mixing and the internal source, i.e. the aging. As for the BC years the boundary value for C is zero, i.e. water exogenous to the model, and thus to Öregrundsgrepen, is assumed to have age 0. Likewise, the initial condition is zero concentration throughout the model domain.

The model has been set up to store the concentration of the age tracer in each basin at hourly intervals. This output has then been post-processed by calculating the basin volume average of the age tracer concentration for each year, which yields time series of the evolution of the average age tracer concentration in each basin. There is a spin-up time during which the concentration increases until a quasi-steady balance between exchange and aging is reached. The spin-up time will vary in the AD years as the Öregrundsgrepen shallows and narrows. Thus, the AvA of each basin has been calculated as the mean for each year excluding the spin-up period.

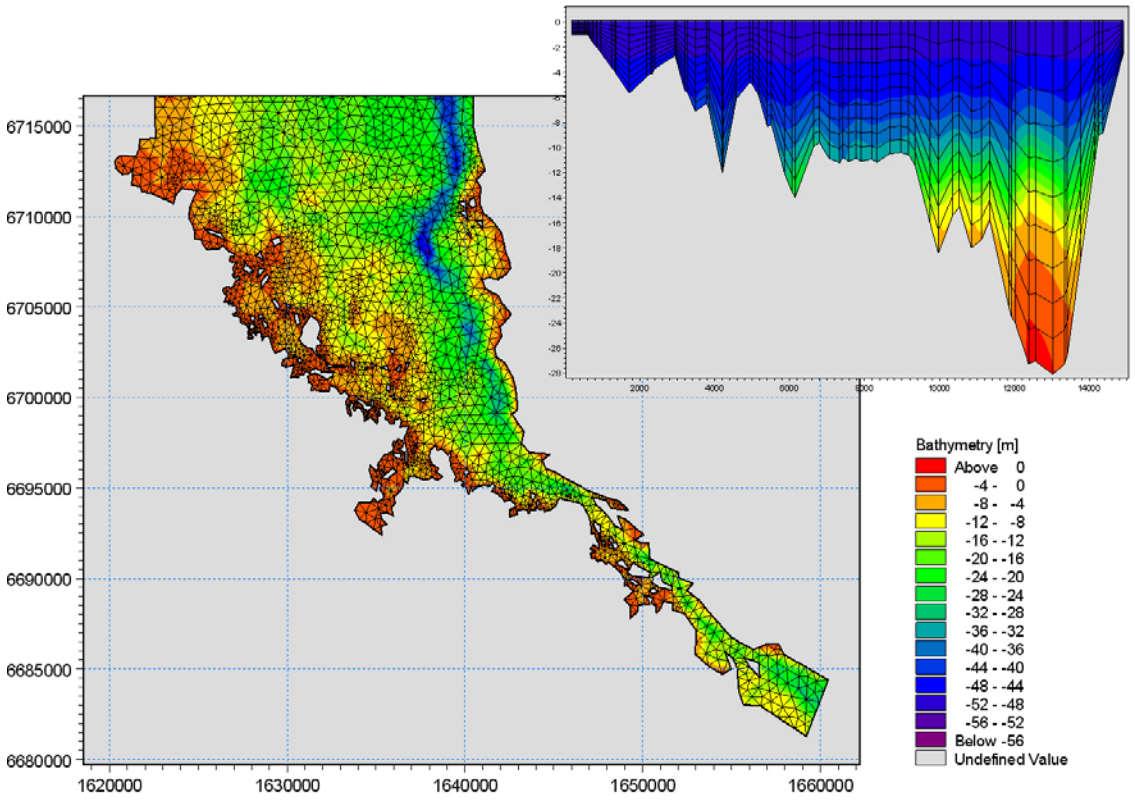

Figure 3-4. *The computational mesh for the year 2020 AD showing horizontal and vertical resolution. Resolution is higher in areas with small basins and straits. The vertical resolution varies with depth as the water column always is described using 10 layers. Thus, the deeper the water, the thicker the layers.*

4 Model input data

Three types of input data are required to setup and run the hydrodynamic models: a bathymetry including the bottom roughness (constant in time for a given year), forcing parameters (variable in time and optionally in space) and initial conditions (variable in space). The relevant forcing parameters are:

1. Meteorological forcing used to calculate exchange of momentum and heat through the sea surface, i.e. wind velocity, air temperature, humidity and cloudiness.
2. Freshwater runoff from land.
3. Sea levels along the open boundaries.
4. Stratification on the open boundaries, i.e. vertical profiles of salinity and temperature.
5. Ice cover.

In addition, the observed cooling water discharge for 2004 from the Forsmark power plant is included as a source in the 2020 AD local model simulation, but not in any other year. Input parameters and data sources are listed in Table 4-1.

As very little is known about the past and future climate, present-day climate has been used as input for all years. The year 2004 has previously been used for modelling purposes in this area /Engqvist and Andrejev 2008/. For the BC years some modifications of the river runoff and initial salinity and temperature fields have been made based on other studies (see Appendix B).

Table 4-1. Input data used for modelling of AD years.

Input data	Source	Reference	File name
Air temperature	SMHI (Örskär station)	Sicada_08_094	temperature_hourly.ascii
Wind	SMHI (Örskär station)	Sicada_08_094	wind.ascii
Precipitation	SMHI (Örskär station)	Sicada_08_094	precip_alexcorr.ascii
Relative humidity	SMHI (Örskär station)	Sicada_08_094	air_humidity_hourly.ascii
Clearness	SMHI (Mueller data-base)	Anders Engqvist	balt04[01-12].txt
Salinity	Baltic Sea model	Anders Engqvist	zts04[01-12].dat
Temperature	Baltic Sea model	Anders Engqvist	zts04[01-12].dat
Sea level	Baltic Sea model	Anders Engqvist	zts04[01-12].dat
Discharge Olandsån		Anders Engqvist	Qf_fors_d_2004a.txt
Discharge Forsmarksån		Anders Engqvist	Qf_fors_d_2004a.txt
Forsmark cooling water discharge		Anders Engqvist	CoolWater3a.xls
DEM	SKB		fm_0_ad, fm_1000ad, fm_2020_ad, fm_3000_ad,…, fm_10000_ad
Basins	SKB	GIS_ Request#08_33_080508	Bassänger.shp
Present-day coastline	SKB	GIS_Request#08_30	FM_Kustlinje_OK.shp
Basin volumes (cor-rected)	SKB	090918 Mårten Strömgren	Forsmark_basins_volume.xls
Original basin volumes (erroneous)	SKB	090210 Mårten Strömgren	Forsmark_basins_volume_FEL.xls
Marine basins	SKB	GIS_ request#08_31_080425	Marina_bassänger_i_Forsmark.shp
Catchment areas for future lakes	SKB	GIS_ request#08_31_080425	Subavrinningsområden_för_fram-tida_sjöar_inom_Forsm.shp

4.1 Bathymetric data

The bathymetry including the shoreline (at mean sea level) for the different years is determined from two digital elevation models (DEM) with a resolution of 20 m and 500 m respectively /Strömgren and Brydsten 2008/, corrected with the Påsse shoreline displacement equation /Söderbäck 2008/. The high resolution DEM almost covers the model area for the local hydrodynamic model whereas the coarser DEM covers the whole Baltic Sea.

4.2 Meteorological forcing

The most important meteorological forcing parameter is the wind. The Baltic Sea model uses databases of analyzed fields of meteorological observations provided by the Swedish Meteorological and Hydrological Institute (SMHI). Two alternatives have been used: the so-called Mueller database (available from SMHI) for the simulation of present-day conditions and the Mesan database (available from SMHI) for the BC years (see Appendix B). In both cases data for the year 2004 have been used. Note that the Mueller database requires adjustment of its geostrophic wind velocities to the 10-m level. A comparison with measured data at the local wind station Örskär /Engqvist and Andrejev 2008/ indicates that both databases underestimate the wind speed. Also, the correlation between the two data sets is poor. As a result the observed wind at Örskär has been selected as forcing for the local model of Öregrundsgrepen. Wind statistics from the station Örskär A is shown in Figure 4-1, where wind measured every three hours during 2004 is presented in a wind rose. The predominant wind direction (38% of the time) is from the sector south to west.

To determine the heat exchange with the atmosphere in the local model, air temperature, humidity and clearness (defined as one minus the cloudiness) are required input data. Observed time series for 2004 from the station Örskär A were used in the model; see Figure 4-2 and Figure 4-3.

4.3 Land runoff

The Baltic Sea model is forced by calculated monthly values for 29 river discharges during 2004. For the BC years these values have been adjusted using the relative change compared to 2000 AD computed by /Gustafsson and Westman 2002/. Also, the source points have been moved to match the altered shoreline (see Appendix B).

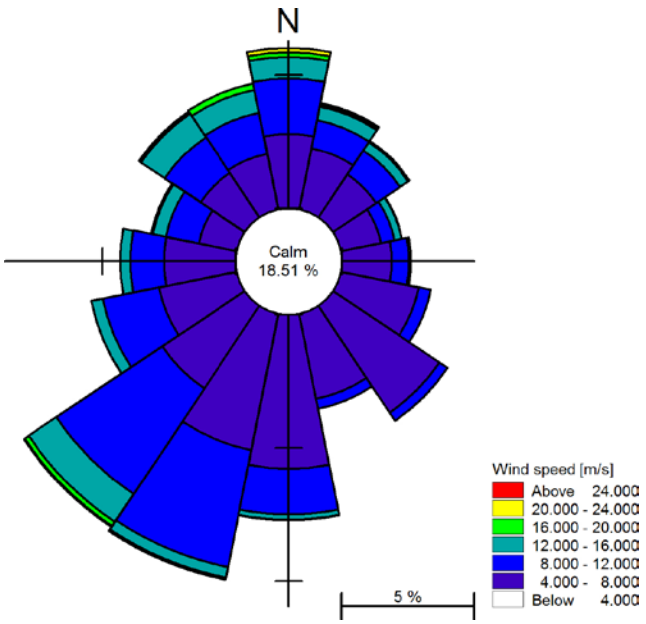

Figure 4-1. *Wind statistics from Örskär A for 2004 (3-hour wind). The predominant wind direction is from the sector south to west.*

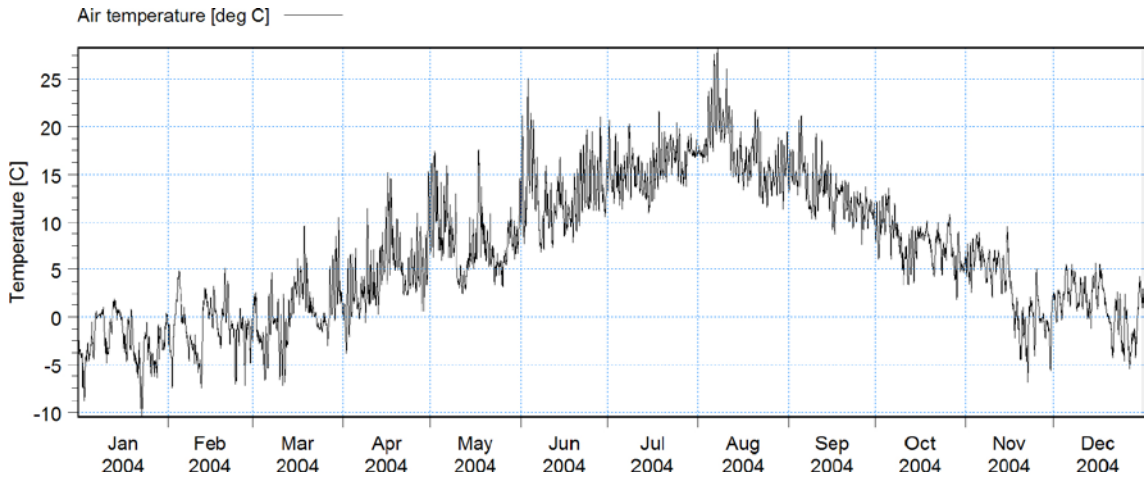

Figure 4-2. *Temperature observations at Örskär in 2004.*

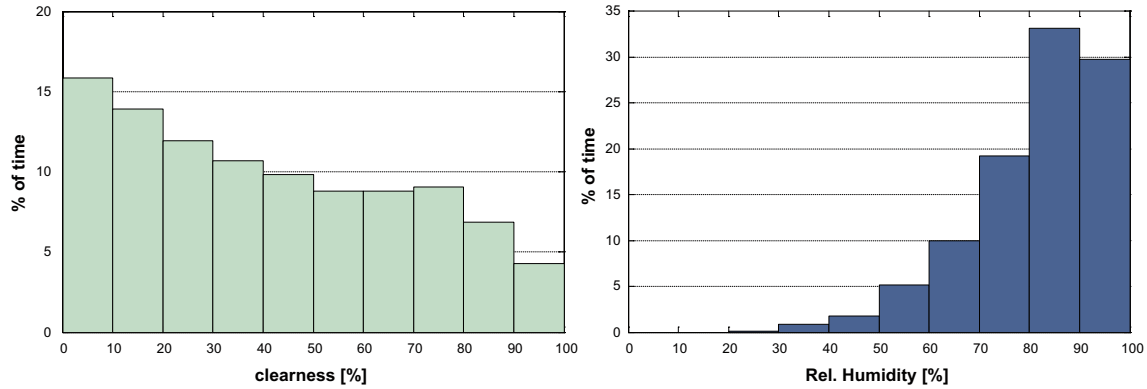

Figure 4-3. *Histograms of relative humidity and clearness factor observed at Örskär in 2004.*

The local model for Öregrundsgrepen uses the daily flows in Forsmarksån and Olandsån for 2004 as input for land runoff to Öregrundsgrepen (see Figure 4-4). For all AD years, the drainage basins for Forsmarksån and Olandsån are more or less unchanged (Lars Brydsten, pers. comm.), and hence present-day flows in Forsmarksån and Olandsån have been used. The source points for future years have been determined from the landscape modelling in which the evolution of the mouths of these two streams can be traced. Water temperature in the streams has been set to the local air temperature since no information is available for this parameter. For all instances of sub-zero air temperature the surface water temperature has been set to zero.

4.4 Sea levels

The Baltic Sea model used for the BC years is forced on its western boundary (Kattegat) by observed sea levels in Göteborg and Fredrikshavn for the year 2004 /Engqvist and Andrejev 2008/.

The local Öregrundsgrepen model is forced by the Baltic Sea model results for 2004, i.e. computed sea levels have been extracted from representative grid points in the Baltic Sea model which coincide with the boundaries of the local model (see Figure 4-5). Note that no horizontal variations have been included, as small perturbations in the horizontal distribution present in the Baltic Sea model caused significant instabilities in the local model. The same forcing – for the year 2004 – has been used for all AD years.

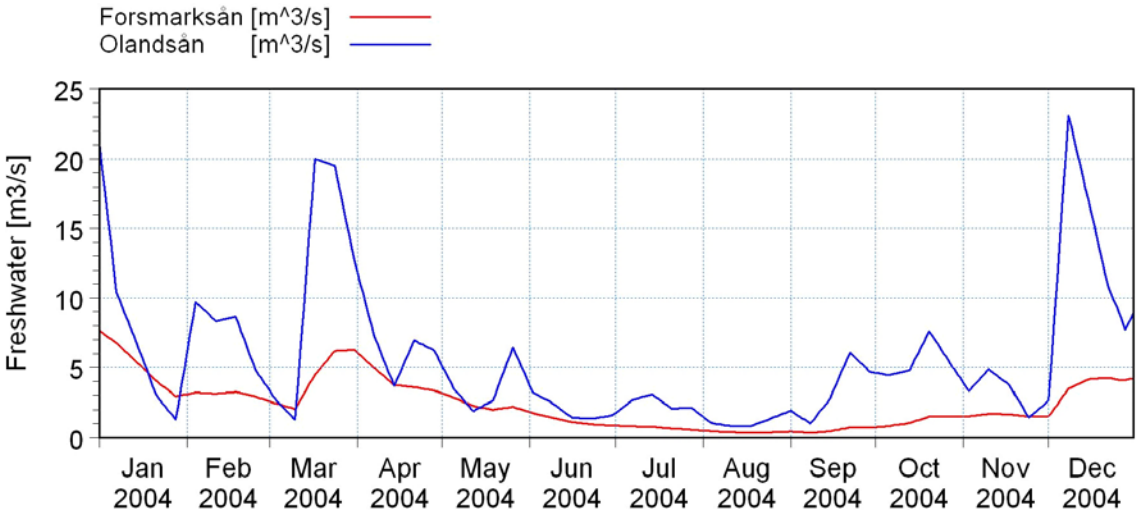

Figure 4-4. *Fresh water discharge from the streams Forsmarksån and Olandsån.*

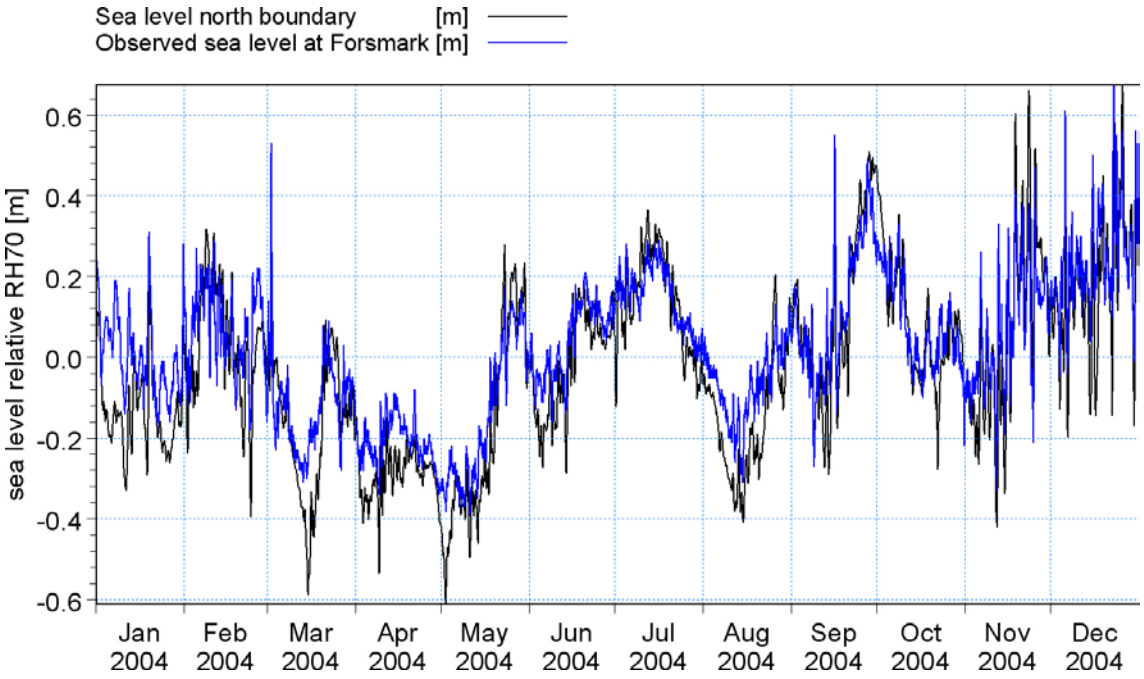

Figure 4-5. *Sea level computed by the Baltic Sea model at the northern boundary in the Öregrundsgrepen model, compared to observations at Forsmark.*

4.5 Stratification

The Baltic Sea model uses climatic averages for the salinity and temperature profiles at its western boundary (Kattegat) /Engqvist and Andrejev 2008/.

The local model uses the computed salinity and temperature profiles from the Baltic Sea model for 2004 as forcing on the northern and southern boundaries. Model results were extracted every hour from equidistant grid points in the Baltic Sea model that roughly matched the locations of the two open boundaries in the local model. For the southern boundary only one grid point was used. These outputs were then interpolated vertically to equidistant depths, such that the resulting grids covered the respective boundaries.

4.6 Ice

Gridded ice cover data from measurements is available for 2004. However, for past and future years no such data is available. Even neglecting climatic variations, the ice cover will differ greatly depending on the geometry, i.e. a small, narrow area will ice over more easily than open sea. Thus, it is hardly relevant to use ice cover data from the year 2004 for other years, when the Öregrundsgrepen area looks much different from today.

The ice formation could be modelled using a separate ice model. However, as a first approximation, and considering other approximations that had to be made, ice has been neglected for all years in the hydrodynamic simulations. In the sensitivity analysis in chapter 7, the effects of no wind forcing is discussed which is similar to an ice covered area.

4.7 Initial conditions

The initial conditions in the Baltic Sea model for the year 2004 was produced by running the model from climatic average salinities and temperatures, starting one month earlier than the desired starting point. Initial conditions are then given as an average of this procedure for a number of times /Wijnbladh et al. 2008/. For the BC years see Appendix B.

For the local model the initial conditions were zero velocities, a constant sea level elevation and a constant vertical stratification throughout the model domain. The initial sea level elevation was set to the value simulated by the Baltic Sea model at the midpoint of the northern boundary on January 1. Likewise, the initial vertical stratification was set to the profile simulated by the Baltic Sea model at the midpoint of the northern boundary on January 1.

5 Results

5.1 General circulation

In Figure 5-1 the modelled surface current distribution for present-day conditions (2020 AD) at a number of representative points is presented as current roses. The colours indicate current speed and the size of the coloured stripes indicates the relative frequency of currents within that particular speed interval. The area of each slice indicates the relative frequency of current directions within that particular interval.

The surface current speed is mostly in the 0–20 cm/s range. The strongest currents are found to the south in the narrow Öregrunds strait, where between 30 and 40 cm/s is not uncommon. The lowest speeds are found along the deeper eastern side of Öregrundsgrepen, where the current speed hardly ever exceeds 10 cm/s. Current speeds are generally higher along the shallower western side of the estuary, though only rarely above 30 cm/s. Note that a typical surface current speed due to the wind is approximately 1 % of the wind speed. This would imply common wind speeds of 10–20 m/s. Observations show that the wind speed exceeded 10 m/s only about 18 % of the time during 2004, and 15 m/s only 2 % of the time. We can conclude that the surface current is only partly forced by the local wind.

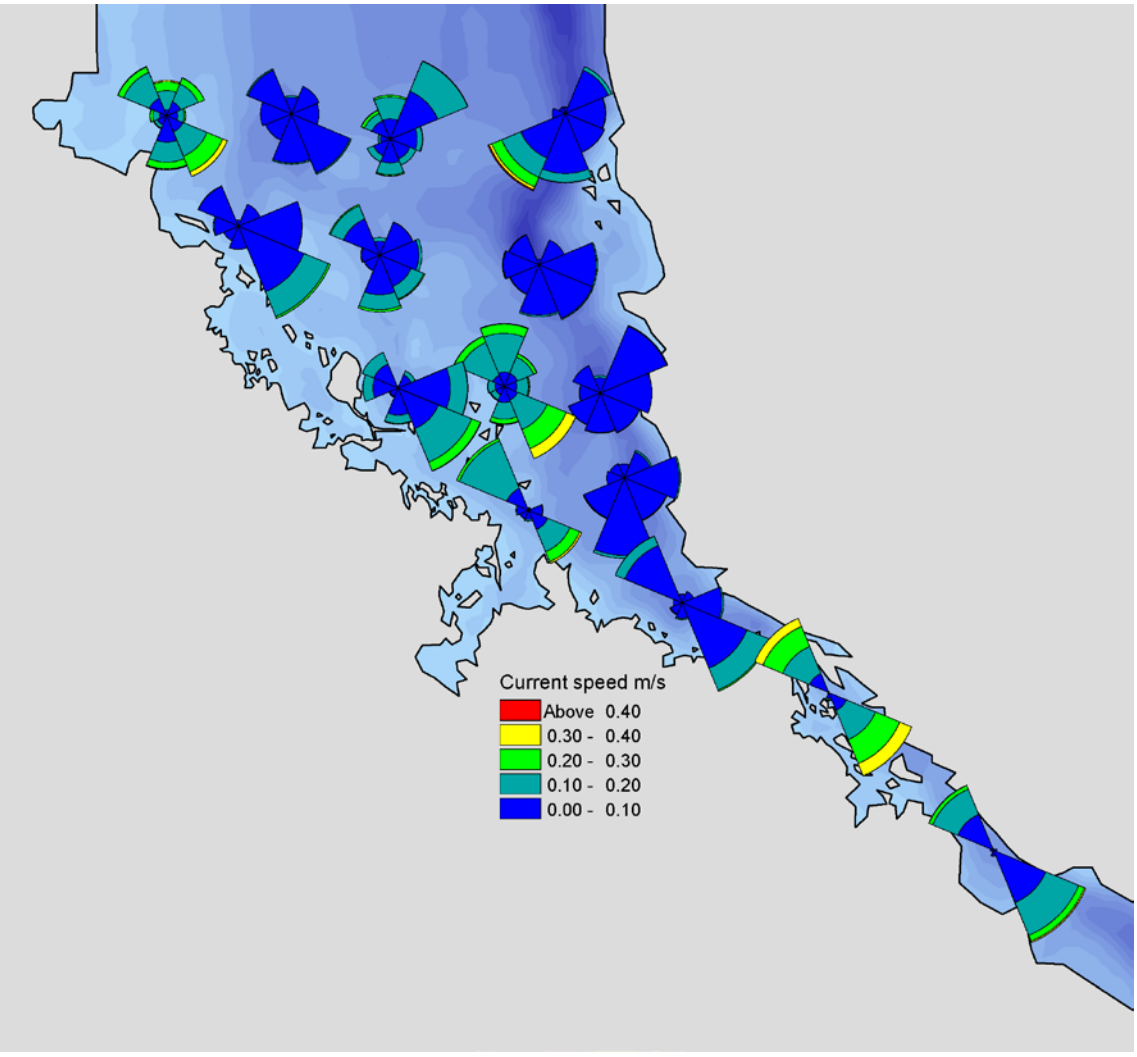

Figure 5-1. *Surface (–0.5 m) current roses at selected points for 2020 AD.*

This last conclusion is also supported if we consider the current direction. In the south the current is clearly in the along-channel direction, as would be expected. Along the western shore the current is primarily directed parallel to the shoreline, whereas in the central parts of the estuary and along the eastern shore current directions vary. According to observations the dominating wind direction is from the SSW (180–225°), which accounts for about 24% of the observations during 2004. No clear prevalence of surface currents in the NNE direction can be discerned.

In Figure 5-2 the depth integrated modelled current for 2020 AD is shown. The vertical average current speed is generally somewhat reduced compared to the surface speeds, but not excessively so. This again indicates that the wind-driven current plays a role but is not altogether dominating, at least in the deeper areas.

The results for the current direction show greater differences. However, in the southern strait the picture resembles that for the surface current. A closer inspection indicates that flow in the southward direction is slightly more common than flow towards the north, supporting the case made in section 2.3 for a net southward flow through Öregrundsgrepen. Along the eastern shore the average current direction is clearly aligned with the deep channel, i.e. the mean flow is guided by the bathymetry. The varying current direction at the surface cannot be seen. Along the western shore the vertically integrated current is aligned parallel to the shore, just as for the surface current. In fact, at most points shown the vertically averaged current appears to be more aligned with the shoreline, with fewer instances of current directions perpendicular to the shoreline.

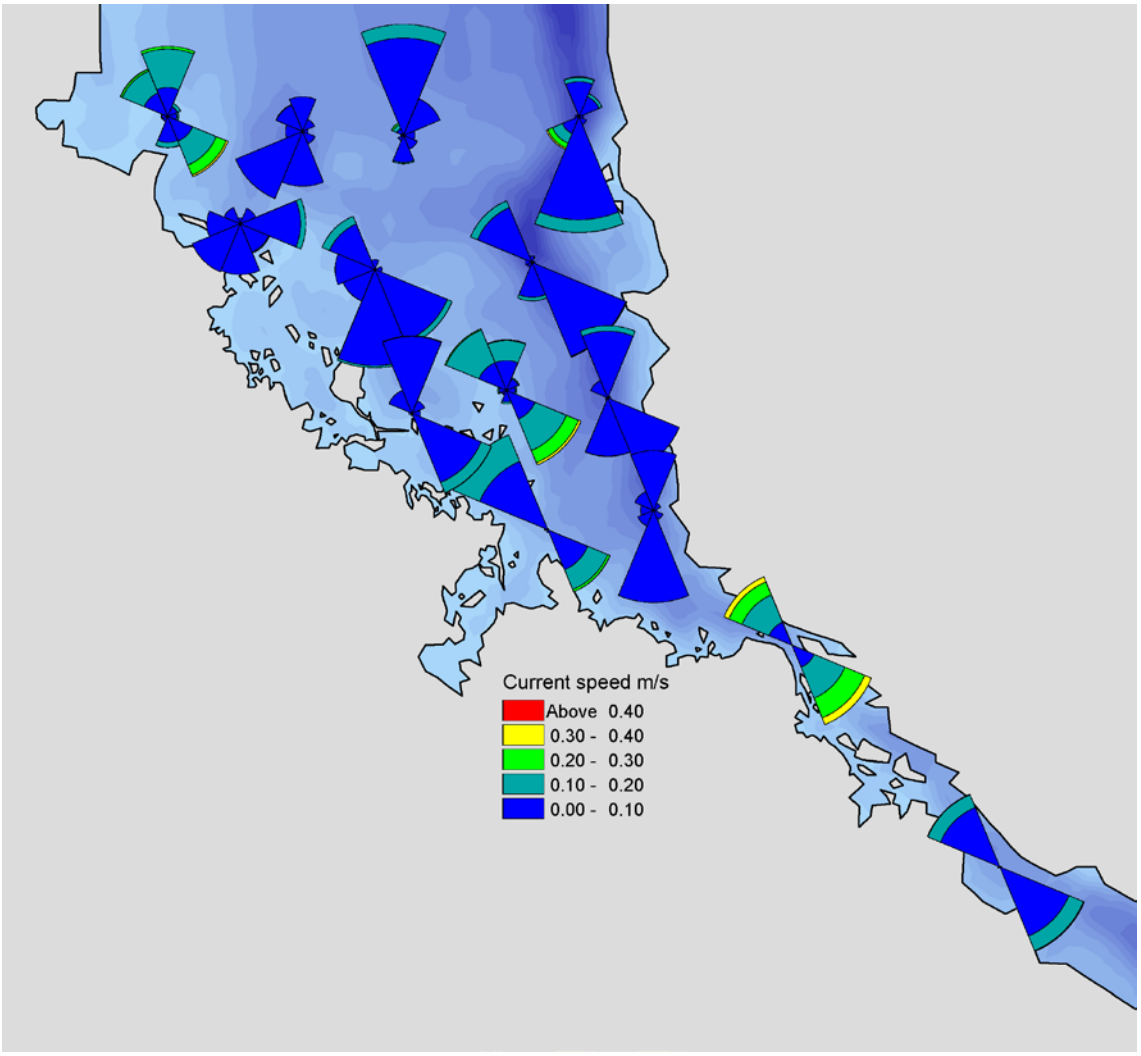

Figure 5-2. *Depth integrated current roses at selected points for 2020 AD.*

One curious feature of the modelled vertically integrated currents is the strong northward component at the central point near the northern boundary. Together with the dominating southward direction at the point in the north-eastern corner, this may indicate a clockwise circulation in the area, with water entering through the boundary at the deep, north-eastern corner and exiting in the middle of the northern boundary. If this feature is physical or an artefact of the model setup is difficult to tell. However, that the northern boundary dominates the water exchange, with concurrent inflows and outflows along different parts of the boundary, is not unexpected.

It should be stated that in previous modelling of the area, a gyre in the opposite direction was found /Engqvist and Andrejev 1999/. However, in that study a different year was modelled which may be the reason behind the disparate results. All in all, the modelled general circulation appears reasonable, both in terms of current magnitudes and directions.

5.2 Basin flows

The mean annual flow between basins has been calculated for the years from 6500 BC to 9000 AD. In Table 5-1 and Table 5-2 the basin flows for the year 2020 AD are shown.

The results show that the magnitude of the flow is primarily determined by the areas of the cross sections between basins. When the cross section between two basins is small, the flow is small and vice versa. For example, basin 105 at 2020 AD has large cross-sectional areas (wide and/or deep) to the basins 100, 101, 110 and 114. This produces large annual mean flows through these sections, and there is also a net through flow between basins. From Table 5-1 we can also see that between basins 120 and 121 the flow is in one direction only. This is due to the cooling water intake located in basin 120.

The positive and negative basin flows in Table 5-1, calculated by the present model for 2020 AD (MIKE 3), have been compared with those calculated for 1988 using the AS3D model, presented in Table 5-3 of /Wijnbladh et al. 2008/. The results are shown in Figure 5-3 and Figure 5-4. It is readily seen that the two models produces both positive and negative flows of the same magnitude, and large differences are found only in a few cases. The largest differences are found in the basin connections situated in the vicinity of the northern boundary. This discrepancy may be due to different forcing for the two modelled years.

For the connections through which the models show different flows, the AS3D model yields larger basin flows, with only a few exceptions. For those basin connections where this is not the case the explanation is probably given in the formulation of the basin connections. An example of this is found in the connections to basins 101 and 100 from basin 105. When adding up the flow from basin 100 and 101 into basin 105 the two models produce comparable results.

Another feature that is illuminated in the comparison is that AS3D produces a smaller exchange over the southern boundary (151 to Baltic) than MIKE 3. In AS3D the average flows are several times smaller than in MIKE 3. However, it should be noted that the two models have their southern boundaries located differently. According to /Engqvist and Andrejev 1999/, a through-flow in the Öregrund strait of 540 m^3/s has been reported, but was not qualified in the original reference if it refers to a mean or a peak flow. This datum cannot be considered as an indication that the flows produced by MIKE 3 are more realistic than AS3D.

Finally, all basin connections in the previous modelling study are not present in this study, and vice versa. This is mainly due to the fact that the two studies use different types of computational grids and resolution. In this study some of the connections were considered too small to include. The grid resolution does not resolve the smallest connections where flows between basins are around 1 m^3/s or less.

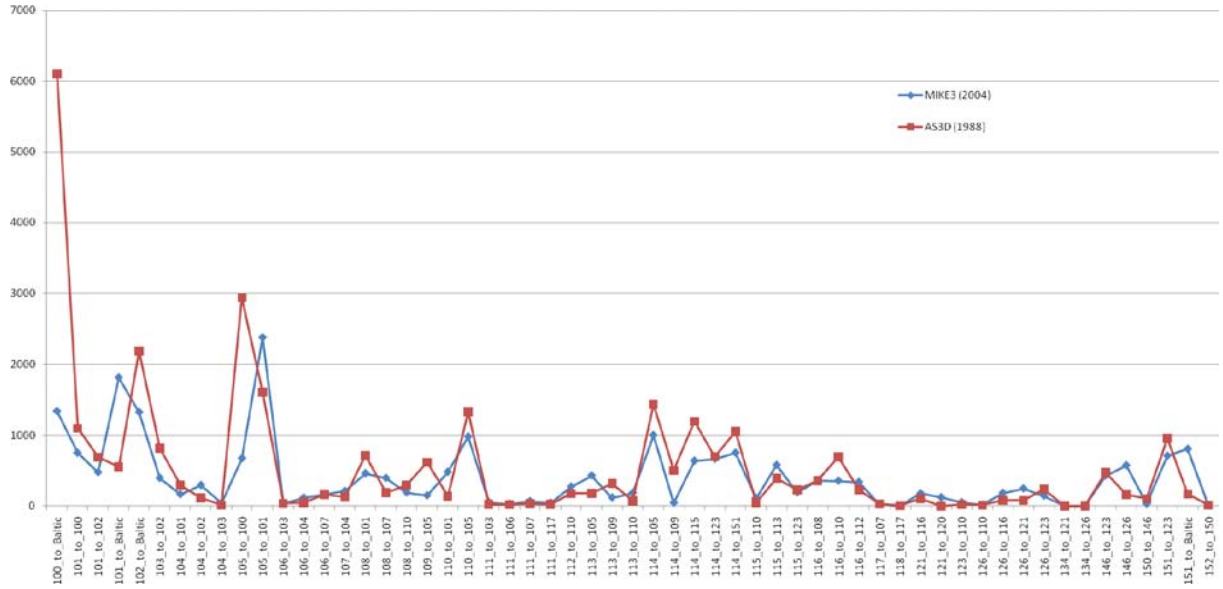

Figure 5-3. *Average positive flows in m³/s between basins in Öregrundsgrepen. The flow direction is indicated by the labelling on the x-axis. Blue line is MIKE 3 results for the year 2004. Red line is AS3D results for 1988.*

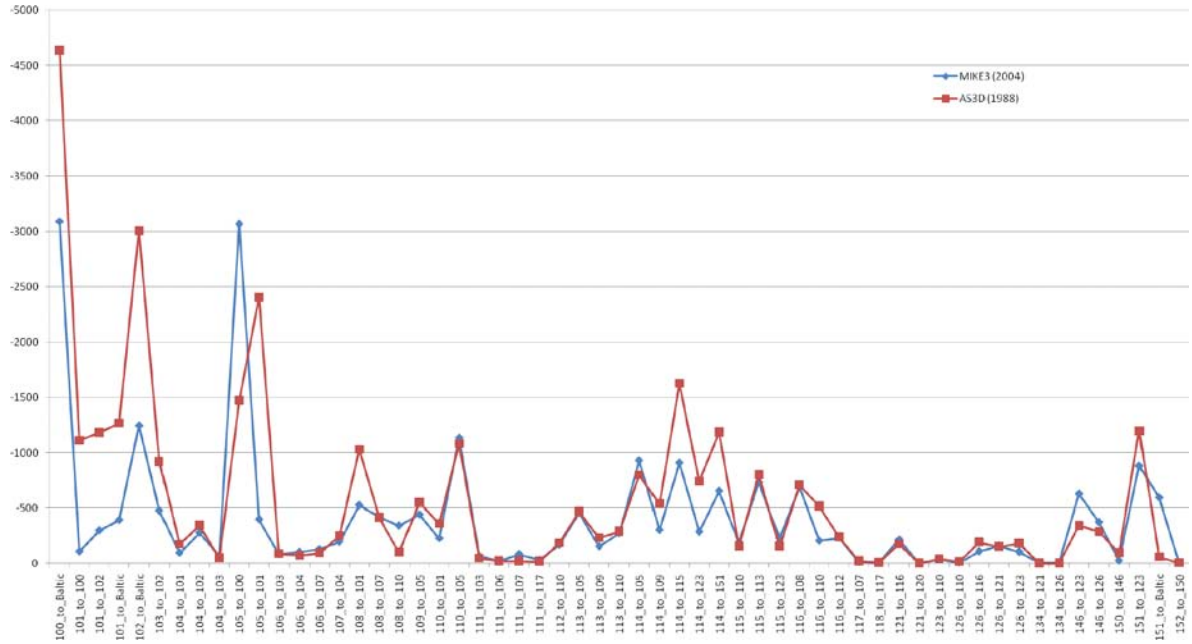

Figure 5-4. *Average negative flows in m³/s between basins in Öregrundsgrepen. The flow direction is opposite to that indicated by the labelling on the x-axis. Blue line is MIKE 3 results for the year 2004. Red line is AS3D results for 1988.*

Table 5-1. Average flows between basins in Öregrundsgrepen for 2020 AD. Positive values signify flow from the first basin 'to' the second basin, and negative flow is thus in the opposite direction.

Basin ID	Pos. flow [m3/s]	Neg. Flow [m3/s]	Net flow [m3/s]
100 to Baltic	1341	-3085	-1743
101 to 100	751	-106	644
101 to 102	477	-299	177
101 to Baltic	1818	-392	1426
102 to Baltic	1326	-1244	82
103 to 102	395	-476	-80
104 to 101	165	-94	70
104 to 102	294	-278	16
104 to 103	43	-67	-25
105 to 100	675	-3063	-2388
105 to 101	2386	-398	1988
106 to 103	38	-82	-44
106 to 104	117	-103	15
106 to 107	166	-127	39
107 to 104	213	-196	17
108 to 101	462	-525	-63
108 to 107	396	-420	-24
108 to 110	191	-341	-150
109 to 105	148	-441	-293
110 to 101	481	-227	254
110 to 105	981	-1135	-154
111 to 103	54	-66	-12
111 to 106	30	-21	9
111 to 107	66	-83	-17
111 to 117	45	-29	17
112 to 110	273	-168	105
113 to 105	431	-457	-26
113 to 109	119	-154	-35
113 to 110	185	-273	-88
114 to 105	1001	-929	73
114 to 109	45	-303	-258
114 to 115	640	-908	-268
114 to 123	666	-287	379
114 to 151	753	-651	102
115 to 110	112	-192	-80
115 to 113	580	-729	-149
115 to 123	191	-230	-39
116 to 108	361	-688	-328
116 to 110	357	-204	153
116 to 112	338	-233	105
117 to 107	26	-10	16
118 to 117	2	-3	0
121 to 116	178	-214	-36
121 to 120	122	0	122
123 to 110	53	-38	14
126 to 110	15	-7	8
126 to 116	185	-108	76
126 to 121	247	-159	88
126 to 123	144	-105	39
134 to 121	3	-5	-2
134 to 126	5	-3	3
146 to 123	430	-626	-196
146 to 126	576	-373	204
150 to 146	32	-24	8
151 to 123	710	-879	-169
151 to Baltic	807	-593	214
152 to 150	14	-7	8

Table 5-2. Average flows in and out of each basin for 2020 AD.

Basin ID	In flow [m3/s]	Out flow [m3/s]	Diff flow
Basin 100	4511	-4511	0 %
Basin 101	4292	-4290	0 %
Basin 102	2410	-2379	1 %
Basin 103	611	-611	0 %
Basin 104	769	-800	4 %
Basin 105	6023	-6023	0 %
Basin 106	342	-342	0 %
Basin 107	850	-853	0 %
Basin 108	1769	-1738	2 %
Basin 109	605	-605	0 %
Basin 110	2549	-2686	5 %
Basin 111	199	-196	2 %
Basin 112	506	-506	0 %
Basin 113	1464	-1464	0 %
Basin 114	3078	-3106	1 %
Basin 115	1791	-1791	0 %
Basin 116	1488	-1378	7 %
Basin 117	58	-57	1 %
Basin 118	3	-2	7 %
Basin 120	122	-122	0 %
Basin 121	464	-464	0 %
Basin 123	2180	-2180	0 %
Basin 126	961	-967	1 %
Basin 134	8	-8	0 %
Basin 146	1030	-1030	0 %
Basin 150	38	-38	0 %
Basin 151	2225	-2168	3 %

5.3 AvA

5.3.1 Entire Öregrundsgrepen

The evolution of Öregrundsgrepen and the resulting water exchange is shown in Figure 5-5, where the AvA for each year simulated after the open sea phase is shown. Overall, the AvA increases with time as the area becomes shallower and more isolated from the Baltic Sea. However, there are variations along the way due to different factors. By analyzing the AvA for the different time steps, the evolution of the Öregrundsgrepen can be divided into three different stages that have different types of main water exchange characteristics (see Figure 5-6 and Table 5-3).

The first stage is between 6500 BC to 0 AD, when the Öregrundsgrepen area is located in the open sea without any physical boundaries restricting water exchange. There is no significant difference in the water exchange, as indicated by the AvA-values, between these three BC years. The value for the entire Öregrundsgrepen area is between five and seven days, and the basin values lie in the same range, with extremes of two and ten days. This is the phase during which the shortest residence times in the evolution of Öregrundsgrepen are found.

The second stage is between the years 0 AD and 3000 AD, when the southern boundary of Öregrundsgrepen has narrowed due to land uplift and thereby restricting the water exchange. The narrowing of the southern boundary results in higher AvA compared to the earlier stage. The net flow through the southern boundary into the Baltic in the 0 AD simulation is reduced four times. Similarly the net flow into Öregrundsgrepen through the northern boundary decreases almost four times. These combined effects increase the residence time for the basin. However, between the years 1000 AD and 3000 AD the AvA is actually reduced, probably due to smaller basin volumes combined with inflows of the same magnitude as for the year 1000 AD. In Figure 5-5 it is apparent that the AvA shows the same topographically controlled steering as the depth integrated current in Figure 5-2. The AvA is by its definition heavily influenced by the dominating current pattern.

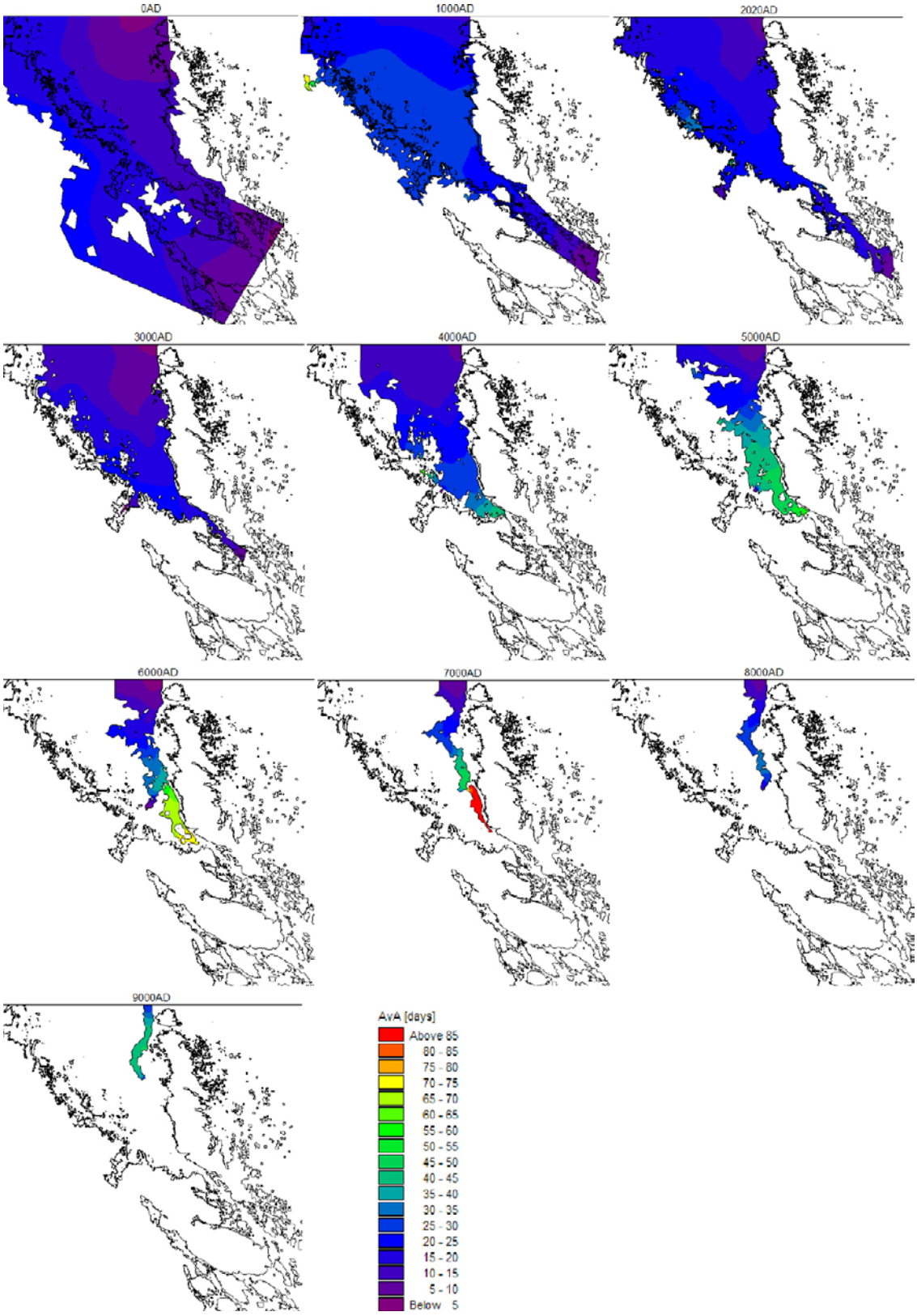

Figure 5-5. *Horizontal distribution of the vertically averaged average age for each simulated AD year.*

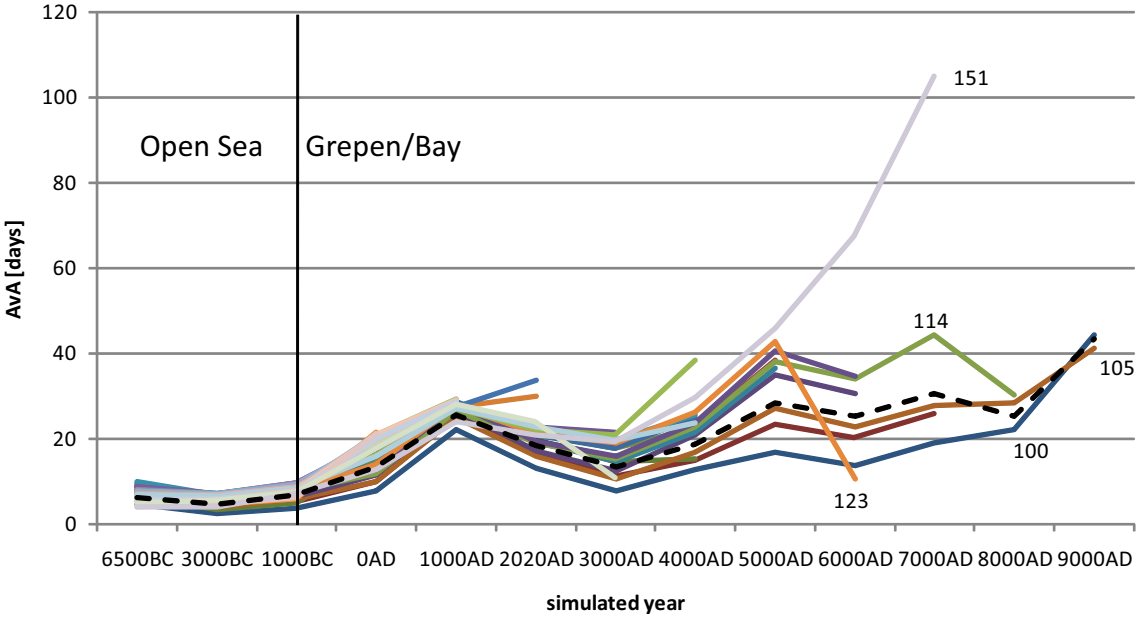

Figure 5-6. *The temporal development of AvA in each basin. Some of the curves are marked with the basin number. The black dotted line is the mean average age for all basins. For basin positions see Figure 2-2.*

The third and last stage of the Öregrundsgrepen begins in the year 4000 AD when the land has risen enough to close the southern boundary. From now on the AvA starts to increase again since exchange only can occur over the northern boundary. As an effect of the change into a one-ended system the inner parts of Öregrundsgrepen only experience very restricted water exchange.

5.3.2 Individual basins

As land rises Öregrundsgrepen becomes more enclosed and more shallow, and the importance of the open sea forcing (sea level and density variations) for the water exchange in individual basins decreases compared to local effects (wind and land runoff). During the period when the area is open-ended, the water exchange is relatively high as water can pass through Öregrundsgrepen. The shortest residence times are found in the basins close to the eastern shore, where the main flow occurs. However, as land continues to rise and the narrow Öregrundssund closes in the south, shallow embayments are formed and the water exchange is reduced. Overall, the AvA increases with time, both on the scale of individual basins and for the entire area, as individual basins become more secluded (Figure 5-5 and Figure 5-6).

When analyzing the AvA of individual basins in terms of their distance to the open sea, there is a strong co-variation. Also the mean depth of basins have been compared to AvA and show that shallow basins have higher AvA, which is not surprising as the largest flows occur in the deeper basins situated along the eastern boundary. Where the small rivers Olandsån and Forsmarksån discharge into Öregrundsgrepen, the AvA is somewhat smaller than surrounding basins. This effect of locally decreased AvA, due to freshwater input, increases with time as Öregrundsgrepen shallows. When basin volumes decrease but freshwater input remains the same, AvA becomes even more affected by land runoff.

When looking at individual basins (Figure 5-6), it is apparent that in 6000 AD the water exchange in basin 123 is much higher than it was in 5000 AD, even though the basin is more enclosed in 6000 AD. As mentioned earlier, fresh water input can have a significant effect on water exchange locally. In 5000 AD the small rivers of Olandsån and Forsmarksån have a common discharge in basin 151. In 6000 AD this discharge has moved to basin 123. At the same time basin 123 is relatively small in volume – compared to basin 151 – and the fresh water thus has a larger local effect on the AvA than for the whole of Öregrundsgrepen. The same phenomenon, though not as pronounced, occurs when a basin has a small volume but relatively large exchange with other basins (large cross-sectional area of its inter-basin connections). The opposite, when the exchange with other basins decreases but the volume in relation to the cross-sectional area of the connections increases, leads to rapidly increasing AvA. This is the case for basin 151 from 3000 AD to 7000 AD before it turns into a lake.

Table 5-3. Volume averaged AvA in days for each basin. These data are computed considering water outside Öregrundsgrepen as exogenous.

Basin	6500 BC	3000 BC	1000 BC	0 AD	1000 AD	2020 AD	3000 AD	4000 AD	5000 AD	6000 AD	7000 AD	8000 AD	9000 AD
100	5	2	3	8	22	13	8	13	17	14	19	22	44
101	7	4	5	10	25	17	11	15	24	20	26		
102	6	3	5	16	25	19	14	15					
103	8	4	6	17	26	20	16						
104	8	4	6	15	27	21	18						
105	7	4	6	10	25	16	11	17	27	23	28	28	41
106	9	5	7	16	27	21	19						
107	9	6	8	16	27	22	19						
108	9	6	8	14	28	21	18	22					
109	7	5	7	11	27	17	12	21	35	31			
110	9	6	8	13	28	19	15	22	36				
111	8	5	8	19	27	24							
112	9	6	8	14	29	21	18	25					
113	8	5	8	13	28	19	16	23	39				
114	6	5	8	12	26	19	15	23	38	34	44	30	
115	8	6	8	13	28	19	16	23	40	35			
116	10	7	9	16	28	22	20	25					
117	8	6	10	19	27	30							
118	9	7	10	19	27	34							
119	7	7	9	20	29								
120	8	7	9	20	28	23							
121	9	7	9	18	27	23	22						
122	7	6	8	21	29								
123	7	6	8	14	28	21	19	26	43	10			
124	8	7	9	19	28								
125	8	7	9	19	28								
126	8	7	9	16	27	22	21	38					
127	9	7	10	19	28								
128	7	7	9	20	29								
129	4	4	6	21									
130	7	6	8	19	28								
131	7	7	9	20	29								
132	5	6	8	21	29								
133	8	7	9	19	28								
134	8	7	9	18	28	24							
135	7	7	9	18	28								
136	7	7	9	20	29								
137	7	7	9	18	28								
138	7	7	9	18	28								
139	7	7	9	19	28								
140	7	7	9	18	28								
141	7	7	8	20	28								
142	5	5	8	21	29								
143	7	7	9	18	28								
144	7	7	9	19	28								
145	6	6	8	18	28								
146	7	6	8	16	27	23	20	23					
147	5	6	8	21	29								
148	6	6	7	20	29								
149	4	5	6	21									
150	5	6	7	18	28	24	11						
151	4	4	7	13	24	21	19	29	46	67	105		
All basins	6	5	7	13	25	19	14	20	31	30	39	26	43

Finally, it might be reasonable to expect a comparison between the modelled residence times for 2020 AD presented here and those presented in the previous study in chapter 5 of /Wijnbladh et al. 2008/. However, performing such a comparison is difficult as it is the "individual" basin AvA that is is tabulated in the previous study, i.e. the AvA for each basin considering all water outside this particular basin as exogenous, whereas in this study only water outside of Öregrundsgrepen is considered exogenous ("collective" AvA). The closest comparison to the individual AvA in the current study is the hydraulic residence time (see next section).

5.4 HRT

The annual average HRT calculated for each basin and year are shown in Table 5-4. Since the HRT is highly dependent on the relationship between basin volume and the cross-sectional areas of the basin's connections to surrounding basins, the HRT can fluctuate up and down and will not necessarily increase as the Öregrundsgrepen develops. The HRT in a basin is also insensitive to the HRT in the neighbouring basins and it is thus difficult to compare the AvA and the HRT.

A comparison between the present model results for 2020 AD and the individual AvA for 1988 tabulated in the previous study (chapter 5 in /Wijnbladh et al. 2008/) is shown in Figure 5-7. The different measures of the residence time are in general of the same magnitude with a few exceptions, namely basins 117, 118 and 150. One possible reason could be that in the present model study there is no connection between basins 117 and 118 whereas in the previous study there is. In this study basin 118 is very secluded and higher calculated HRT is to be expected. As for basin 150, it is possible that the land runoff – both Forsmarksån and Olandsån discharge into basin 150 in 2020 AD – differs between the two modelled years.

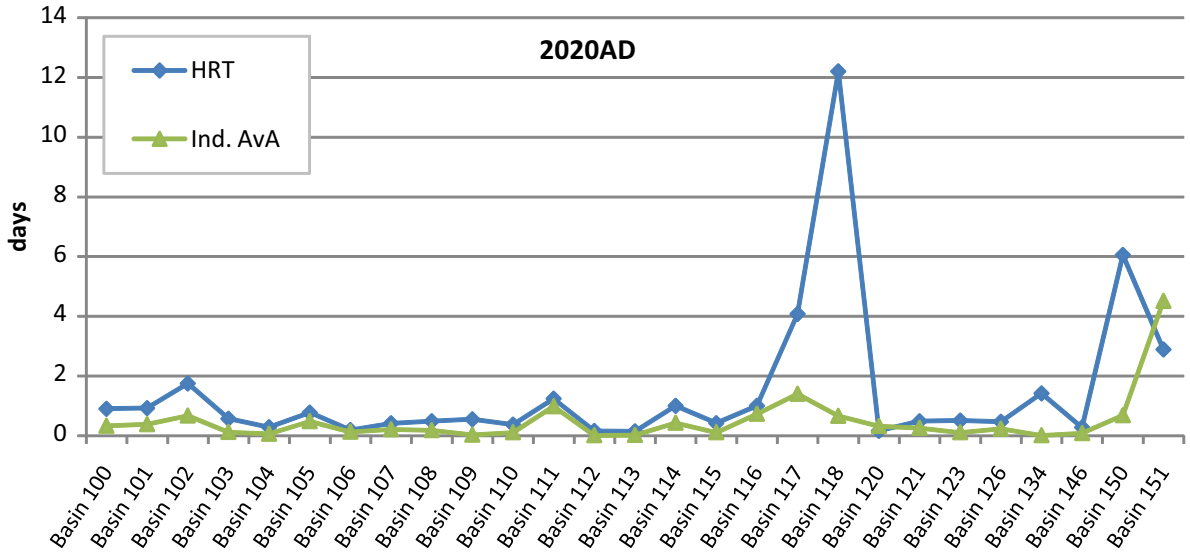

Figure 5-7. *HRT calculated in the present study for 2020 AD compared to individual AvA for 1988 tabulated in chapter 5 of /Wijnbladh et al. 2008/.*

Table 5-4. Volume averaged HRT in days for each basin. These data are computed considering water outside each basin as exogenous.

Basin	6500 BC	3000 BC	1000 BC	0 AD	1000 AD	2020 AD	3000 AD	4000 AD	5000 AD	6000 AD	7000 AD	8000 AD	9000 AD
100	1.58	1.30	1.42	0.65	1.34	0.91	0.73	0.80	2.78	3.61	5.17	14.94	21.49
101	1.77	1.36	1.30	0.94	1.50	0.93	0.74	0.60	1.44	0.56	0.30		
102	3.13	2.68	2.65	2.15	2.03	1.76	2.52	3.00					
103	1.11	1.10	1.08	0.68	0.54	0.58	42.78						
104	0.66	0.62	0.60	0.46	0.34	0.29	0.38						
105	1.47	1.11	1.13	0.68	1.12	0.78	0.66	0.69	1.54	1.36	2.16	14.79	22.45
106	0.58	0.49	0.46	0.34	0.23	0.20	0.50						
107	1.06	0.82	0.75	0.61	0.47	0.43	0.74						
108	1.07	0.78	0.73	0.63	0.62	0.50	0.65	1.12					
109	0.55	0.43	0.40	0.23	0.36	0.56	0.43	0.42	0.42	0.22			
110	0.99	0.75	0.73	0.51	0.59	0.38	0.37	0.60	18.31				
111	1.60	1.42	1.43	0.64	0.74	1.25							
112	0.36	0.29	0.28	0.20	0.25	0.17	0.23	0.37					
113	0.45	0.30	0.28	0.16	0.30	0.15	0.15	0.14	0.18				
114	1.25	0.95	0.99	0.50	0.90	1.01	1.45	1.31	2.10	3.02	12.82	19.44	
115	0.72	0.55	0.54	0.27	0.51	0.43	0.52	0.52	0.64	0.90			
116	1.51	1.28	1.33	0.96	0.97	1.01	1.51	4.52					
117	1.47	1.30	1.26	0.57	0.55	4.09							
118	0.45	0.39	0.33	0.20	0.20	19.13							
119	0.13	0.10	0.10	0.04	0.11								
120	0.57	0.49	0.50	0.24	0.28	0.17							
121	0.75	0.64	0.59	0.40	0.43	0.49	0.65						
122	0.44	0.38	0.37	0.18	0.24								
123	0.82	0.68	0.69	0.32	0.42	0.52	0.81	0.88	0.98	2.44			
124	0.17	0.15	0.15	0.08	0.10								
125	0.19	0.14	0.14	0.07	0.07								
126	0.95	0.83	0.83	0.44	0.39	0.48	0.71	8.17					
127	0.27	0.22	0.22	0.11	0.19								
128	0.11	0.09	0.09	0.04	0.05								
129	0.73	0.83	0.68	0.65									
130	0.17	0.12	0.12	0.06	0.09								
131	0.14	0.12	0.11	0.04	18.18								
132	0.47	0.32	0.32	0.17	0.48								
133	0.16	0.14	0.14	0.05	0.08								
134	0.44	0.37	0.39	0.18	0.26	1.43							
135	0.12	0.08	0.08	0.04	0.06								
136	0.45	0.38	0.39	0.17	0.28								
137	0.06	0.05	0.06	0.02	0.02								
138	0.10	0.07	0.08	0.03	0.04								
139	0.28	0.22	0.23	0.09	0.22								
140	0.10	0.09	0.09	0.03	0.03								
141	0.23	0.20	0.20	0.08	0.09								
142	0.58	0.47	0.47	0.25	0.57								
143	0.17	0.12	0.12	0.05	0.07								
144	0.29	0.21	0.21	0.08	0.12								
145	0.22	0.17	0.18	0.07	0.12								
146	0.74	0.62	0.61	0.30	0.27	0.29	0.36	1.74					
147	0.15	0.15	0.15	0.06	0.10								
148	0.63	0.52	0.56	0.21	0.35								
149	0.58	0.51	0.50	0.21									
150	1.06	0.92	1.07	0.50	1.41	6.06	4.53						
151	3.01	2.02	2.51	1.46	2.23	2.90	5.05	4.93	7.26	21.68	30.02		

6 Model validation

6.1 Baltic Sea model

The Baltic Sea model has earlier been validated against observations in the vicinity of the Stockholm archipelago by /Engqvist and Andrejev 2003/. They concluded that the model reproduced the observed salinity and temperature profiles acceptably well but with an offset in the salinity. However, the model shows an inability to maintain the salinity stratification over a period of a whole year, showing a decreasing trend that is absent in the observations /Engqvist and Andrejev 2008/. Note that the resolution of 2 nautical miles means that the model cannot be expected to correctly simulate the coastal circulation, e.g. the influence of the discharge from the river Dalälven north of Öregrundsgrepen.

6.2 Öregrundsgrepen model

A validation of the local model used for the AD years has been made for the year 2004, comparing measurements of sea level, salinity and temperature in Öregrundsgrepen with model results.

In Figure 6-1 a comparison is made between observed (SMHI, station PFM010039, SICADA_08_102) and modelled sea levels at Forsmark. The time series are well correlated (correlation coefficient 0.89) but in general the modelled sea level is somewhat lower than the observed. The root mean square error is 12.5 cm and the maximum difference is –44 cm. When comparing the modelled sea levels and the sea levels from the Baltic model used as forcing, it becomes clear that the forcing data produces the offset. Öregrundsgrepen responds quickly to sea level variations at the north boundary and the modelled levels at Forsmark are a direct reflection of the forcing data. Overall there is a reasonable correspondence between modelled and measured data and this implies that the circulation due to sea level variations is modelled realistically.

Figure 6-2 and Figure 6-3 compare modelled and measured temperatures and salinities (SMHI station Fo13, SICADA station ID PFM002655, SICADA_08_101), forcing data from the Baltic Sea model and data from the Water Forecast (DHI's operational model for the Baltic Sea).

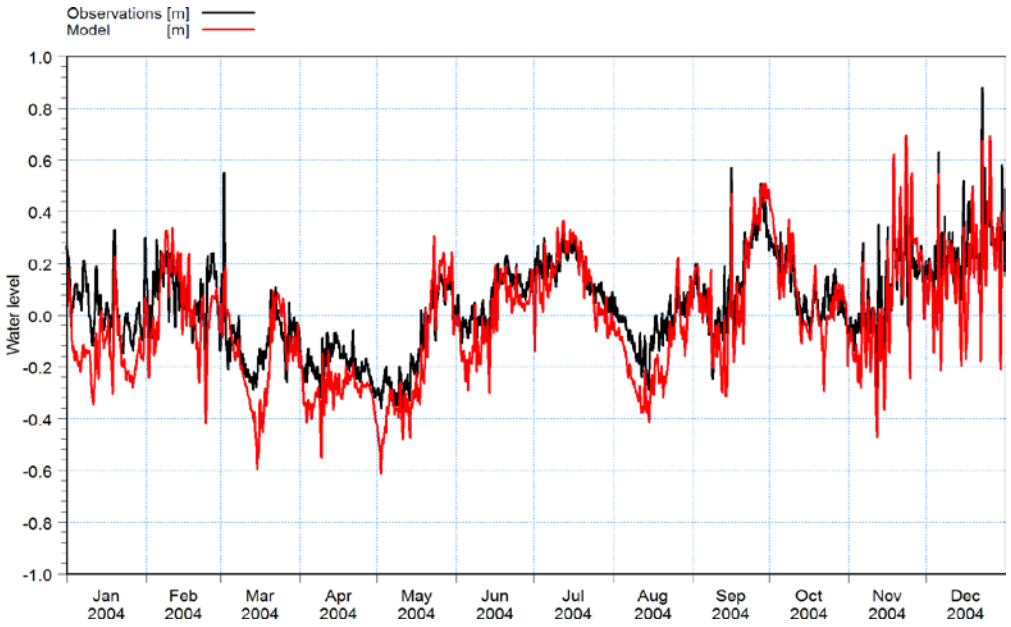

Figure 6-1. *Observed (SMHI) and modelled sea levels at Forsmark.*

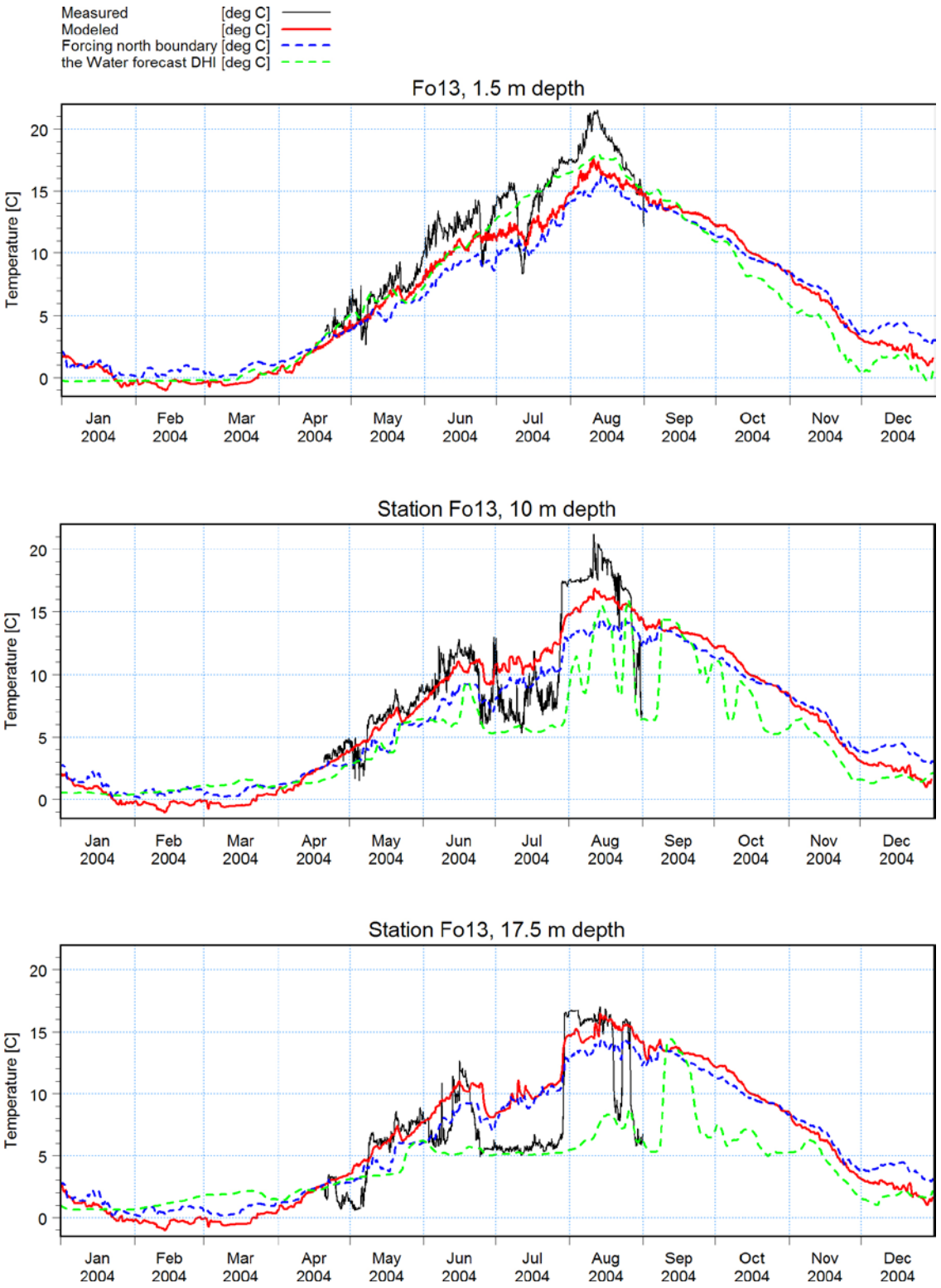

Figure 6-2. *Observed and modelled temperatures at station Fo13 compared to the forcing temperature at the north boundary, as well as corresponding temperatures produced by the Water Forecast model.*

Figure 6-2 compares modelled (red line) to observed (black line) temperature at the station Fo13 at three different depths. The correspondence between measured and modelled temperature data is acceptable. In summer, however, particularly near the surface (1.5 m), the model underestimates the observed temperature.

At the two deeper levels there is a marked decrease in temperature by the end of June which remains for the whole of July. This could be an effect of so called upwelling, meaning that colder water from deeper levels in the Baltic is shifted upwards to the surface near the coast, often as a result of wind-induced transport of surface water out from the coast. The model does not fully capture the upwelling of cold water in July. Since the upwelling is unlikely to be an effect caused by local factors in Öregrundsgrepen, the lack of response in the local model is due to the weak signal in the forcing data, as shown by the dashed blue line in Figure 6-2.

The temperatures calculated by the Water Forecast model (dashed green line) show a somewhat better agreement with the measured temperatures, compared to the forcing from the Baltic Sea model, for the near-surface temperature and for the upwelling event. However, the Water Forecast model often underestimates the temperature at the two deeper levels.

The model consistently overestimates the salinity in Öregrundsgrepen (see Figure 6-3). There is an offset between modelled and observed salinities of more than 0.5 psu. However, the modelled variability agrees reasonable well with the observed variability. The modelled data correlates well with the forcing on the northern boundary but the forcing has a higher mean salinity than that observed inside Öregrundsgrepen. There appears to be a somewhat better match between measured salinity and the salinity modelled by the Water Forecast model at the deeper levels, as the Water Forecast model generally produces lower salinities. On the other hand, the Water Forecast model clearly underestimates the surface salinity.

Hence, either the local model does not correctly describe how the salinity at the open boundary penetrates into Öregrundsgrepen or the forcing boundary salinities produced by the Baltic Sea model are too high. To ensure that no mistakes have been made, the forcing data on the boundary has been compared to the files originating from the Baltic Sea model. No errors due to data treatment were found. In the previous study /Engqvist and Andrejev 2008/ no large offset between modelled and observed salinities was found at station Fo13. On the other hand, the model results of /Engqvist and Andrejev 2008/ close to the boundary (station Fo11) , which to some degree should reflect their boundary conditions, is on a significantly lower level than the forcing data DHI received (compare Figure 3-4 in /Engqvist and Andrejev 2008/ with Figure 6-3).

According to Anders Engqvist the forcing data for the local MIKE 3 Öregrundsgrepen model used in this study was produced by running a new simulation with the Baltic Sea model, in which the Mueller meteorological data set was used instead of the Mesan data set used previously for 2004 /Engqvist and Andrejev 2008/. This could indicate that the stratification computed by the Baltic Sea model in the vicinity of Öregrundsgrepen is sensitive to the meteorological forcing. However, the modelled salinities presented in /Engqvist and Andrejev 2008/ at Fo11 do not explicitly represent the forcing used, particularly during periods of northerly flow (out from the local model), and thus it remains to be seen whether the boundary forcing really does differ between this study and previous studies by Engqvist and Andrejev.

To summarize, the model results are in good agreement with observed sea levels and temperatures. The agreement is not good when comparing modelled and observed salinities, but the discrepancy is mainly an almost constant offset. The model captures most of the variability in the observations. Since it is the differences in the density stratification – and not the absolute values – that produce water movement, the model is expected to produce realistic estimates of the water exchange. It should be mentioned that there are questions about the quality of both measurements /Engqvist and Andrejev 2008/ and the forcing data from the Baltic Sea model (see section 6.1). Hence, it is difficult to quantitatively determine the quality of the local model, particularly as it is very much dependent on the quality of the forcing.

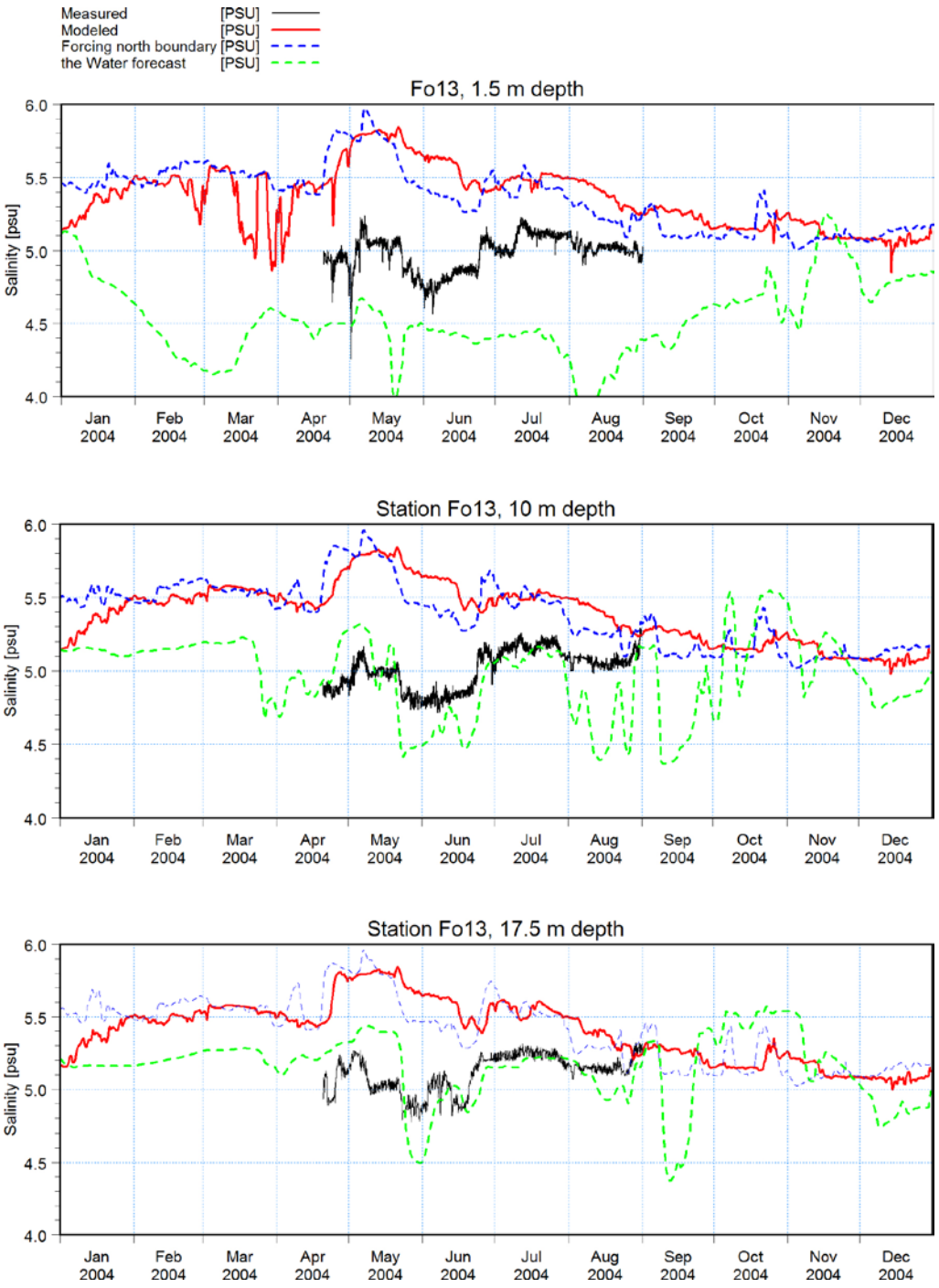

Figure 6-3. *Observed and modelled salinity at station Fo13 compared to the forcing salinity at the north boundary as well as corresponding salinities produced by the Water Forecast.*

7 Sensitivity analysis

7.1 BC model

No sensitivity analysis has been performed for the Baltic Sea model as part of the present study, as it was outside the scope of the project. However, the actual method for interpolating the modelled currents to the basin connections and solving the differential equations for the AvA has been checked for sensitivity to different numerical parameters. No significant sensitivity has been discovered and the results appear robust in this respect.

7.2 AD model

The sensitivity of the MIKE 3 model set up for Öregrundsgrepen to the different driving forces has been tested by varying the forcing parameters that control the hydrodynamics. Simulations of two separate years in the evolution of Öregrundsgrepen have been used to illuminate the differences in dynamics when the area transforms from having two connections with the open Baltic to becoming an enclosed bay. The two years used are 2020 AD and 5000 AD. For these two years four sets of model runs have been performed. The four different runs examine the effect of wind forcing, river runoff, sea level variations and salinity stratification by removing one forcing in each run. All runs with changed forcing have been related to the original reference run for comparison.

Changes in water exchange are discussed both for the entire Öregrundsgrepen area and for a few selected basins. For the entire Öregrundsgrepen area the horizontal distribution of the AvA is presented, derived by averaging the model results over the entire water column for each computational cell in the horizontal, comparable to the AvA presented in Figure 5-5. For the selected basins, the temporal development of the volume averaged age tracer is analyzed. As the AvA is defined as a temporal average, this time varying average over each basin volume is termed the volume averaged age of the water.

7.2.1 Wind forcing

When wind forcing is removed from the 2020 AD simulation, the model yields much higher AvA in the shallower parts of the area. As can be seen from Figure 7-1, AvA for the whole western part of Öregrundsgrepen is some 30–60% higher than in the case with wind forcing. For the deeper parts of Öregrundsgrepen this is not as prominent as in the shallower areas, which is due to the fact that wind forcing is relatively more important in shallow areas. In the north-eastern part of Öregrundsgrepen, an area with reduced AvA is found. Such a change is probably caused by altered current pattern both in the east-west direction and over the boundaries when wind forced currents are removed.

Removing wind forcing when Öregrundsgrepen is an enclosed bay in 5000 AD (see Figure 7-2) produces noticeable and even larger changes for the area as a whole than in 2020 AD. The effect of the wind is readily illustrated by the increase in AvA both in the southern and northern parts of the bay. Also, east-westerly gradients are more pronounced in the case without wind.

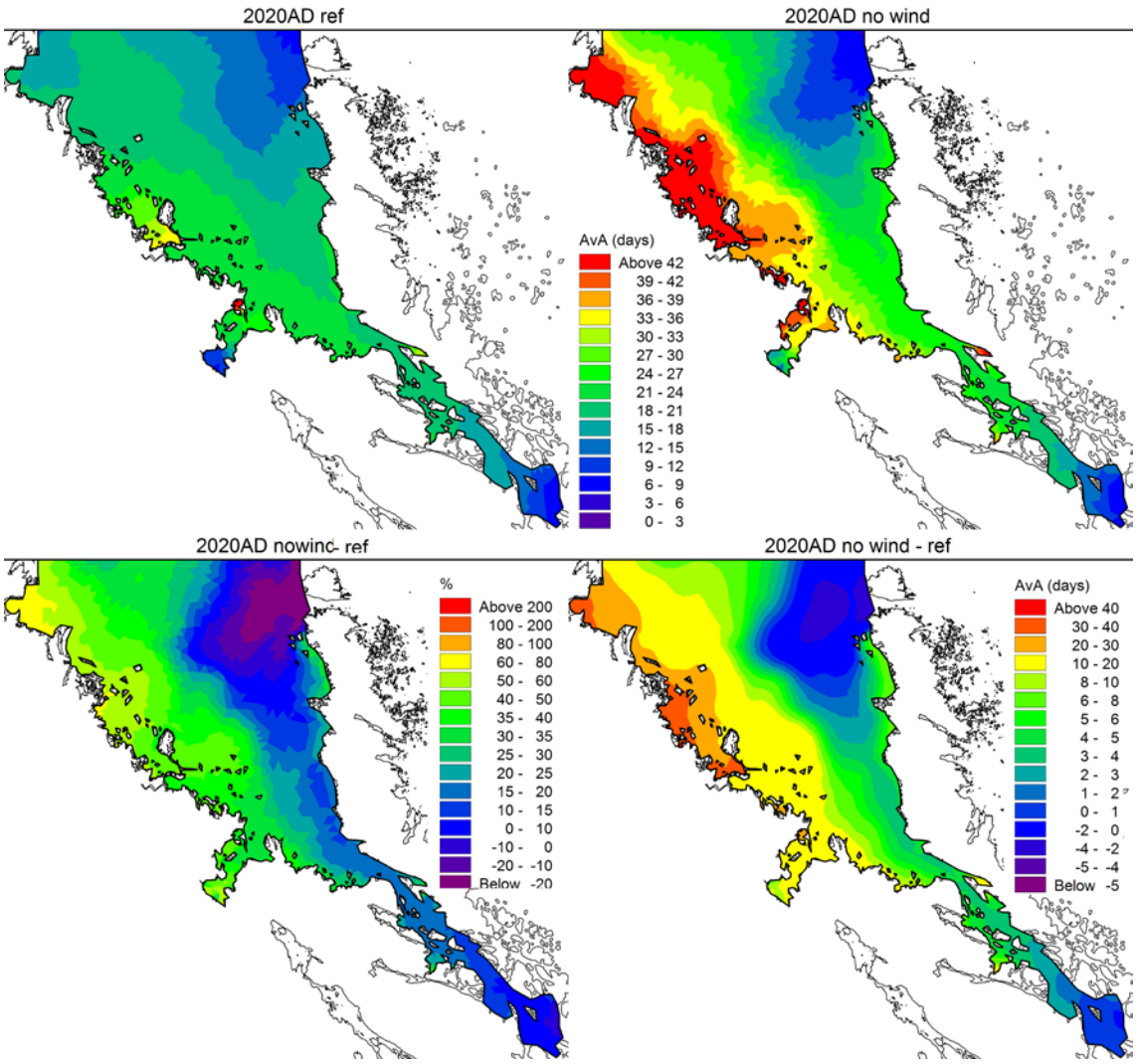

Figure 7-1. *Horizontal distribution of vertically averaged AvA in 2020 AD: the reference run (upper left), the zero wind run (upper right), the difference in percent (lower left) and in days (lower right). Positive values signify higher AvA in the zero wind run.*

7.2.2 Sea level variations

When the sea level variations at the boundaries are removed, i.e. the sea level is fixed at a constant value, the normal southward net through-flow is removed. Instead of a net flow out through the south boundary of some 200 m^3/s there is now a net flow into Öregrundsgrepen of about 150 m^3/s. This results in higher AvA in the northern and deeper parts of Öregrundsgrepen and lower in the southern strait (Figure 7-3). It is apparent that circulation is dominated by the wind in the western parts while the eastern parts are more influenced by sea level differences.

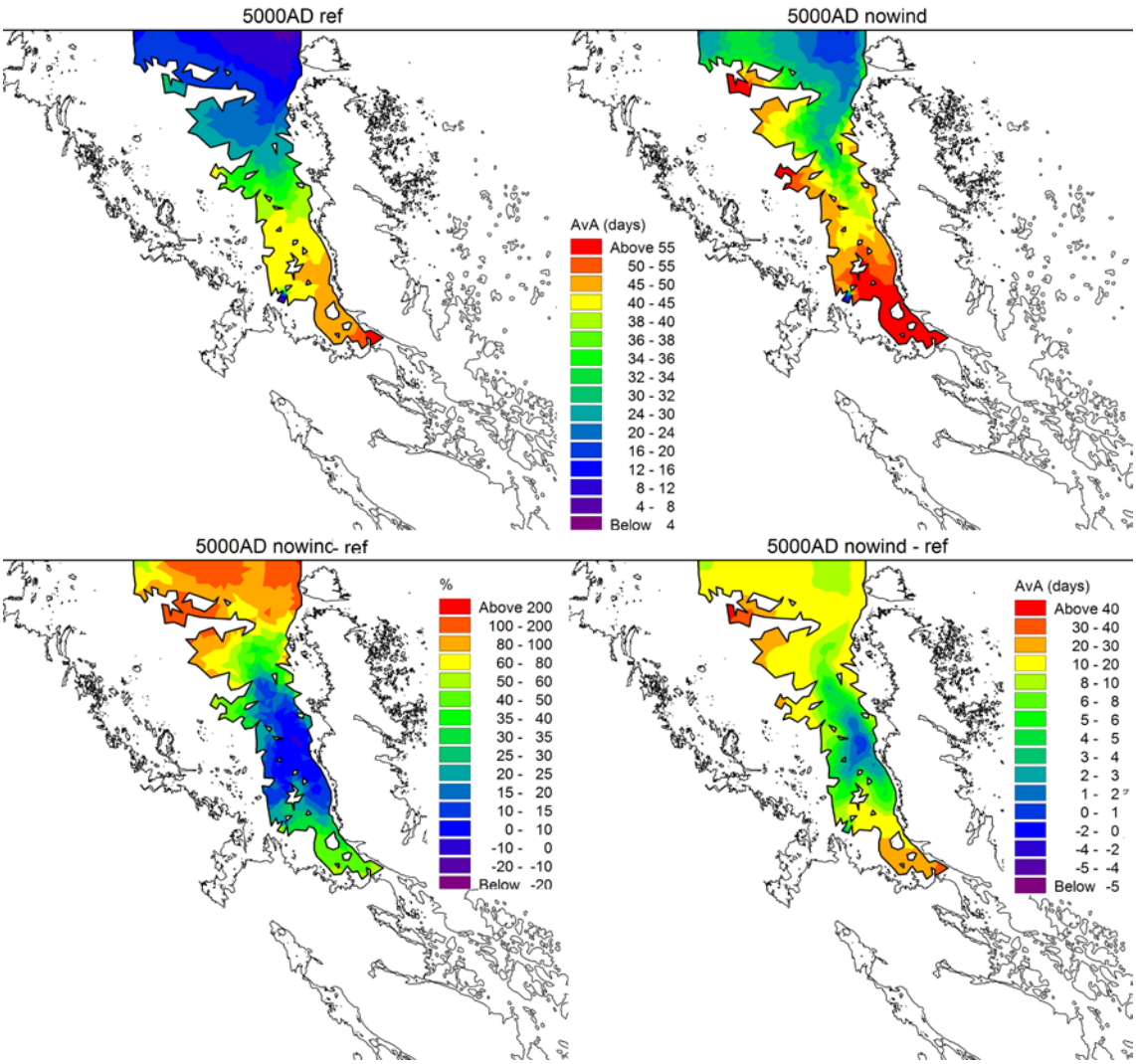

Figure 7-2. *Horizontal distribution of vertically averaged AvA in 5000 AD: the reference run (upper left), the zero wind run (upper right), the difference in percent (lower left) and in days (lower right). Positive values signify higher AvA in the zero wind run.*

The effect of removing sea level variations in 2020 AD can be interpreted as hindering the exogeneous water from entering Öresundsgrepen. Without barotropic pressure gradients acting on the water only density differences and wind induced currents produce exchange. The baroclinic effects are weak in this area due to the generally weak vertical density stratification and cannot penetrate all the way to the inner parts of the area as effectively as barotropically forced currents. Also due to the increased importance of baroclinic effects the southern boundary is now more active in the water budget than when the barotropic effects are included.

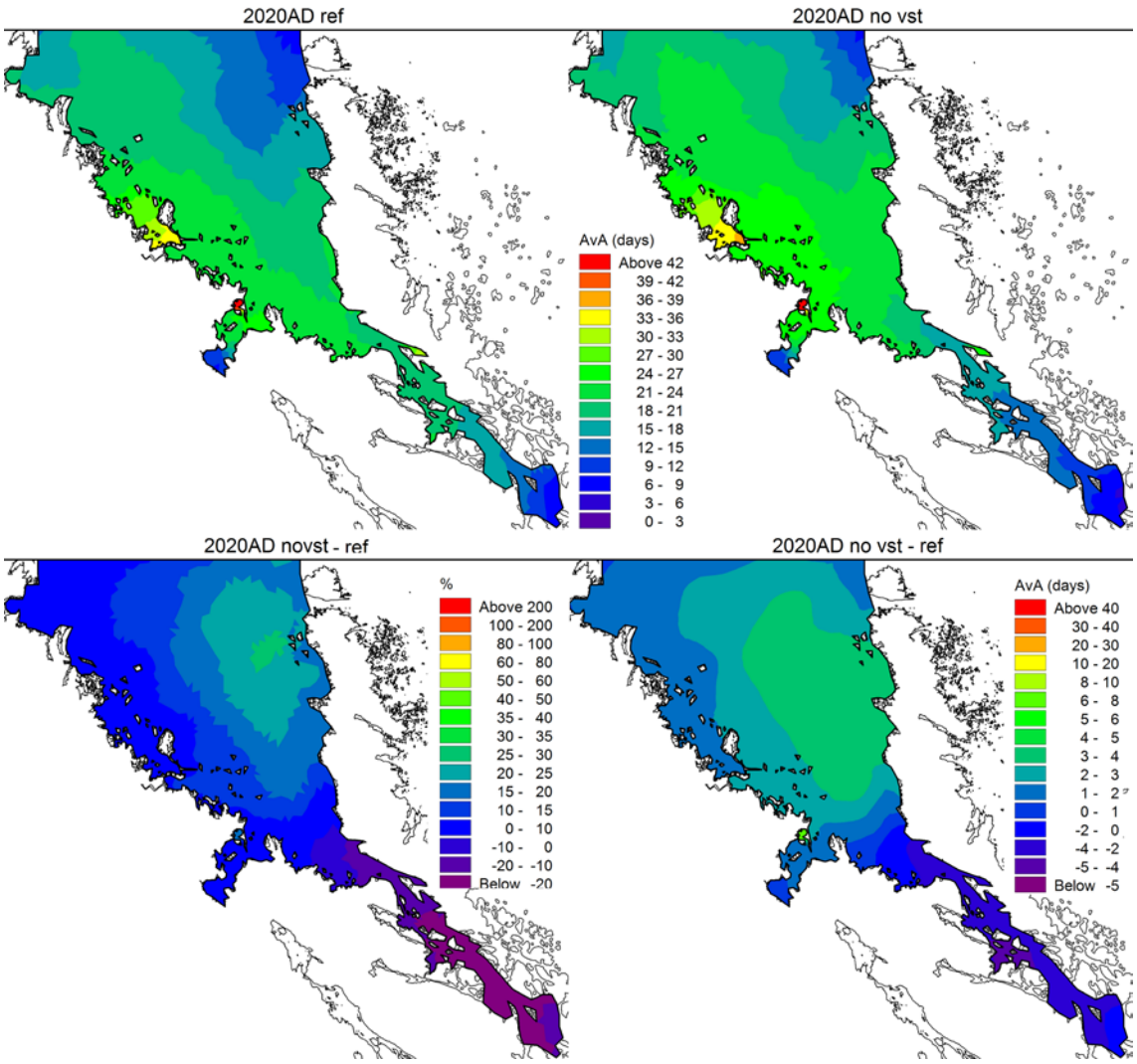

Figure 7-3. *Horizontal distribution of vertically averaged AvA in 2020 AD: the reference run (upper left), the run with constant sea level (upper right), the difference in percent (lower left) and in days (lower right). Positive values signify higher AvA in the run with constant sea level.*

Sea level variations at the northern boundary are of less importance when Öregrundsgrepen has turned into a bay (Figure 7-4). This is primarily due to the fact that sea level differences between the boundary and the inner parts of the bay are rapidly equalized, as the sea level signal travels quickly into the bay in the form of a long wave. This equalizing requires very little volume transport if the sea level difference is small. In the case of an open-ended system the sea level difference is maintained by exterior factors.

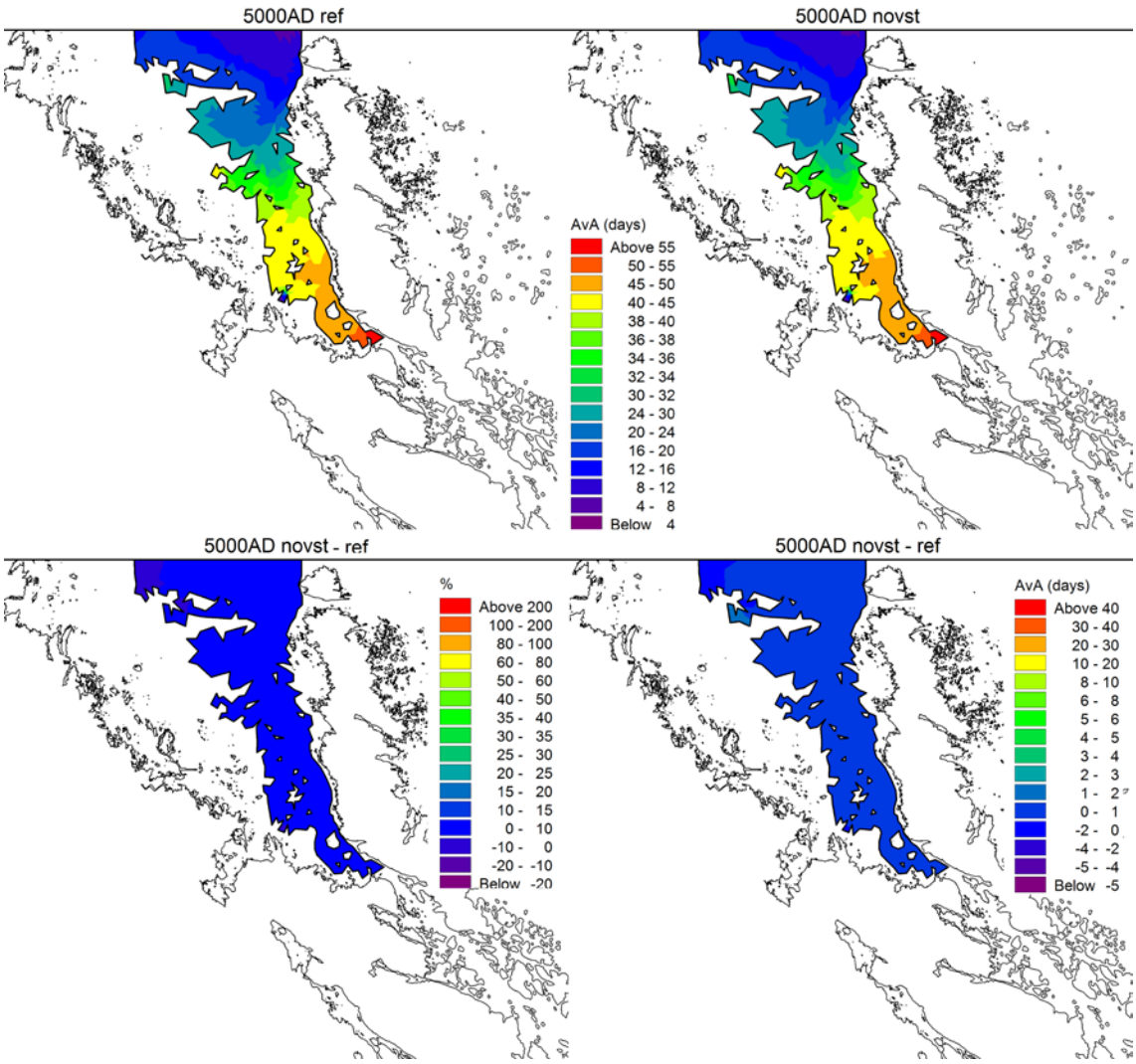

Figure 7-4. *Horizontal distribution of vertically averaged AvA in 5000 AD: the reference run (upper left), the run with constant sea level (upper right), the difference in percent (lower left) and in days (lower right). Positive values signify higher AvA in the run with constant sea level.*

7.2.3 Local river runoff

The effect of removing the local river runoff of Olandsån och Forsmarksån is barely identifiable in the larger parts of Öregrundsgrepen in 2020 AD. As can be interpreted from Figure 7-5, the relative and absolute differences with or without river runoff are very small. The only exception is in the basin where the rivers are situated. This basin changes dramatically from being a generally well ventilated area to an area with very restricted exchange. Land runoff is very important in a small and enclosed basin but negligible for the area as a whole in 2020 AD.

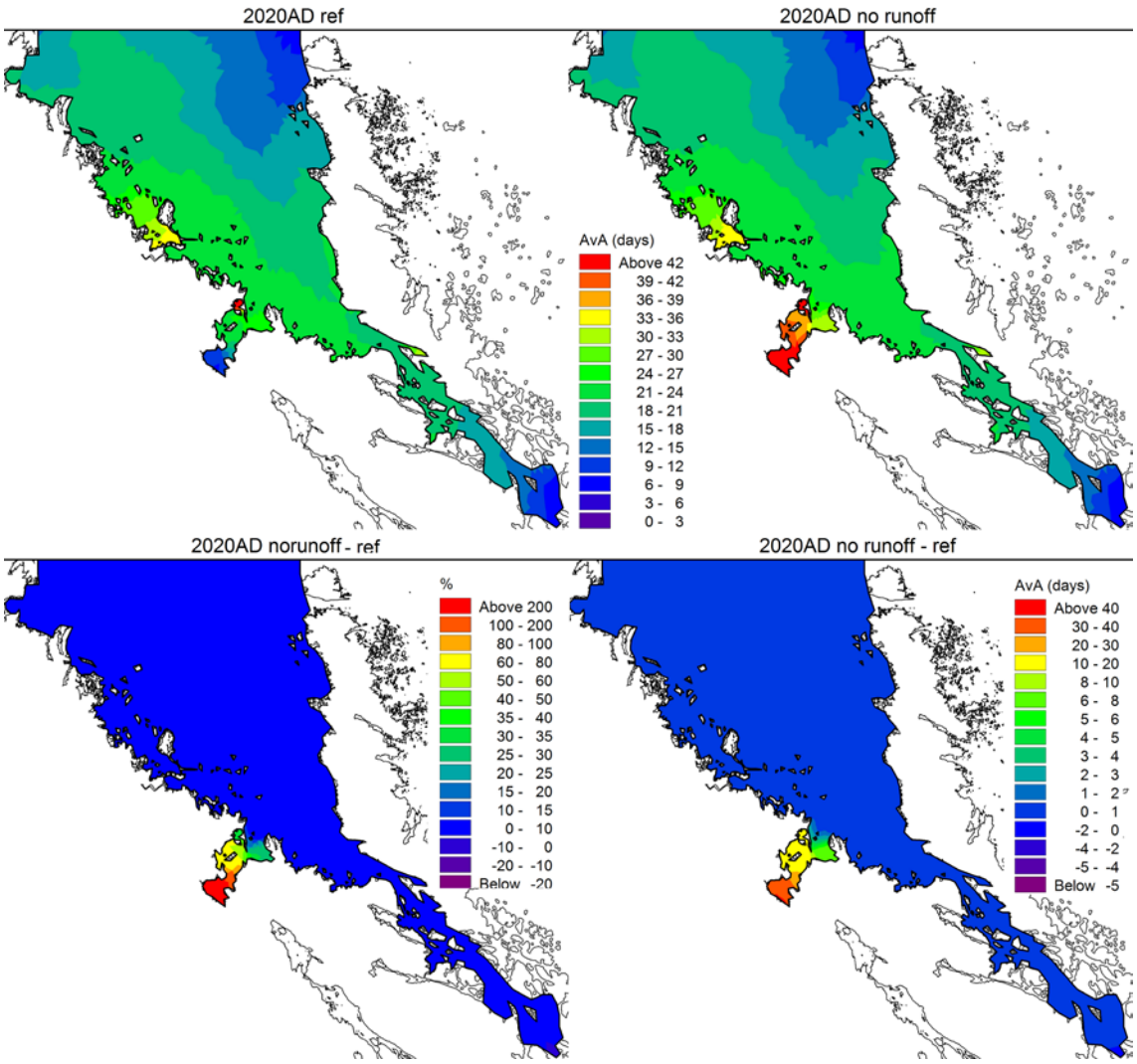

Figure 7-5. *Horizontal distribution of vertically averaged AvA in 2020 AD: the reference run (upper left), the run with no runoff (upper right), the difference in percent (lower left) and in days (lower right). Positive values signify higher AvA in the run with no runoff.*

In 5000 AD the removal of local river runoff affects the AvA in most of the inner parts of Öregrundsgrepen (Figure 7-6). The combined water volume in the area is now much smaller and there is no net through-flow. The largest increases in AvA are found close to the river mouths but extend towards both the north and the south. In the southern half of the bay the AvA increases by about 25% corresponding to about 10 days.

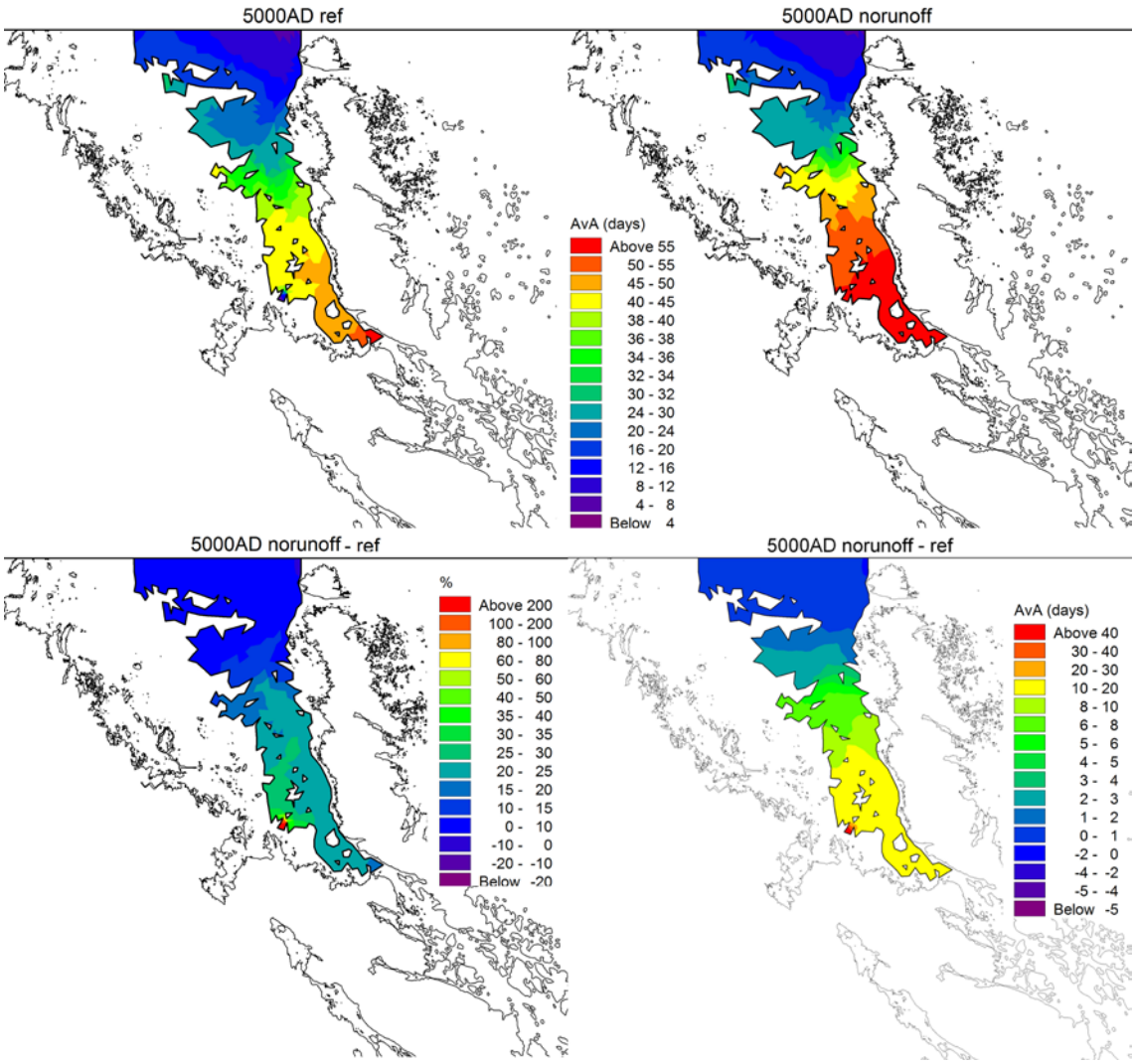

Figure 7-6. *Horizontal distribution of vertically averaged AvA in 5000 AD: the reference run (upper left), the run with no runoff (upper right), the difference in percent (lower left) and in days (lower right). Positive values signify higher AvA in the run with no runoff.*

7.2.4 Salinity stratification

When the 2020 AD model no longer is forced with vertical salinity variations but still varies in time, no great differences can be seen (Figure 7-7). The relatively small increases in AvA are in the order of 4–10% relative to the reference run and occur in the shallower parts of the area. The small effect that results from running the model without salinity stratification is partly due to the weak density contrast in the area. In short, the baroclinic forcing only has a limited influence on the exchange. If a stronger salinity gradient had been removed larger differences would have been expected.

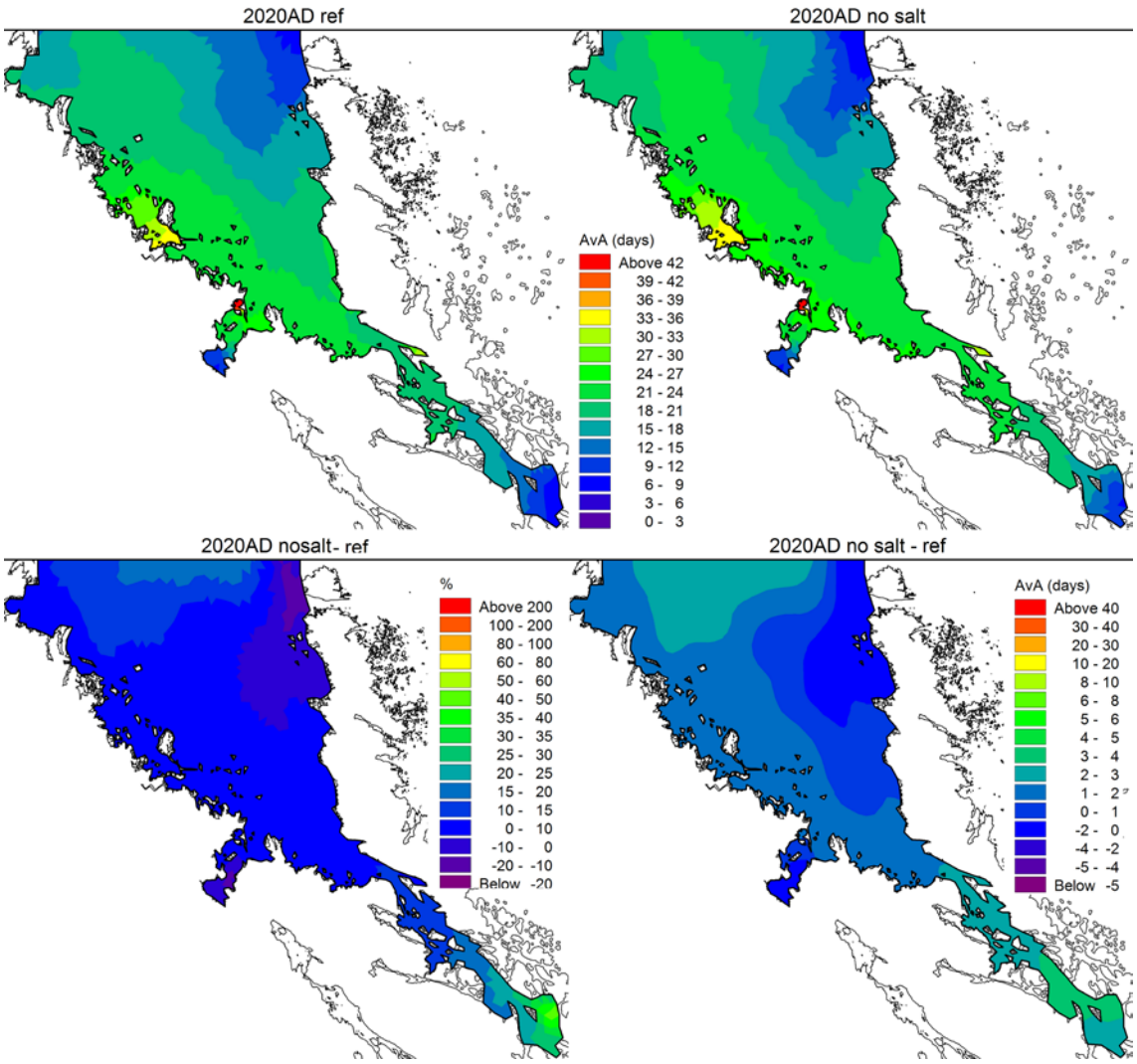

Figure 7-7. *Horizontal distribution of vertically averaged AvA in 2020 AD: the reference run (upper left), the run with no salinity stratification (upper right), the difference in percent (lower left) and in days (lower right). Positive values signify higher AvA in the run with no salinity stratification.*

Salinity variations become more important when Öregrundsgrepen has turned into a bay (see Figure 7-8). Baroclinic effects now dominate the water exchange since the importance of the barotropic forcing has been greatly reduced. For the inner parts of Öregrundsrepen, AvA is increased by 20% when the salinity stratification is removed. The bay behaves more like an estuary, with a circulation driven by the density difference between more saline deep water on the boundary and fresh water influenced surface water inside.

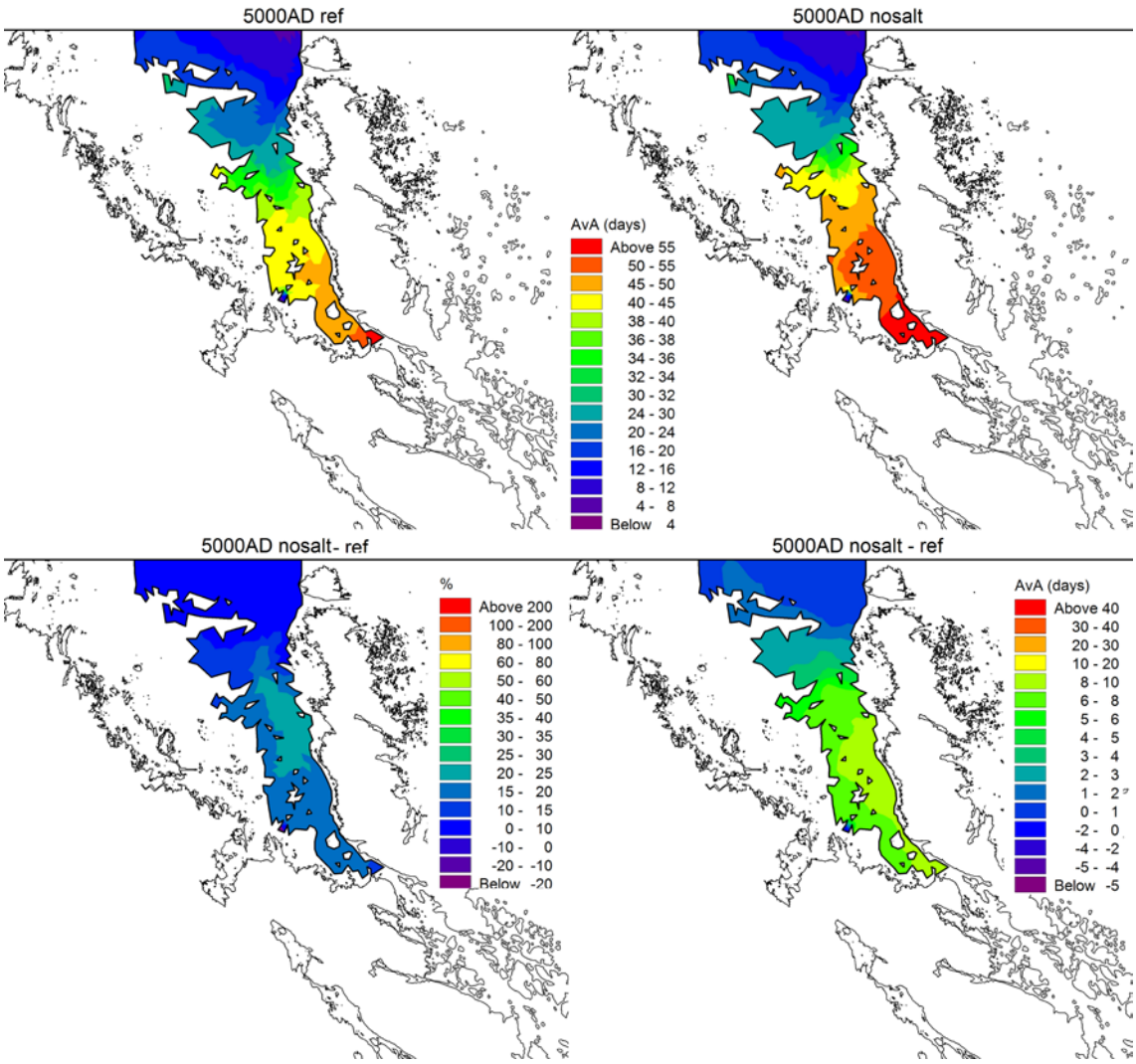

Figure 7-8. *Horizontal distribution of vertically averaged AvA in 5000 AD: the reference run (upper left), the run with no salinity stratification (upper right), the difference in percent (lower left) and in days (lower right). Positive values signify higher AvA in the run with no salinity stratification.*

7.2.5 Basin 103

Basin 103 is shallow and situated at the north-western boundary.

In 2020 AD basin 103 is relatively insensitive to all of the prescribed forcing changes except for removing the wind (Figure 7-9). When the wind is set to zero the AvA continues to increase after the general spin up time that is common for the other forcing changes. The location and characteristics of basin 103 makes it sensitive to wind generated mixing and water exchange, which is reflected in the age development of the water.

Basin 103 is above sea level in 5000 AD.

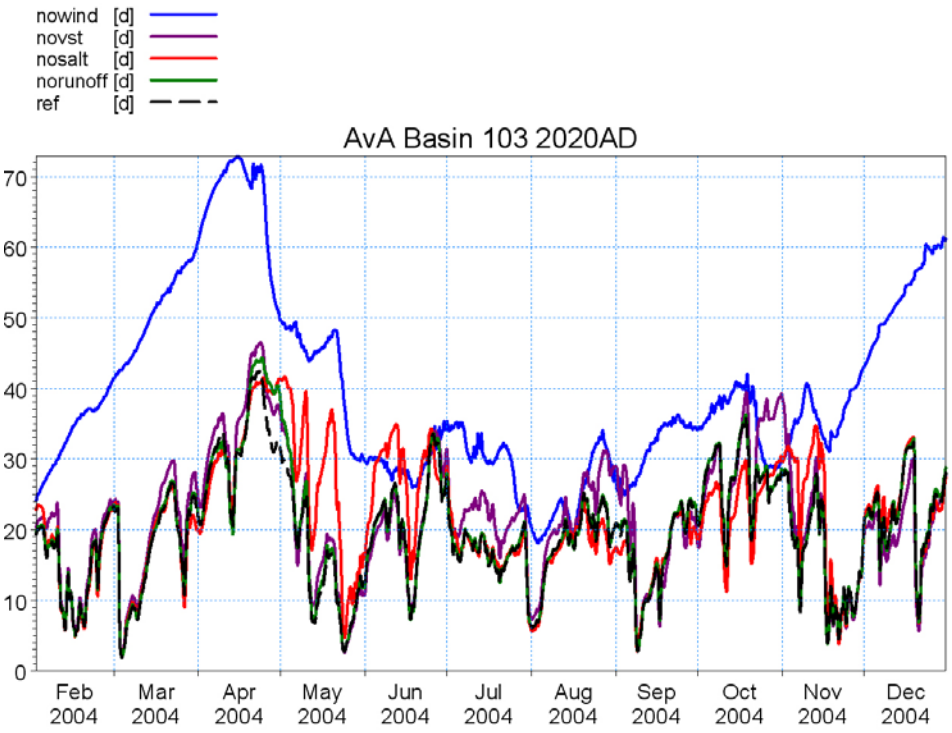

Figure 7-9. *Time series of the volume averaged age for Basin 103 in 2020 AD. Black line is the reference run, blue line is with zero wind, purple line is with constant sea level, red line is with no salinity stratification, and green line is with no river runoff.*

7.2.6 Basin 105

Basin 105 is situated on the north eastern boundary and includes both the deepest part of Öregrundsgrepen as well as more shallow areas.

In 2020 AD this basin, due to it being situated near the open boundary, is strongly influenced by all forcing factors except for river runoff (Figure 7-10). Wind dominates the upper layers while sea level changes dominate the deep water. From the individual mean basin flows it is found that 60% of the northward flow into basin 105 is lost when the wind is set to zero. Similarly, 40% of the mean southward flow is removed when sea level variations are removed. It is difficult to describe in general how the basin is influenced by different forcing factors. Some months show reduced exchange when a particular forcing is removed while other months show the opposite. The relative importance of a particular forcing appears to be seasonally dependent. It is however apparent that large differences in the water age relative to the standard run occur during all parts of the year when removing forcing due to wind, salinity stratification and sea level changes.

In 5000 AD basin 105 has shrunk noticeably and many characteristics of Öregrundsgrepen have changed. Sea level variations are no longer important for the exchange, as discussed earlier (Figure 7-11). River runoff and salinity stratification are important during late spring while the removal of wind forcing seems to induce generally lower water exchange (greater age) throughout the year.

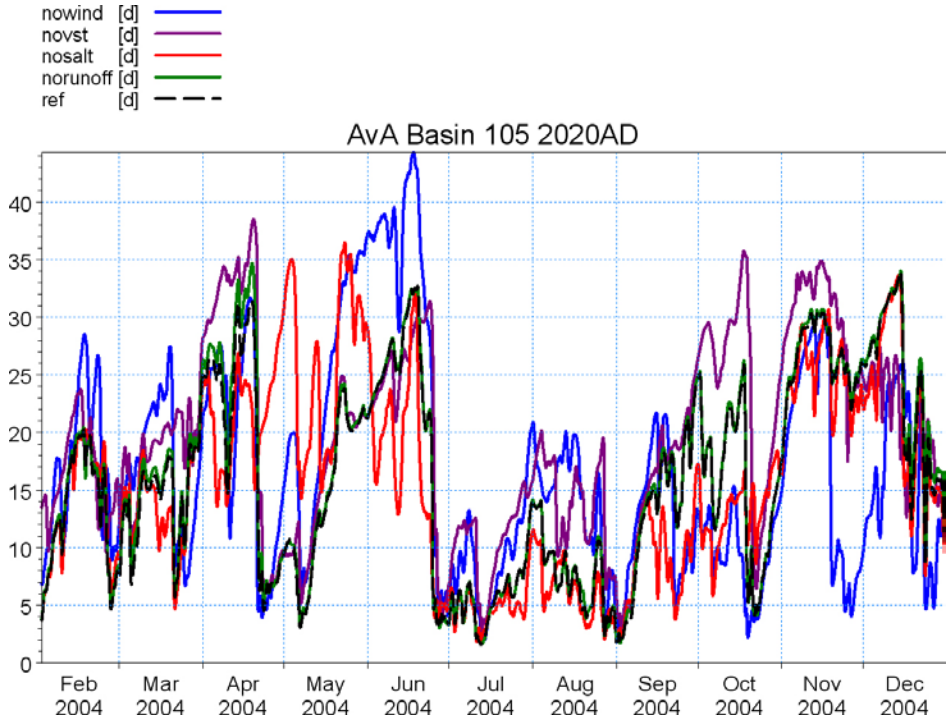

Figure 7-10. *Time series of the volume averaged age for Basin 105 in 2020 AD. Black line is the reference run, blue line is with zero wind, purple line is with constant sea level, red line is with no salinity stratification, and green line is with no river runoff.*

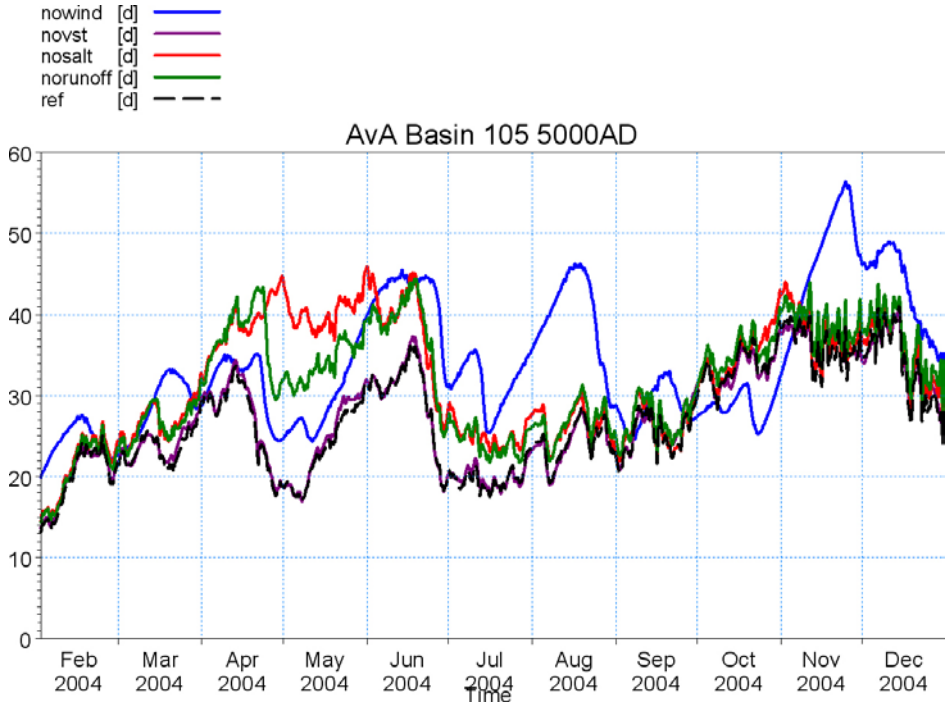

Figure 7-11. *Time series of the volume averaged age for Basin 105 in 5000 AD. Black line is the reference run, blue line is with zero wind, purple line is with constant sea level, red line is with no salinity stratification, and green line is with no river runoff.*

7.2.7 Basin 118

This basin is located centrally near the western shoreline and is a shallow area inside an archipelago.

In 2020 AD the exchange in basin 118 is dominated by the local wind (Figure 7-12). All other changes relative the reference run are small in comparison.

Basin 118 is above sea level in 5000 AD.

7.2.8 Basin 151

This basin is the southernmost basin and includes both deep and shallow areas. In 2020 AD the basin also includes the southern open boundary.

In 2020 AD (Figure 7-13) the age of the water increases when the wind is removed, probably due to water of greater age entering the basin from the northwest. Neither sea level variations nor river runoff have any major influence on the water exchange. During late spring there is an increase in the water age for the simulation without salinity stratification, indicating some influence from the baroclinic forcing on the open boundaries.

In 5000 AD the age of the water in basin 151 is largely determined by density differences (Figure 7-14). Density differences are caused by river runoff and salinity stratification on the open boundary, and are influenced by wind mixing. As in the case of basin 105, the sensitivity to changes in salinity stratification and river runoff is greater during the first half of the year, while removing the wind influences the water exchange mainly in the summer and winter.

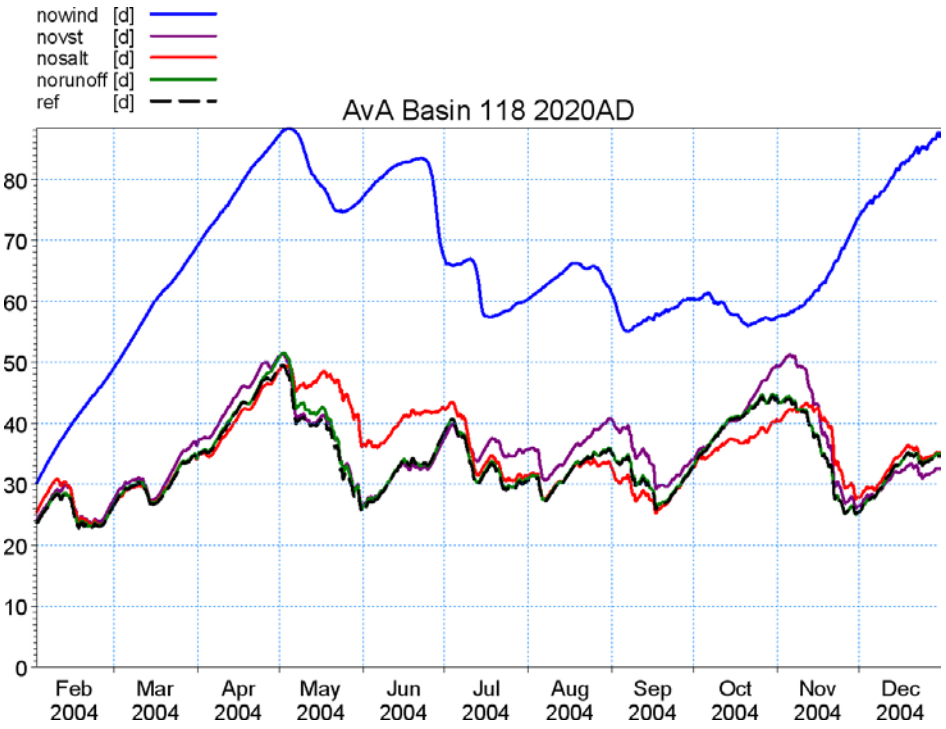

Figure 7-12. *Time series of the volume averaged age for Basin 118 in 2020 AD. Black line is the reference run, blue line is with zero wind, purple line is with constant sea level, red line is with no salinity stratification, and green line is with no river runoff.*

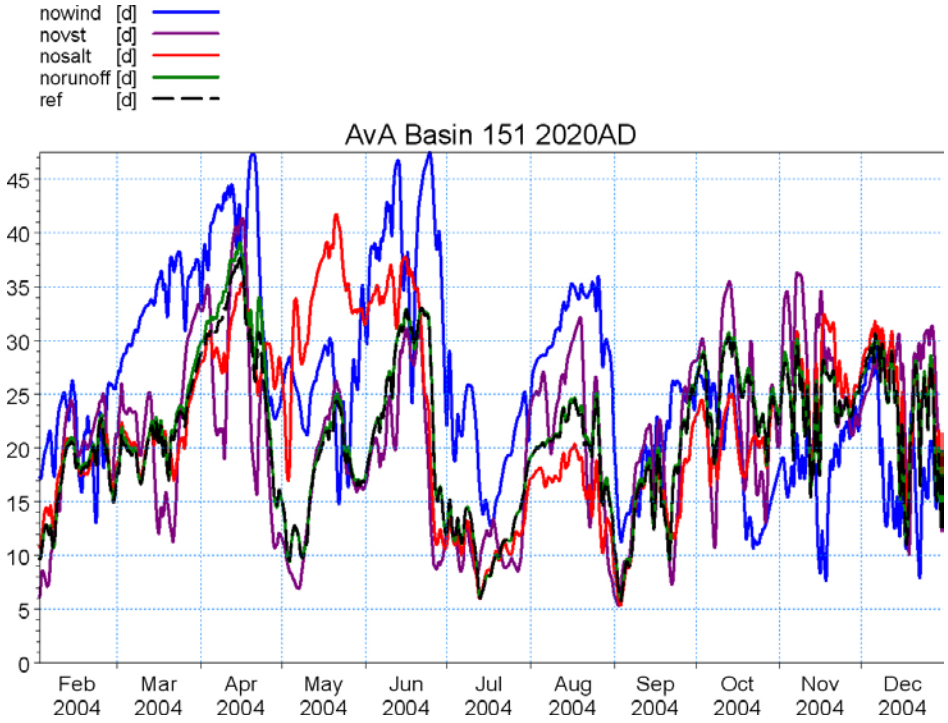

Figure 7-13. *Time series of the volume averaged age for Basin 151 in 2020 AD. Black line is the reference run, blue line is with zero wind, purple line is with constant sea level, red line is with no salinity stratification, and green line is with no river runoff.*

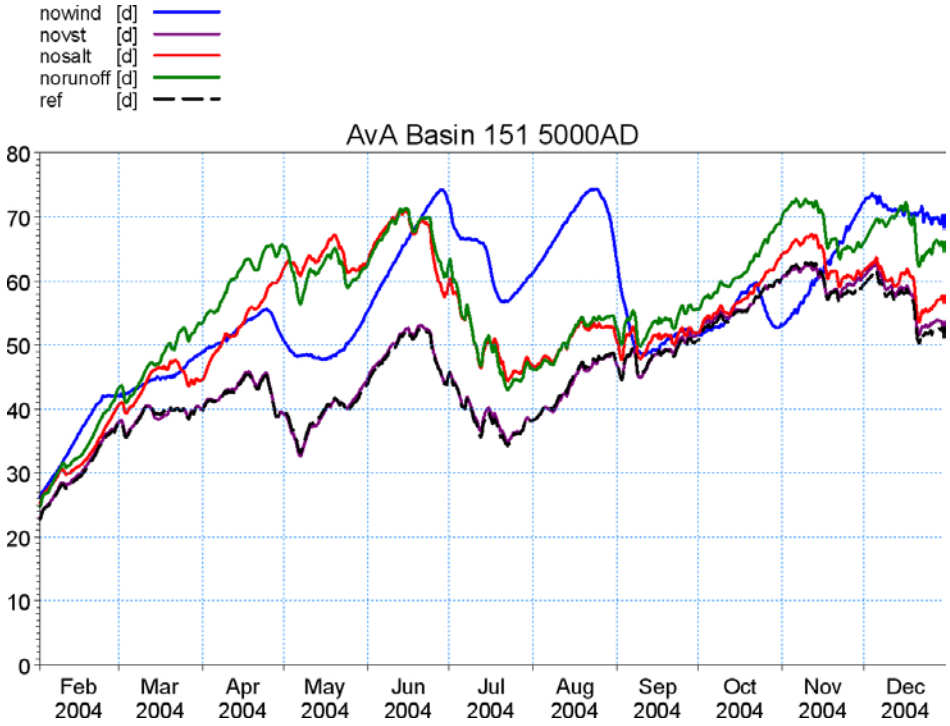

Figure 7-14. *Time series of the volume averaged age for Basin 151 in 5000 AD. Black line is the reference run, blue line is with zero wind, purple line is with constant sea level, red line is with no salinity stratification, and green line is with no river runoff.*

7.3 Future climate scenarios

Future changes in climate have the potential to alter the water exchange characteristics of the Forsmark area /The BACC Author Team 2008/. Given the long time period that is being considered it is difficult to estimate how much relevant parameters will change. In a recent study /Kjellström et al. 2009/, estimates of variations in the parameters temperature, precipitation and runoff are presented for a 100,000-year perspective. Three scenarios have been simulated. However, only the warm scenario is applicable to the present study, as the other two scenarios describe a much cooler climate in which Öregrundsgrepen is either covered by an ice sheet or is located above sea level (permafrost scenario).

The warm scenario roughly corresponds to a climate a couple of thousand years in the future, which is partly the rationale for doing the sensitivity analysis for the year 5000 AD. In the climate study, the results for the warm scenario show an increase in air temperature of 3.6°C and an increase in runoff of 21% for the Forsmark area. As the authors discuss, this falls within the range of the scenarios produced for the late 21st century. Consequently the sensitivity analysis in the present study was also carried out for present-day conditions, i.e. 2020 AD.

Changes in air temperature have not been considered in the sensitivity analysis in the previous section. A higher air temperature would affect the heat exchange between the sea and the atmosphere. However, it is the temporal and spatial variations that influence the water exchange. The average temperature change is thus not expected to be of large importance to the exchange, unless it in turn affects the variability. A temperature change of 3.6°C has approximately the same effect on the density as a salinity difference of about 0.7 psu. As discussed below, the Baltic Sea salinities may very well change more than this over long time scales, as it has in the past /Gustafsson and Westman 2002/. However, the temperature signal is expected to be manifested in winter, resulting in a new seasonal cycle that approximates the present-day period March-November. In short, present-day winter conditions would no longer exist.

Examining the monthly evolution of the volume averaged age in Figure 7-11 and Figure 7-14 shows no clear indication that the winter months February and December are different in terms of water exchange. The low values in February are probably a result of spin-up, i.e. the model does not spin up as quickly in the year 5000 AD as in 2020 AD. Hence, it would seem that differences in the average air temperature does not create large changes in the average water exchange. It should be mentioned that the model does not include ice. It would be reasonable to assume that ice cover during the winter would reduce the influence of the wind, reducing water exchange. Less ice in the future would then cause a higher water exchange during the winter

As for the projected changes in river runoff for present-day elevations it is readily seen that the amount of freshwater entering Öregrundsgrepen really only affects a very small area in the south-eastern corner (Figure 7-5). A projected increase of 20% would probably not change the present situation much. For the year 5000 AD the situation is different (Figure 7-6). River runoff dominates the volume-averaged age in large parts of the area and an increase would probably be noticeable, although small, resulting in higher water exchange and lower AvA.

Future scenarios are very vague in their projections of wind changes, but typical changes lie in the range of +20%. Increased windiness over the area, for both 2020 AD and 5000 AD, would likely result in decreased AvA, particularly in shallow areas.

Salinity is also a highly dynamical variable that has proven very difficult to project future changes of. The changes presented in the Baltic Sea assessment report lie in the order of a 8 to 50% decrease. Just as for the air temperature, mean changes in salinity will only have a noticeable impact on the AvA if they alter the gradients in salinity. A higher fresh water runoff could sharpen the vertical gradients, but could also – if large enough – push the halocline to depths below the bottom depths of Öregrundsgrepen. As discussed in /Gustafsson 2004/, the salinity stratification is to a greater degree determined by short-term variability in meteorological conditions. Should the gradient of the vertical stratification decrease, the sensitivity analysis points to a reduced water exchange, yielding higher AvA, particularly for the enclosed bay of 5000 AD. Completely removing stratification produces a reduction in the AvA by about 25%, or about 5 days (Figure 7-8).

All in all it may be relatively safe to state that all the projected changes in climatic variables would induce a higher rate of water exchange, the only exception being if the stratification at depths above approximately 30 m in the Baltic Sea is reduced.

8 Conclusions

The hydrodynamic conditions of the Forsmark marine area (present-day Öregrundsgrepen) have successfully been modelled for both past and future conditions spanning 15,000 years. Based on the modelled circulation two outputs have been calculated: the annual mean flows between adjacent basins and a measure of the residence time termed the Average Age (AvA) for each basin. Two different methods have been used. For the years 6500, 3000 and 1000 BC, the circulation simulated using a model for the entire Baltic Sea has been used to estimate the basin flows and AvA in the Forsmark area. For the years 0 to 9000 AD a high-resolution local model has been set up for Öregrundsgrepen and used to compute flows and AvA. The local model has in turn been forced by the results of the Baltic Sea model for the year 2004. The local model has been validated against hydrographic observations, compared to an earlier model study and a sensitivity analysis has been performed.

The results for the basin flows show the following. Overall, the individual basin flows are primarily a function of the cross-sectional areas of each connection between adjacent basins. Furthermore, for the BC years, the flows are higher, usually in the order of 10^2–10^3 m^3/s. For the AD years the flows are smaller by about half an order of magnitude and tend to decrease for future years. The present results for 2020 AD agree well with the results presented in chapter 5 of /Wijnbladh et al. 2008/ for the year 1988.

The AvA more clearly than the basin flows shows how the Forsmark marine area evolves through three major stages: an open sea stage (6500 BC–0 AD), an open-ended coastal area (0–3000 AD) and a bay with only one open boundary (3000–9000 AD). During the open sea stage the AvA is more or less the same for all basins, with values between 2 and 10 days, with a mean for the entire area of about 6 days. During the second stage, a net through-flow is possible. The AvA increases and then decreases as a result of a complex interplay between a narrower southern boundary, decreasing basin volumes and decreasing cross-sectional areas between adjacent basins. The AvA varies between 8 and 34 days, with the mean for the entire area increasing from 13 up to 25 and then decreasing to 14 days again. In general, the shallow western basins have higher AvA than then deeper eastern basins. During the third stage, basins are gradually becoming more enclosed and are one by one transformed into lakes. The AvA for the entire area increases from 14 to 43 days, but with a wide spread between basins, varying from 13 to 105 days, where the innermost basins in the system have the highest AvA.

As the previous modelling study did not calculate the same AvA measure as was used here, the hydraulic residence time (HRT) was calculated and compared to the “individual” AvA in the previous study for present-day conditions (2020 AD vs. 1988). The agreement was good with a few exceptions that can be explained by the fact that the models have different computational grids and used forcing from different years for the simulations. The HRT for 2020 AD produced slightly higher values for the residence time than the “individual” AvA, which is consistent with the fact that the HRT does not include exchange due to diffusive processes.

A validation of the local model showed good agreement between modelled and observed sea levels. A reasonably good agreement was found for the temperature at a station in the centre of Öregrundsgrepen, except that the model does not completely capture the magnitude of the temperature decrease in the deeper water during an upwelling event. The agreement for salinity is not entirely satisfactory, as there is an offset between observed and modelled salinities of about 0.5 psu. However, the variability is fairly well captured by the model. The validation also clearly demonstrated how the model is sensitive to the forcing on the open boundaries, particularly the wide northern boundary. As this forcing has been created using the Baltic Sea model mentioned earlier, it cannot be expected to mirror reality exactly.

A sensitivity analysis has also been performed for the local model for the years 2020 and 5000 AD. This was carried out by completely removing one of the major forcing mechanisms at a time and comparing the results for the AvA with the reference simulation. The results show that the present-day stage, when Öregrundsgrepen is open-ended, is primarily forced by the wind and sea levels. After the southern entrance has closed and Öregrundsgrepen has been transformed into a bay, the

baroclinic forcing due to variations in stratification and runoff from land come into play, whereas the barotropic forcing becomes insignificant. Wind still plays an important role, though. As can be expected the AvA increases as a forcing mechanism is removed, with some local exceptions. Overall, the sensitivity of the AvA values to the complete removal of a forcing mechanism was less than 50% in relative terms, or less than about 10 days in absolute terms. Some specific basins could show higher sensitivity, at least for parts of the year, such as basin 118 where AvA approximately doubled when the wind was removed.

As for future climate scenarios, the only relevant scenario, on the time scales considered in this study for which any predictions are available, is a warmer climate with increased rainfall. A higher average air temperature is on its own not expected to significantly alter the water exchange. However, reduced ice cover in winter may produce higher exchange in the winter months and thus a lower AvA. Increased land runoff would also cause lower AvA, but probably only in directly affected basins and is unlikely to cause any changes in the order of magnitude if the projected increase of about 20% is realistic.

It is difficult to estimate changes in the water exchange due to climate-induced changes in the wind or Baltic Sea salinity, as projections for these variables are very vague. Particularly in the case of the salinity stratification, the projections are for the Baltic Sea mean salinity, whereas it is strength of the stratification that primarily induces water exchange. A projected increase in wind should result in an increased water exchange and lower AvA. If the vertical salinity stratification decreases, the sensitivity analysis indicates an increase in AvA, with the greatest effect when Öregrundsgrepen is an enclosed bay. Even so, completely removing salinity stratification only increases the AvA by about 25%.

9 References

Brydsten L, 2006. A model for landscape development in terms of shoreline displacement, sediment dynamics, lake formation, and lake choke-up processes. SKB TR-06-40, Svensk Kärnbränslehantering AB.

DHI, 2007. MIKE21 & MIKE3 Flow Model, Hydrodynamic and Transport Module, Scientific Documentation. DHI Water Environment Health, Hørsholm, Denmark.

DHI, 2008. ECO Lab – Short Scientific Description. MIKE by DHI. DHI Water Environment Health, Hørsholm, Denmark.

Engqvist A, Andrejev O, 1999. Water exchange of Öregrundsgrepen. A baroclinic 3D-model study. SKB TR-99-11, Svensk Kärnbränslehantering AB.

Engqvist A, Andrejev O, 2000. Sensitivity analysis with regard to variations of physical forcing including two possible future hydrographic regimes for the Öregrundsgrepen. A follow-up baroclinic 3D-model study. SKB TR-00-01, Svensk Kärnbränslehantering AB.

Engqvist A, Andrejev O, 2003. Water exchange of the Stockholm archipelago – A cascade framework modeling approach. Journal of Sea Research 49, 275–294.

Engqvist A, Andrejev O, 2008. Validation of coastal oceanographic models at Forsmark. Site descriptive modelling, SDM-Site Forsmark. SKB TR-08-01, Svensk Kärnbränslehantering AB.

Engqvist A, Döös K, Andrejev O, 2006. Modeling water exchange and contaminant transport through a Baltic coastal region. Ambio 35 (8), 435–447.

Erichsen A C, Møhlenberg F, Closter R M, Sandberg J, 2010. Models for transport and fate of carbon, nutrients and radionuclides in the aquatic ecosystem at Öregrundsgrepen. SKB R-10-10, Svensk Kärnbränslehantering AB.

Fonselius S, 1996. Västerhavets och Östersjöns oceanografi. SMHI.

Gustafsson B G, 2004. Sensitivity of the Baltic Sea salinity to large perturbations in climate. Clim. Res. 27 (3), 237–251.

Gustafsson B G, Westman P, 2002. On the causes for salinity variations in the Baltic Sea during the last 8500 years. Paleoceanography 17 (3), doi:10.1029/2000PA000572.

Kjellström E, Strandberg G, Brandefelt J, Näslund J-O, Smith B, Wohlfarth B, 2009. Climate conditions in Sweden in a 100,000-year time perspective. SKB TR-09-04, Svensk Kärnbränslehantering AB.

SKB, 2006. The biosphere at Forsmark. Data, assumptions and models used in the SR-Can assessment. SKB R-06-82, Svensk Kärnbränslehantering AB.

Strömgren M, Brydsten L, 2008. Digital elevation models of Forsmark. Site descriptive modelling, SDM-Site Forsmark. SKB R-08-62, Svensk Kärnbränslehantering AB.

Söderbäck B (ed), 2008. Geological evolution, palaeoclimate and historical development of the Forsmark and Laxemar-Simpevarp areas. Site descriptive modelling, SDM-Site. SKB R-08-19, Svensk Kärnbränslehantering AB.

The BACC Author Team, 2008. Assesment of Climate Change for the Baltic Sea Basin. (H.-J. Bolle, M. Menenti, & I. Rasool, Eds.) Berlin, Heidelberg: Springer.

Westman P, Wastegård S, Schoning K, Gustafsson B, Omstedt A, 1999. Salinity change in the Baltic Sea during the last 8,500 years: evidence, causes and models. SKB TR-99-38, Svensk Kärnbränslehantering AB.

Wijnbladh E, Aquilonius K, Floderus S, 2008. The marine ecosystems at Forsmark and Laxemar-Simpevarp. Site descriptive modelling SDM-Site. SKB R-08-03, Svensk Kärnbränslehantering AB.

Appendix A

Model results

Deliveries of model output

The model output which has been delivered are annual mean positive, negative and net flows between all adjacent basins, AvA for each basin and HRT for each basin, for each simulated year. The following deliveries have been made:

1. “090202” (February 2, 2009)
2. “090306” (March 6, 2009)
3. “090306_rev_090316” (revision March 16, 2009)
4. “Leverans091102” (November 2, 2009)

Output data tables

The model output is reported as follows:

- Basin flows: Table A-1 through Table A-13
- AvA: Table A-14
- HRT: Table A-15

Table A-1. Average flows between basins in Öregrundsgrepen for 6500 BC. Positive values signify flow from the first basin 'to' the second basin, and negative flow is thus in the opposite direction.

Basin ID	Pos. flow [m³/s]	Neg. flow [m³/s]	Net flow [m³/s]
100_to_Baltic	7,927	–6,874	1,053
101_to_100	2,188	–1,788	400
101_to_102	1,278	–870	408
101_to_Baltic	2,603	–2,072	531
102_to_152	1,704	–1,850	–146
102_to_Baltic	9,584	–7,640	1,944
103_to_102	3,049	–2,616	433
104_to_101	411	–567	–156
104_to_102	1,561	–1,248	313
104_to_103	280	–207	74
105_to_100	5,425	–4,860	565
105_to_101	4,128	–3,177	951
105_to_Baltic	1,724	–2,079	–356
106_to_103	461	–318	143
106_to_104	658	–573	85
106_to_107	617	–842	–225
107_to_104	1,134	–980	155
108_to_101	2,496	–2,151	345
108_to_107	1,239	–862	377
108_to_110	338	–486	–148
109_to_105	1,748	–1,447	301
110_to_101	794	–582	212
110_to_105	2,128	–2,243	–115
111_to_102	2,458	–1,836	622
111_to_103	1,720	–1,500	220
111_to_106	479	–460	18
111_to_107	444	–500	–56
111_to_117	2,840	–3,536	–696
111_to_152	1,190	–1,336	–145
112_to_110	863	–840	23
113_to_105	968	–698	270
113_to_109	651	–615	36
113_to_110	415	–270	145
114_to_105	3,733	–3,015	718
114_to_109	872	–599	273
114_to_115	3,421	–2,964	458
114_to_123	2,580	–2,840	–260
114_to_151	2,369	–3,125	–756
114_to_Baltic	1,893	–2,107	–214
115_to_110	394	–299	95
115_to_113	1,922	–1,459	463
115_to_123	664	–802	–138
116_to_108	2,823	–2,202	621
116_to_110	1,521	–1,672	–151
116_to_112	984	–958	26
117_to_107	856	–818	39
117_to_108	427	–454	–28
117_to_116	176	–173	2
117_to_152	893	–981	–88
118_to_116	569	–531	37
118_to_117	1,551	–1,262	289
120_to_117	1,906	–1,614	292
120_to_118	1,697	–1,444	253
120_to_119	317	–367	–50
121_to_116	1,943	–1,728	215
121_to_118	336	–263	74
121_to_120	370	–278	92
122_to_119	331	–280	51
122_to_120	740	–679	61
123_to_110	529	–426	103
124_to_121	280	–266	14
125_to_120	657	–535	122
125_to_121	217	–185	31
125_to_124	294	–375	–81
126_to_110	191	–193	–2
126_to_116	1,265	–1,023	242
126_to_121	579	–443	136
126_to_123	1,257	–1,225	32
127_to_121	727	–743	–16
128_to_120	76	–58	17

Basin ID	Pos. flow [m³/s]	Neg. flow [m³/s]	Net flow [m³/s]
128_to_125	165	–137	28
129_to_120	980	–865	115
129_to_122	217	–213	3
129_to_152	1,128	–1,189	–60
130_to_121	559	–461	98
131_to_120	304	–251	52
132_to_120	72	–90	–18
132_to_122	699	–575	124
132_to_129	270	–208	61
132_to_152	259	–297	–38
133_to_121	62	–81	–19
133_to_127	274	–243	31
134_to_121	797	–704	93
134_to_126	435	–427	8
134_to_130	102	–108	–7
135_to_130	236	–185	52
135_to_134	91	–126	–35
136_to_124	613	–518	94
136_to_125	218	–174	44
136_to_127	166	–210	–44
136_to_128	344	–299	45
136_to_131	368	–307	60
136_to_133	367	–354	13
137_to_126	263	–230	33
138_to_137	218	–185	33
139_to_121	427	–360	68
139_to_130	272	–220	53
139_to_134	144	–180	–37
139_to_135	157	–140	17
140_to_126	237	–223	14
140_to_138	80	–64	15
141_to_136	1089	–980	110
141_to_139	186	–206	–20
142_to_120	606	–537	69
142_to_131	65	–72	–7
142_to_132	701	–580	120
142_to_136	289	–304	–16
142_to_152	469	–482	–13
143_to_138	257	–219	38
143_to_140	87	–95	–7
144_to_126	142	–126	15
144_to_134	930	–775	155
144_to_138	86	–108	–22
144_to_139	169	–135	34
144_to_143	158	–201	–43
145_to_126	335	–313	22
145_to_140	198	–162	35
145_to_143	413	–340	73
145_to_144	180	–144	36
146_to_123	1,383	–1,534	–151
146_to_126	1,671	–1,321	349
147_to_136	296	–254	41
148_to_136	168	–132	36
148_to_139	560	–485	75
148_to_141	616	–529	87
148_to_144	313	–320	–7
148_to_147	530	–499	32
149_to_136	316	–287	29
149_to_142	716	–571	145
149_to_147	257	–249	8
149_to_148	291	–310	–19
150_to_123	333	–295	38
150_to_144	715	–605	109
150_to_145	1,112	–944	168
150_to_146	1,852	–1,670	182
150_to_148	869	–696	172
150_to_Baltic	442	–569	–128
151_to_123	2,615	–1,982	634
151_to_150	1,930	–1,605	325
151_to_Baltic	18,187	–19,658	–1,470
152_to_148	595	–516	79
152_to_149	1,389	–1,221	167
152_to_150	2,508	–2,289	219

Table A-2. Average flows between basins in Öregrundsgrepen for 3000 BC. Positive values signify flow from the first basin 'to' the second basin, and negative flow is thus in the opposite direction.

Basin ID	Pos. flow [m^3/s]	Neg. flow [m^3/s]	Net flow [m^3/s]
100_to_Baltic	3,444	–7,924	–4,481
101_to_100	536	–1,978	–1,442
101_to_102	568	–1,980	–1,412
101_to_Baltic	644	–2,585	–1,941
102_to_152	317	–302	15
102_to_Baltic	2,314	–8,970	–6,656
103_to_102	950	–2,368	–1,417
104_to_101	810	–241	569
104_to_102	374	–1,468	–1,094
104_to_103	72	–321	–249
105_to_100	2,655	–5,318	–2,663
105_to_101	1,549	–5,166	–3,617
105_to_Baltic	2,394	–742	1,652
106_to_103	137	–641	–504
106_to_104	123	–376	–253
106_to_107	1,075	–280	795
107_to_104	251	–760	–509
108_to_101	996	–2,161	–1,165
108_to_107	599	–1,835	–1,236
108_to_110	710	–222	489
109_to_105	637	–1,754	–1,117
110_to_101	233	–1,007	–774
110_to_105	1,819	–1,537	282
111_to_102	764	–2,875	–2,111
111_to_103	368	–1,008	–640
111_to_106	158	–173	–15
111_to_107	385	–196	188
111_to_117	3,250	–838	2,412
111_to_152	412	–109	303
112_to_110	549	–663	–114
113_to_105	367	–1,373	–1,006
113_to_109	208	–385	–177
113_to_110	151	–692	–541
114_to_105	988	–4,034	–3,046
114_to_109	455	–1,422	–967
114_to_115	1,673	–3,282	–1,609
114_to_123	2,338	–1,358	980
114_to_151	4,003	–1,008	2,995
114_to_Baltic	2,050	–1,077	973
115_to_110	149	–467	–318
115_to_113	696	–2,442	–1,746
115_to_123	808	–286	522
116_to_108	960	–3,109	–2,149
116_to_110	1,328	–886	442
116_to_112	731	–856	–125
117_to_107	366	–480	–113
117_to_108	273	–168	105
117_to_116	68	–70	–2
117_to_152	382	–173	209
118_to_116	143	–256	–113
118_to_117	563	–1,548	–984
120_to_117	496	–1,503	–1,007
120_to_118	496	–1,343	–847
120_to_119	318	–148	171
121_to_116	605	–1,446	–840
121_to_118	136	–388	–252
121_to_120	201	–514	–314
122_to_119	94	–260	–166
122_to_120	330	–534	–204
123_to_110	166	–548	–382
124_to_121	79	–113	–35
125_to_120	231	–654	–423
125_to_121	57	–162	–105
125_to_124	421	–142	279
126_to_110	80	–81	–2
126_to_116	489	–1,353	–863
126_to_121	277	–734	–456
126_to_123	429	–629	–200
127_to_121	502	–453	49
128_to_120	31	–97	–67

Basin ID	Pos. flow [m³/s]	Neg. flow [m³/s]	Net flow [m³/s]
128_to_125	47	–141	–94
129_to_120	175	–519	–344
129_to_122	78	–62	16
129_to_152	366	–289	76
130_to_121	185	–544	–360
131_to_120	76	–258	–181
132_to_120	105	–31	74
132_to_122	189	–619	–431
132_to_129	113	–373	–260
132_to_152	181	–53	127
133_to_121	100	–29	71
133_to_127	67	–165	–98
134_to_121	250	–587	–337
134_to_126	155	–198	–43
134_to_130	59	–33	26
135_to_130	84	–274	–189
135_to_134	180	–56	124
136_to_124	178	–494	–316
136_to_125	80	–230	–150
136_to_127	260	–98	162
136_to_128	103	–264	–161
136_to_131	113	–325	–212
136_to_133	216	–251	–35
137_to_126	89	–212	–124
138_to_137	63	–186	–123
139_to_121	120	–374	–254
139_to_130	91	–286	–195
139_to_134	229	–76	153
139_to_135	45	–110	–65
140_to_126	68	–116	–49
140_to_138	35	–100	–64
141_to_136	439	–832	–393
141_to_139	164	–71	92
142_to_120	143	–365	–222
142_to_131	56	–23	33
142_to_132	267	–726	–459
142_to_136	186	–107	79
142_to_152	147	–153	–6
143_to_138	82	–229	–147
143_to_140	68	–36	32
144_to_126	40	–99	–58
144_to_134	318	–929	–612
144_to_138	140	–49	91
144_to_139	55	–196	–141
144_to_143	262	–86	176
145_to_126	89	–167	–78
145_to_140	69	–210	–140
145_to_143	136	–428	–291
145_to_144	64	–210	–145
146_to_123	1,303	–734	569
146_to_126	644	–1,920	–1,277
147_to_136	91	–235	–144
148_to_136	79	–215	–136
148_to_139	157	–449	–292
148_to_141	190	–493	–303
148_to_144	155	–111	43
148_to_147	214	–342	–128
149_to_136	73	–162	–89
149_to_142	242	–798	–556
149_to_147	81	–94	–13
149_to_148	205	–107	98
150_to_123	95	–235	–140
150_to_144	219	–659	–440
150_to_145	346	–1,004	–659
150_to_146	620	–1,288	–667
150_to_148	317	–1,013	–696
150_to_Baltic	697	–167	530
151_to_123	1,212	–3,503	–2,291
151_to_150	621	–1,944	–1,323
151_to_Baltic	17,339	–12,798	4,541
152_to_148	148	–459	–310
152_to_149	355	–914	–559
152_to_150	713	–1,463	–750

Table A-3. Average flows between basins in Öregrundsgrepen for 1000 BC. Positive values signify flow from the first basin 'to' the second basin, and negative flow is thus in the opposite direction.

Basin ID	Pos. flow [m³/s]	Neg. flow [m³/s]	Net flow [m³/s]
100_to_Baltic	2,355	–4,480	–2,125
101_to_100	490	–1,126	–635
101_to_102	774	–1,231	–457
101_to_Baltic	604	–1,453	–849
102_to_152	144	–158	–13
102_to_Baltic	2,169	–3,867	–1,698
103_to_102	811	–1,260	–449
104_to_101	486	–326	160
104_to_102	367	–737	–371
104_to_103	81	–147	–67
105_to_100	2,007	–2,820	–813
105_to_101	1,582	–3,272	–1,690
105_to_Baltic	977	–561	415
106_to_103	162	–288	–126
106_to_104	86	–178	–92
106_to_107	576	–337	238
107_to_104	191	–386	–195
108_to_101	873	–1,309	–436
108_to_107	701	–1,016	–315
108_to_110	421	–259	163
109_to_105	614	–1,070	–456
110_to_101	264	–552	–288
110_to_105	1,231	–1,131	100
111_to_102	608	–918	–310
111_to_103	239	–477	–238
111_to_106	73	–104	–31
111_to_107	202	–177	25
111_to_117	1,193	–679	514
111_to_152	107	–81	26
112_to_110	369	–408	–39
113_to_105	429	–826	–397
113_to_109	155	–198	–44
113_to_110	181	–380	–199
114_to_105	903	–2,060	–1,157
114_to_109	540	–1,003	–462
114_to_115	1,332	–2,016	–684
114_to_123	1,202	–899	302
114_to_151	2,264	–1,025	1,240
114_to_Baltic	823	–579	243
115_to_110	163	–300	–136
115_to_113	737	–1,411	–674
115_to_123	422	–248	174
116_to_108	957	–1,593	–636
116_to_110	733	–616	117
116_to_112	498	–541	–43
117_to_107	206	–269	–63
117_to_108	122	–117	6
117_to_116	29	–37	–9
117_to_152	73	–59	14
118_to_116	79	–112	–33
118_to_117	433	–692	–259
120_to_117	302	–508	–206
120_to_118	356	–582	–226
120_to_119	133	–96	37
121_to_116	393	–635	–242
121_to_118	356	–582	–226
121_to_120	169	–250	–81
122_to_119	72	–111	–39
122_to_120	165	–208	–43
123_to_110	133	–252	–120
124_to_121	37	–48	–11
125_to_120	169	–277	–108
125_to_121	40	–68	–28
125_to_124	179	–107	72
126_to_110	46	–44	2
126_to_116	414	–682	–269
126_to_121	270	–422	–152
126_to_123	312	–314	–2
127_to_121	243	–231	12
128_to_120	19	–35	–16

Basin ID	Pos. flow [m³/s]	Neg. flow [m³/s]	Net flow [m³/s]
128_to_125	34	–58	–25
129_to_120	95	–173	–78
129_to_122	21	–24	–3
129_to_152	133	–93	40
130_to_121	139	–241	–102
131_to_120	54	–101	–47
132_to_120	35	–18	17
132_to_122	134	–245	–111
132_to_129	68	–116	–47
132_to_152	18	–13	5
133_to_121	40	–21	19
133_to_127	43	–70	–27
134_to_121	172	–271	–99
134_to_126	87	–97	–10
134_to_130	26	–18	8
135_to_130	69	–123	–54
135_to_134	85	–49	36
136_to_124	127	–211	–84
136_to_125	61	–100	–39
136_to_127	110	–71	39
136_to_128	66	–107	–41
136_to_131	76	–130	–54
136_to_133	112	–123	–10
137_to_126	58	–92	–35
138_to_137	44	–80	–35
139_to_121	84	–157	–72
139_to_130	72	–128	–56
139_to_134	92	–53	39
139_to_135	29	–47	–19
140_to_126	34	–47	–14
140_to_138	26	–42	–17
141_to_136	266	–349	–83
141_to_139	62	–39	22
142_to_120	93	–153	–60
142_to_131	19	–12	8
142_to_132	152	–245	–93
142_to_136	57	–45	12
142_to_152	55	–64	–9
143_to_138	58	–97	–39
143_to_140	32	–23	9
144_to_126	26	–43	–17
144_to_134	231	–393	–162
144_to_138	61	–37	24
144_to_139	36	–72	–36
144_to_143	108	–62	46
145_to_126	47	–70	–22
145_to_140	51	–88	–37
145_to_143	97	–173	–76
145_to_144	45	–83	–38
146_to_123	823	–551	272
146_to_126	572	–1,012	–440
147_to_136	65	–96	–31
148_to_136	51	–79	–28
148_to_139	105	–182	–77
148_to_141	136	–201	–65
148_to_144	61	–52	9
148_to_147	111	–137	–26
149_to_136	43	–65	–22
149_to_142	127	–235	–108
149_to_147	32	–38	–5
149_to_148	57	–41	16
150_to_123	59	–97	–38
150_to_144	142	–256	–115
150_to_145	243	–418	–175
150_to_146	412	–575	–164
150_to_148	229	–409	–180
150_to_Baltic	238	–110	129
151_to_123	1,152	–2,188	–1,037
151_to_150	417	–766	–349
151_to_Baltic	6,221	–4,754	1,467
152_to_148	93	–174	–81
152_to_149	205	–323	–118
152_to_150	313	–498	–185

Table A-4. Average flows between basins in Öregrundsgrepen for 0 AD. Positive values signify flow from the first basin 'to' the second basin, and negative flow is thus in the opposite direction.

Basin ID	Pos. flow [m³/s]	Neg. flow [m³/s]	Net flow [m³/s]
100_to_Baltic	3,436	–8,111	–4,676
101_to_100	853	–2,816	–1,963
101_to_102	995	–210	785
101_to_Baltic	1,652	–622	1,030
102_to_Baltic	2,741	–1,679	1,062
103_to_102	1,118	–1,100	19
104_to_101	102	–319	–217
104_to_102	680	–371	309
104_to_103	114	–101	13
105_to_100	2,286	–4,999	–2,713
105_to_101	2,961	–2,441	520
106_to_103	206	–162	44
106_to_104	253	–215	38
106_to_107	275	–426	–151
107_to_104	356	–290	66
108_to_101	583	–1,155	–572
108_to_107	816	–572	244
108_to_110	194	–368	–174
109_to_105	1,226	–1,524	–298
110_to_101	464	–343	121
110_to_105	1,058	–1,751	–694
111_to_102	901	–951	–51
111_to_103	499	–536	–38
111_to_106	53	–121	–69
111_to_107	157	–203	–45
111_to_117	1,374	–1,171	203
112_to_110	432	–460	–28
113_to_105	593	–828	–235
113_to_109	448	–556	–108
113_to_110	176	–334	–159
114_to_105	2,136	–3,103	–966
114_to_109	563	–754	–191
114_to_115	2,776	–3,234	–457
114_to_123	2,444	–1,588	856
114_to_151	3,110	–2,352	759
115_to_110	125	–286	–161
115_to_113	1,184	–1,685	–501
115_to_123	601	–396	205
116_to_108	976	–1,559	–583
116_to_110	660	–698	–38
116_to_112	489	–517	–28
117_to_107	254	–237	17
117_to_108	126	–82	43
117_to_116	26	–60	–34
118_to_116	12	–196	–184
118_to_117	736	–848	–111
120_to_117	391	–456	–65
120_to_118	461	–684	–223
120_to_119	196	–142	53
121_to_116	293	–535	–242
121_to_118	173	–246	–73
121_to_120	337	–318	20
122_to_119	108	–161	–53
122_to_120	153	–151	2
123_to_110	315	–376	–61
124_to_121	24	–39	–14
125_to_120	226	–366	–140
125_to_121	44	–50	–6
125_to_124	191	–140	50
126_to_110	98	–50	49
126_to_116	747	–703	45
126_to_121	379	–503	–124
126_to_123	154	–567	–413
127_to_121	207	–225	–18
128_to_120	38	–58	–20
128_to_125	46	–74	–28

Basin ID	Pos. flow [m³/s]	Neg. flow [m³/s]	Net flow [m³/s]
129_to_120	52	–50	2
129_to_122	5	–8	–3
130_to_121	175	–316	–141
131_to_120	88	–130	–42
132_to_120	58	–51	7
132_to_122	147	–195	–48
132_to_129	45	–46	–1
133_to_121	61	–40	21
133_to_127	77	–99	–21
134_to_121	214	–346	–133
134_to_126	162	–81	81
134_to_130	27	–33	–6
135_to_130	92	–163	–71
135_to_134	125	–57	67
136_to_124	146	–210	–64
136_to_125	83	–150	–68
136_to_127	153	–150	3
136_to_128	83	–130	–48
136_to_131	107	–176	–68
136_to_133	156	–156	0
137_to_126	120	–134	–14
138_to_137	96	–109	–14
139_to_121	121	–197	–76
139_to_130	85	–149	–63
139_to_134	137	–37	100
139_to_135	39	–43	–4
140_to_126	112	–81	31
140_to_138	10	–66	–57
141_to_136	336	–465	–129
141_to_139	100	–49	51
142_to_120	37	–100	–63
142_to_131	46	–20	26
142_to_132	142	–184	–42
142_to_136	131	–96	35
143_to_138	98	–138	–40
143_to_140	68	–13	54
144_to_126	66	–50	16
144_to_134	312	–536	–224
144_to_138	101	–18	83
144_to_139	50	–94	–44
144_to_143	168	–56	112
145_to_126	101	–139	–38
145_to_140	63	–143	–80
145_to_143	158	–256	–98
145_to_144	41	–93	–52
146_to_123	1,241	–1,240	0
146_to_126	751	–1,271	–520
147_to_136	59	–126	–67
148_to_136	69	–116	–48
148_to_139	213	–264	–51
148_to_141	217	–295	–78
148_to_144	147	–51	96
148_to_147	121	–156	–35
149_to_136	25	–61	–36
149_to_142	56	–100	–44
149_to_147	34	–66	–31
149_to_148	103	–27	75
150_to_123	99	–57	43
150_to_144	285	–385	–101
150_to_145	335	–604	–268
150_to_146	328	–848	–520
150_to_148	281	–468	–188
151_to_123	2,221	–2,973	–752
151_to_150	276	–600	–324
151_to_Baltic	5,981	–4,146	1,835
152_to_148	249	–253	–4
152_to_149	185	–222	–36
152_to_150	788	–1,468	–680

Table A-5. Average flows between basins in Öregrundsgrepen for 1000 AD. Positive values signify flow from the first basin 'to' the second basin, and negative flow is thus in the opposite direction.

Basin ID	Pos. flow [m³/s]	Neg. flow [m³/s]	Net flow [m³/s]
100_to_Baltic	1,438	–2,287	–849
101_to_100	532	–736	–203
101_to_102	326	–138	188
101_to_Baltic	1,052	–272	780
102_to_Baltic	1,696	–1,784	–88
103_to_102	737	–932	–195
104_to_101	119	–97	21
104_to_102	508	–544	–36
104_to_103	75	–140	–66
105_to_100	1,311	–1,957	–646
105_to_101	1,790	–917	873
106_to_103	124	–202	–77
106_to_104	198	–246	–48
106_to_107	348	–269	80
107_to_104	279	–311	–32
108_to_101	329	–636	–307
108_to_107	584	–709	–125
108_to_110	149	–233	–84
109_to_105	666	–554	112
110_to_101	344	–166	178
110_to_105	751	–769	–18
111_to_102	132	–177	–45
111_to_103	360	–412	–52
111_to_106	37	–83	–46
111_to_107	98	–156	–58
111_to_117	570	–369	201
112_to_110	296	–169	127
113_to_105	213	–318	–105
113_to_109	296	–130	166
113_to_110	56	–296	–240
114_to_105	1,226	–988	238
114_to_109	409	–463	–54
114_to_115	1,022	–1,274	–252
114_to_123	937	–338	599
114_to_151	1,040	–1,571	–531
115_to_110	94	–301	–207
115_to_113	394	–572	–179
115_to_123	360	–226	134
116_to_108	581	–1,172	–590
116_to_110	767	–229	538
116_to_112	380	–253	127
117_to_107	183	–113	71
117_to_108	114	–40	74
117_to_116	21	–24	–3
118_to_116	14	–56	–43
118_to_117	397	–488	–91
120_to_117	46	–14	32
120_to_118	239	–340	–101
120_to_119	12	–22	–10
121_to_116	283	–271	12
121_to_118	107	–140	–33
121_to_120	190	–208	–18
122_to_119	20	–10	10
122_to_120	7	–19	–12
123_to_110	208	–221	–13
124_to_121	24	–6	18
125_to_120	76	–127	–50
125_to_121	14	–10	4
125_to_124	60	–32	28

Basin ID	Pos. flow [m³/s]	Neg. flow [m³/s]	Net flow [m³/s]
126_to_110	70	–31	39
126_to_116	564	–455	109
126_to_121	436	–420	16
126_to_123	177	–365	–188
127_to_121	38	–38	0
128_to_125	17	–19	–2
130_to_121	52	–82	–30
132_to_120	2	–1	1
132_to_122	6	–8	–2
133_to_121	5	–4	1
133_to_127	19	–17	1
134_to_121	91	–139	–48
134_to_126	99	–60	39
134_to_130	7	–16	–9
135_to_130	25	–45	–21
135_to_134	45	–24	20
136_to_124	45	–55	–10
136_to_125	40	–56	–17
136_to_127	31	–33	–2
136_to_128	17	–19	–2
136_to_131	0	0	0
136_to_133	36	–34	2
137_to_126	77	–70	8
138_to_137	21	–14	8
139_to_121	12	–11	1
139_to_130	23	–23	0
139_to_134	25	–13	12
139_to_135	5	–5	–1
140_to_126	44	–18	26
140_to_138	14	–26	–12
141_to_136	89	–112	–23
141_to_139	28	–14	13
142_to_120	13	–13	0
142_to_132	7	–8	–1
142_to_136	20	–19	1
143_to_138	26	–27	–1
143_to_140	24	–13	11
144_to_126	19	–6	14
144_to_134	56	–107	–51
144_to_138	45	–24	21
144_to_143	39	–16	23
145_to_140	61	–59	2
145_to_143	25	–38	–13
146_to_123	1,063	–996	67
146_to_126	757	–867	–110
147_to_136	11	–17	–5
148_to_136	12	–13	–1
148_to_139	35	–35	0
148_to_141	74	–83	–10
148_to_144	20	–14	6
148_to_147	11	–17	–5
150_to_123	54	–25	29
150_to_144	21	–20	1
150_to_145	86	–97	–11
150_to_146	191	–235	–43
150_to_148	129	–139	–10
151_to_123	1,178	–1,833	–655
151_to_150	49	–90	–41
151_to_Baltic	1,690	–1,524	166
152_to_150	17	–9	8

Table A-6. Average flows between basins in Öregrundsgrepen for 2020 AD. Positive values signify flow from the first basin 'to' the second basin, and negative flow is thus in the opposite direction.

Basin ID	Pos. flow [m³/s]	Neg. flow [m³/s]	Net flow [m³/s]
100_to_Baltic	1,341	–3,085	–1,743
101_to_100	751	–106	644
101_to_102	477	–299	177
101_to_Baltic	1,818	–392	1,426
102_to_Baltic	1,326	–1,244	82
103_to_102	395	–476	–80
104_to_101	165	–94	70
104_to_102	294	–278	16
104_to_103	43	–67	–25
105_to_100	675	–3,063	–2,388
105_to_101	2,386	–398	1,988
106_to_103	38	–82	–44
106_to_104	117	–103	15
106_to_107	166	–127	39
107_to_104	213	–196	17
108_to_101	462	–525	–63
108_to_107	396	–420	–24
108_to_110	191	–341	–150
109_to_105	148	–441	–293
110_to_101	481	–227	254
110_to_105	981	–1,135	–154
111_to_103	54	–66	–12
111_to_106	30	–21	9
111_to_107	66	–83	–17
111_to_117	45	–29	17
112_to_110	273	–168	105
113_to_105	431	–457	–26
113_to_109	119	–154	–35
113_to_110	185	–273	–88
114_to_105	1,001	–929	73
114_to_109	45	–303	–258
114_to_115	640	–908	–268
114_to_123	666	–287	379
114_to_151	753	–651	102
115_to_110	112	–192	–80
115_to_113	580	–729	–149
115_to_123	191	–230	–39
116_to_108	361	–688	–328
116_to_110	357	–204	153
116_to_112	338	–233	105
117_to_107	26	–10	16
118_to_117	2	–3	0
121_to_116	178	–214	–36
121_to_120	122	0	122
123_to_110	53	–38	14
126_to_110	15	–7	8
126_to_116	185	–108	76
126_to_121	247	–159	88
126_to_123	144	–105	39
134_to_121	3	–5	–2
134_to_126	5	–3	3
146_to_123	430	–626	–196
146_to_126	576	–373	204
150_to_146	32	–24	8
151_to_123	710	–879	–169
151_to_Baltic	807	–593	214
152_to_150	14	–7	8

Table A-7. Average flows between basins in Öregrundsgrepen for 3000 AD. Positive values signify flow from the first basin 'to' the second basin, and negative flow is thus in the opposite direction.

Basin ID	Pos. flow [m^3/s]	Neg. flow [m^3/s]	Net flow [m^3/s]
100_to_Baltic	1,451	–2,541	–1,091
101_to_100	746	–181	564
101_to_102	341	–247	94
101_to_Baltic	1,409	–521	889
102_to_Baltic	588	–477	111
103_to_102	3	–3	0
104_to_101	48	–57	–9
104_to_102	118	–100	18
105_to_100	912	–2,567	–1,655
105_to_101	1,975	–584	1,391
106_to_107	18	–18	0
107_to_104	69	–60	10
108_to_101	349	–284	65
108_to_107	70	–60	10
108_to_110	147	–239	–92
109_to_105	274	–476	–202
110_to_101	286	–186	100
110_to_105	762	–962	–201
112_to_110	85	–56	29
113_to_105	380	–316	64
113_to_109	78	–76	2
113_to_110	13	–24	–11
114_to_105	542	–504	38
114_to_109	44	–187	–143
114_to_115	458	–420	38
114_to_123	302	–123	179
114_to_151	270	–321	–50
115_to_110	62	–58	4
115_to_113	421	–366	55
115_to_123	79	–95	–16
116_to_108	150	–167	–17
116_to_110	104	–96	8
116_to_112	128	–99	29
121_to_116	52	–45	7
126_to_116	46	–33	13
126_to_121	52	–45	7
126_to_123	37	–29	8
146_to_123	190	–210	–20
146_to_126	137	–109	28
150_to_146	10	–2	8
151_to_123	257	–403	–146
151_to_Baltic	242	–145	97

Table A-8. Average flows between basins in Öregrundsgrepen for 4000 AD. Positive values signify flow from the first basin 'to' the second basin, and negative flow is thus in the opposite direction.

Basin ID	Pos. flow [m³/s]	Neg. flow [m³/s]	Net flow [m³/s]
100_to_Baltic	823	–1,231	–408
101_to_100	667	–334	333
101_to_102	218	–129	90
101_to_Baltic	648	–322	327
102_to_Baltic	237	–147	89
105_to_100	860	–1,600	–741
105_to_101	1,490	–736	754
108_to_101	89	–99	–9
108_to_110	54	–51	3
109_to_105	247	–227	20
110_to_101	40	–36	4
110_to_105	290	–284	6
112_to_110	11	–6	5
113_to_105	182	–154	28
113_to_109	61	–41	20
114_to_105	283	–323	–40
114_to_109	84	–84	0
114_to_115	386	–338	48
114_to_123	210	–187	23
114_to_151	283	–314	–31
115_to_113	239	–191	48
116_to_108	17	–23	–6
116_to_110	12	–10	1
116_to_112	16	–11	5
146_to_123	11	–3	8
146_to_126	3	–3	0
151_to_123	183	–215	–31

Table A-9. Average flows between basins in Öregrundsgrepen for 5000 AD. Positive values signify flow from the first basin 'to' the second basin, and negative flow is thus in the opposite direction.

Basin ID	Pos. flow [m³/s]	Neg. flow [m³/s]	Net flow [m³/s]
100_to_Baltic	179	–171	8
105_to_100	377	–369	8
105_to_101	368	–369	0
109_to_105	104	–89	15
110_to_105	3	–3	0
113_to_109	43	–33	10
114_to_105	105	–112	–7
114_to_109	57	–53	4
114_to_115	183	–173	10
114_to_123	61	–62	–1
114_to_151	113	–119	–7
115_to_113	44	–33	10
151_to_123	62	–61	1

Table A-10. Average flows between basins in Öregrundsgrepen for 6000 AD. Positive values signify flow from the first basin 'to' the second basin, and negative flow is thus in the opposite direction.

Basin ID	Pos. flow [m^3/s]	Neg. flow [m^3/s]	Net flow [m^3/s]
100_to_Baltic	73	–64	8
105_to_100	229	–221	8
105_to_101	302	–302	0
109_to_105	79	–59	20
114_to_105	72	–84	–12
114_to_109	79	–59	20
114_to_115	45	–45	0
114_to_123	1	–9	–8
114_to_151	29	–29	0

Table A-11. Average flows between basins in Öregrundsgrepen for 7000 AD. Positive values signify flow from the first basin 'to' the second basin, and negative flow is thus in the opposite direction.

Basin ID	Pos. flow [m^3/s]	Neg. flow [m^3/s]	Net flow [m^3/s]
100_to_Baltic	41	–33	8
105_to_100	115	–107	8
105_to_101	135	–135	0
114_to_105	23	–15	8
114_to_151	10	–10	0

Table A-12. Average flows between basins in Öregrundsgrepen for 8000 AD. Positive values signify flow from the first basin 'to' the second basin, and negative flow is thus in the opposite direction.

Basin ID	Pos. flow [m^3/s]	Neg. flow [m^3/s]	Net flow [m^3/s]
100_to_Baltic	26	–18	8
105_to_100	19	–11	8
114_to_105	13	–5	8

Table A-13. Average flows between basins in Öregrundsgrepen for 9000 AD. Positive values signify flow from the first basin 'to' the second basin, and negative flow is thus in the opposite direction.

Basin ID	Pos. flow [m^3/s]	Neg. flow [m^3/s]	Net flow [m^3/s]
100_to_Baltic	16	–8	8
105_to_100	10	–2	8

Table A-14. AvA time in years for each basin, volume averaged. These data are computed considering water outside Öregrundsgrepen as exogenous.

Basin	6500 BC	3000 BC	1000 BC	0 AD	1000 AD	2020 AD	3000 AD	4000 AD	5000 AD	6000 AD	7000 AD	8000 AD	9000 AD
100	0.013	0.006	0.009	0.021	0.060	0.036	0.021	0.035	0.046	0.038	0.052	0.060	0.121
101	0.019	0.011	0.014	0.027	0.069	0.046	0.031	0.041	0.064	0.056	0.071		
102	0.017	0.009	0.013	0.043	0.069	0.053	0.040	0.041					
103	0.021	0.012	0.017	0.047	0.071	0.054	0.043						
104	0.021	0.012	0.017	0.040	0.075	0.057	0.048						
105	0.018	0.011	0.016	0.028	0.069	0.043	0.029	0.046	0.074	0.062	0.076	0.078	0.113
106	0.024	0.014	0.020	0.045	0.074	0.058	0.052						
107	0.025	0.016	0.022	0.044	0.075	0.060	0.052						
108	0.026	0.015	0.021	0.039	0.076	0.058	0.048	0.061					
109	0.019	0.013	0.018	0.031	0.073	0.047	0.034	0.057	0.095	0.084			
110	0.023	0.016	0.021	0.034	0.076	0.053	0.040	0.059	0.100				
111	0.022	0.014	0.021	0.052	0.073	0.065							
112	0.026	0.017	0.023	0.038	0.078	0.058	0.049	0.068					
113	0.021	0.015	0.021	0.034	0.077	0.052	0.043	0.063	0.105				
114	0.017	0.014	0.021	0.032	0.073	0.051	0.042	0.062	0.104	0.093	0.121	0.083	
115	0.021	0.016	0.022	0.035	0.076	0.053	0.043	0.064	0.111	0.095			
116	0.027	0.018	0.024	0.043	0.076	0.061	0.053	0.070					
117	0.023	0.017	0.026	0.052	0.075	0.082							
118	0.023	0.018	0.026	0.051	0.075	0.092							
119	0.020	0.018	0.024	0.055	0.078								
120	0.021	0.018	0.025	0.054	0.077	0.064							
121	0.024	0.019	0.025	0.049	0.074	0.062	0.059						
122	0.018	0.017	0.023	0.056	0.079								
123	0.018	0.016	0.022	0.038	0.076	0.058	0.052	0.071	0.117	0.028			
124	0.021	0.019	0.025	0.052	0.077								
125	0.021	0.019	0.025	0.053	0.077								
126	0.022	0.019	0.024	0.044	0.074	0.061	0.057	0.105					
127	0.024	0.020	0.026	0.052	0.077								
128	0.020	0.019	0.025	0.054	0.078								
129	0.012	0.012	0.016	0.059									
130	0.019	0.018	0.022	0.051	0.077								
131	0.019	0.018	0.025	0.055	0.079								
132	0.015	0.015	0.023	0.057	0.080								
133	0.021	0.019	0.026	0.053	0.078								
134	0.021	0.019	0.025	0.050	0.076	0.065							
135	0.020	0.018	0.024	0.050	0.076								
136	0.019	0.018	0.025	0.054	0.078								
137	0.020	0.019	0.024	0.049	0.076								
138	0.019	0.018	0.024	0.049	0.077								
139	0.019	0.019	0.025	0.052	0.078								
140	0.019	0.018	0.024	0.049	0.077								
141	0.019	0.018	0.023	0.054	0.078								
142	0.014	0.015	0.023	0.057	0.080								
143	0.018	0.018	0.024	0.049	0.077								
144	0.018	0.018	0.024	0.051	0.077								
145	0.017	0.018	0.023	0.049	0.077								
146	0.018	0.018	0.023	0.044	0.074	0.062	0.054	0.064					
147	0.015	0.016	0.021	0.057	0.079								
148	0.015	0.016	0.020	0.054	0.078								
149	0.011	0.013	0.017	0.058									
150	0.014	0.016	0.020	0.049	0.077	0.066	0.030						
151	0.011	0.011	0.020	0.035	0.066	0.057	0.053	0.081	0.125	0.184	0.287		
All basins	0.017	0.012	0.018	0.036	0.070	0.051	0.039	0.054	0.085	0.082	0.106	0.070	0.118

Table A-15. HRT in years for each basin, volume averaged. These data are computed considering water outside each basin as exogenous.

Basin	6500 BC	3000 BC	1000 BC	0 AD	1000 AD	2020 AD	3000 AD	4000 AD	5000 AD	6000 AD	7000 AD	8000 AD	9000 AD
100	0.004	0.004	0.004	0.002	0.004	0.002	0.002	0.002	0.008	0.010	0.014	0.041	0.059
101	0.005	0.004	0.004	0.003	0.004	0.003	0.002	0.002	0.004	0.002	0.001		
102	0.009	0.007	0.007	0.006	0.006	0.005	0.007	0.008					
103	0.003	0.003	0.003	0.002	0.001	0.002	0.117						
104	0.002	0.002	0.002	0.001	0.001	0.001	0.001						
105	0.004	0.003	0.003	0.002	0.003	0.002	0.002	0.002	0.004	0.004	0.006	0.041	0.062
106	0.002	0.001	0.001	0.001	0.001	0.001	0.001						
107	0.003	0.002	0.002	0.002	0.001	0.001	0.002						
108	0.003	0.002	0.002	0.002	0.002	0.001	0.002	0.003					
109	0.001	0.001	0.001	0.001	0.001	0.002	0.001	0.001	0.001	0.001			
110	0.003	0.002	0.002	0.001	0.002	0.001	0.001	0.002	0.050				
111	0.004	0.004	0.004	0.002	0.002	0.003							
112	0.001	0.001	0.001	0.001	0.001	0.000	0.001	0.001					
113	0.001	0.001	0.001	0.000	0.001	0.000	0.000	0.000	0.001				
114	0.003	0.003	0.003	0.001	0.002	0.003	0.004	0.004	0.006	0.008	0.035	0.053	
115	0.002	0.002	0.001	0.001	0.001	0.001	0.001	0.001	0.002	0.002			
116	0.004	0.003	0.004	0.003	0.003	0.003	0.004	0.012					
117	0.004	0.004	0.003	0.002	0.002	0.011							
118	0.001	0.001	0.001	0.001	0.001	0.052							
119	0.000	0.000	0.000	0.000	0.000								
120	0.002	0.001	0.001	0.001	0.001	0.000							
121	0.002	0.002	0.002	0.001	0.001	0.001	0.002						
122	0.001	0.001	0.001	0.000	0.001								
123	0.002	0.002	0.002	0.001	0.001	0.001	0.002	0.002	0.003	0.007			
124	0.000	0.000	0.000	0.000	0.000								
125	0.001	0.000	0.000	0.000	0.000								
126	0.003	0.002	0.002	0.001	0.001	0.001	0.002	0.022					
127	0.001	0.001	0.001	0.000	0.001								
128	0.000	0.000	0.000	0.000	0.000								
129	0.002	0.002	0.002	0.002									
130	0.000	0.000	0.000	0.000	0.000								
131	0.000	0.000	0.000	0.000	0.050								
132	0.001	0.001	0.001	0.000	0.001								
133	0.000	0.000	0.000	0.000	0.000								
134	0.001	0.001	0.001	0.001	0.001	0.004							
135	0.000	0.000	0.000	0.000	0.000								
136	0.001	0.001	0.001	0.000	0.001								
137	0.000	0.000	0.000	0.000	0.000								
138	0.000	0.000	0.000	0.000	0.000								
139	0.001	0.001	0.001	0.000	0.001								
140	0.000	0.000	0.000	0.000	0.000								
141	0.001	0.001	0.001	0.000	0.000								
142	0.002	0.001	0.001	0.001	0.002								
143	0.000	0.000	0.000	0.000	0.000								
144	0.001	0.001	0.001	0.000	0.000								
145	0.001	0.000	0.000	0.000	0.000								
146	0.002	0.002	0.002	0.001	0.001	0.001	0.001	0.005					
147	0.000	0.000	0.000	0.000	0.000								
148	0.002	0.001	0.002	0.001	0.001								
149	0.002	0.001	0.001	0.001									
150	0.003	0.003	0.003	0.001	0.004	0.017	0.012						
151	0.008	0.006	0.007	0.004	0.006	0.008	0.014	0.014	0.020	0.059	0.082		
All basins	0.004	0.004	0.004	0.002	0.004	0.002	0.002	0.002	0.008	0.010	0.014	0.041	0.059

Errors in earlier deliveries

When quality control was performed on earlier deliveries, errors were found regarding the calculations of flows in and out of basins and also in the basin volumes delivered by SKB. These errors were considered grave enough to warrant re-calculation of previously delivered results. A new corrected delivery was made on 2009-11-02. The following errors were addressed:

1. An incorrect method had been used in the post-processing when calculating flows between adjacent basins. The method used did not separate all in- and outflows for those adjacent basins where their common boundary consisted of more than one line segment. This resulted in errors in the estimates of positive and negative flows, though the estimates of net flows were correct. Since the HRT-calculations are based on the in- and outflows these estimates were also affected. However, the AvA estimates were not affected since these are computed directly from the model output.
2. Erroneous basin volumes had been delivered by SKB. When a comparison was made between the basin volumes in MIKE and those delivered from SKB large differences were found in some cases. It turned out that the volumes delivered by SKB (2009-02-10) contained errors. The errors affect the results of the AD simulations. The errors were due to including land points when calculating the mean depth of basins partly above sea level. New basin volumes were delivered to DHI on 2009-09-18. As the basin volumes are used for the calculations of HRT and mean AvA for the entire Forsmark area, these had to be re–calculated after the new delivery.

The magnitude of the errors has not been estimated, as this would require a comparison of all old and new calculations. However, the largest errors are caused by using incorrect basin volumes. In the calculation of the mean AvA for the entire Öregrundsgrepen the sum of the basin volumes is used. As can be seen from Figure A-1 the error becomes very large for the later AD years.

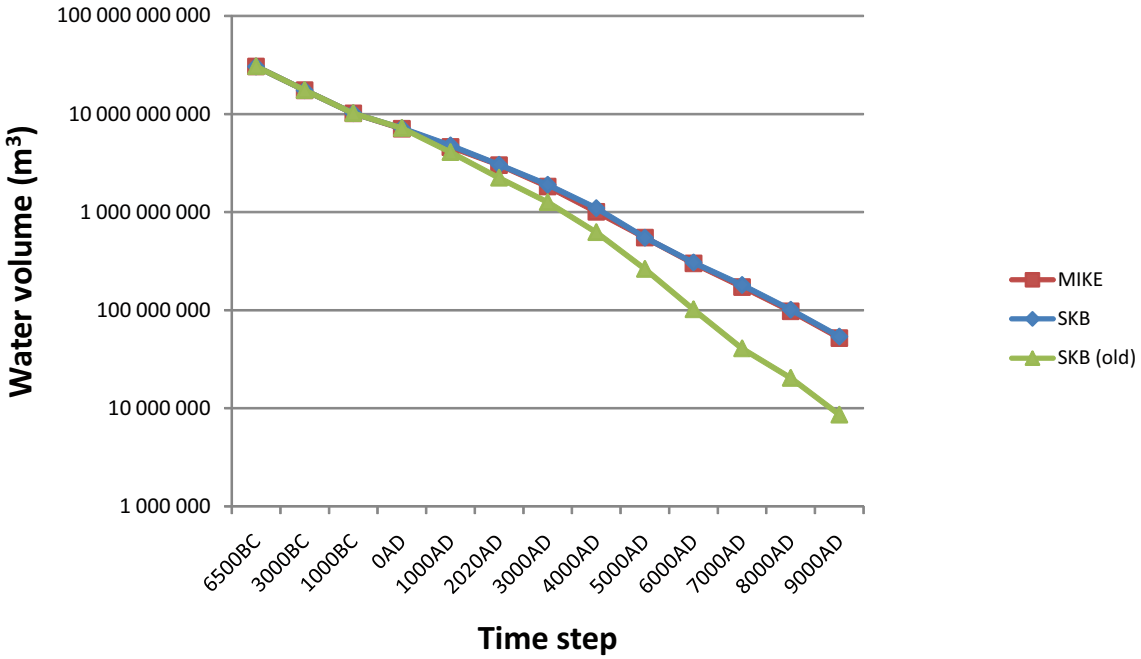

Figure A-1. *Temporal development of total volume of Öregrundsgrepen for all simulated years. Red line shows model volumes (MIKE 3), blue line corrected SKB volumes and green line erroneous SKB volumes.*

Appendix B

Paleooceanographic water exchange computation of three earlier submerged stages of the present time Forsmark coastal area

by Anders Engqvist, Division of Water Resources Engineering, KTH, SE-100 44 Stockholm, Sweden

Report date: 2009-01-20

Abstract

Three distinct phases in the prehistoric development of the Baltic Sea have been simulated for a full year cycle namely 6500 BC, 3000 BC and 1000 BC. The best-known fact about the Baltic at those times is presumably the bathymetry. Forcing factors have mainly been the same as for a particular contemporary year 2004 with two exceptions: (i) the initial salinity distribution close to the surface layer of the Forsmark coast, for which prescribed values have been adhered to and (ii) the freshwater discharge. Literature values have been used for the all-Baltic yearly discharge consistent with the estimated salinities. All other forcing data pertain to the year 2004.

The resulting velocity profiles at model grid points corresponding to the location of the Forsmark coast of the three actual above-mentioned phases are saved and passed on to DHI (Danish Hydraulic Institute) for their further analysis and presentation. The 2D-velocity fields for the layer closest to the bottom are presented here in a succinct manner. The representative velocities are found to be in the range of 2–3 cm/s. This means that the average residence time of hypothetically released nuclides would be determined by the time they are advected off the greatest sub-basin area (with a length-scale of three nautical miles) into which the corresponding location of the present Öregrundsgrepen is partitioned. This time-scale is found to be a little less than two days, i.e. somewhat longer than has been estimated for the present time situation.

1 The assignment

From SKB was assigned 2008-09-29 the task of assisting and guiding DHI's undertaking to perform numerical model estimates of the water exchange of the Forsmark coastal area in the future when this area is subjected to anticipated shoreline displacement. In a meeting between SKB and DHI 2008-11-13 it was decided that the paleooceanographic models should not be performed by DHI, but were reassigned to be attempted by the present author. The computation task consists of estimating the flow-field in the vicinity of the location where the present Forsmark area was located 6500 BC, 3000 BC and 1000 BC. Originally this was restricted to estimating the currents just above the bottom, but in discussion with DHI this was expanded to cover all layers from bottom to surface. The 3D-model employed has a horizontal resolution of 2 × 2 nautical miles and the site of the Öregrundsgrepen area is safely contained by the corner coordinates: 60°14′N; 17°59′E (SW) and 60°32′N; 18°31′E (NE) representing the center points of the scalar properties (e.g. salinity and temperature) in a so-called Arakawa C-grid. Though the N/S(E/W)-velocities are staggered one half grid cell length to the north (east), the saved velocities denoted V(U) are averaged so that they also represent the velocities at the same position as the scalars. For the saved data these items correspond to a 10 × 9 matrix with the longer side in the N/S-direction.

2 Materials and methods

Simulation of processes taking place in the distant past historical times or in the far future is a delicate matter. This applies certainly also to the water circulation of the Baltic Sea. The degree of confidence one can invest in such endeavors is entirely a matter of the adequacy as to how its oceanographic conditions are assessed and as how accurately the forcing data are historically reconstructed or projected into the future. From an oceanographic point of view this task comprises both the bathymetry and the forcing that may deviate considerably from the present time values. Such reconstruction must of course be based on literature data (inferred from proxy ditto) since the oldest reliable oceanographic records are typically younger than 200 years.

2.1 Bathymetry (including strait section areas and depths)

The original DEM /SKB 2006/ is given in projected coordinates (RT90 2.5 gon W) with grid cell side lengths 500 × 500 m. To transform this array to the spherical coordinate system that the 3D-numerical model (AS3D) demands with a 2′ × 2′ (nautical mile) grid, each of the center points of this latter grid was transformed back to the RT90 DEM and the average depth of the wet 7 × 7 grid cells centered around the corresponding midpoint was calculated. This is because two nautical miles (3,704 m) equals roughly 7 times 500 m. If the number of comprised wet grid cells was 24 or more, then this new transformed grid cell was considered wet. This procedure results in rather rugged contour lines, so a Laplacian smoothing procedure with an over-relaxation constant of 0.6 was performed a couple of times. This was also performed for the DEM of the present time and the comparison (Figure B-1) to Warnemuende data seems satisfactory. Uninterrupted connection of narrow channels may not ensue, so corrections of the grid were performed to the Sound and the Danish straits where a few grid cells were adjusted to arrange for passage. The depth of these passages was set to the shallowest of the non-manipulated adjacent ones. The resulting bathymetric grids are shown in Figures B-2 trough B-4 for 6500 BC, 3000 BC and 1000 BC respectively.

2.2 Atmospheric forcing

The atmospheric forcing was for various reasons, but foremost because this had been used in an earlier validation study /Engqvist and Andrejev 2008/, decided to be based on a data set that has been derived from so-called Mesan-data. This set contains in addition to the wind components also air pressure, air temperature and relative humidity, but lacks data for precipitation and insolation.

2.3 Ice conditions

No information about the ice cover of the Baltic has been possible to obtain. It seems safe, however, to assume that the last remainder of land ice had melted at the time of the earliest of these simulations i.e. 6500 BC /Sjöberg 1992/.

2.4 Boundary forcing

The length of the Kattegat boundary varies between the three simulations. The salinity across this zonal cross-section between Denmark and Sweden has been extended in both horizontal and vertical direction maintaining the original data that have been based on 20 years' climatologically averaged data assessed 1970 through 1989. This recourse was necessitated by the lack of paleooceanographic information about the historic state of the adjacent waters of Kattegat. This unavailability also encompasses data about Skagerrak, the North Sea and even the north Atlantic.

2.5 Initial salinity fields

From /Westin and Gustafsson 2002/ the range of the salinity of the entire Baltic has been computed and from these data the local coastal water salinities have been estimated /Gustafsson 2004/, see Table B-1 for the years in question. The initialization procedure has been to arrange for a north/south and a surface/bottom salinity gradient that complies with these specified ranges and simultaneously adjust the surface salinity off the Forsmark coast to initially attain the specified mean value.

Table B-1. Estimates of salinity range for the entire Baltic Sea and the coastal water offshore the Forsmark area. The present corresponding ranges based on measurements have been added for comparison.

	Baltic Sea salinity		Forsmark salinity		
Year	min	max	min	mean	max
6500 BC	0.00	0.00	0.00	0.00	0.00
3000 BC	10.00	15.00	9.26	11.76	14.26
1000 BC	8.00	10.00	7.03	8.03	9.03
2000 AD	6.50	8.00	5.00	5.75	6.50

2.6 Initial temperature fields

No data are suggested for the temperature ranges. Since the forcing was tacitly agreed to be based on so-called Mesan data, this data set has been adhered to. For the 6500 BC condition with freshwater in the entire Baltic, initialization for the winter period is susceptible to numerical problems caused by artificially induced unstable stratification. In order to circumvent such problems, the initialization was set to the summer period with a stable gradient ranging from 20°C at the surface to 4°C at maximum depth throughout the entire computational domain. Both these salinity and temperature fields were then spun-up for one half year and the resulting state by the end of December was used as the initial state for the whole year cycle run. This procedure was used for all three paleooceanographic simulations.

2.7 Freshwater discharge

The freshwater discharge of Baltic Sea has also been computed by /Gustafsson and Westman 2002/ departing from the salinities of the corresponding time periods, see Table B-2. Evidently the uncertainties are large. The mean value of 2000 AD also deviates from the climatologically derived value ($13.5 \cdot 10^3$ m^3/s) that has been used for the present time simulations /Engqvist and Andrejev 1999/. Relative this all-Baltic discharge value the chosen total increase for 6500 BC is 33% and a decrease of 20% (4%) for the year 3000 BC (1000 BC). For these periods with an altered coastline, the river discharge points have been relocated to the nearest coast mainly by backtracking their specified discharge directions. The distribution along the Baltic coast and with regard to the resolved monthly values has thus been retained in direct proportion to the nominal present time distribution.

3 Results

As agreed with Olof Liungman, DHI, the entire velocity profiles from the bottom to the top layers were saved each hour for the 9 × 10 velocity grid points that cover the Öregrund coastal area in the east/west and the north/south-direction respectively. The approximate coverage of the contemporary coastline is depicted in Figure B-5. Since a more detailed analysis of the water exchange of the whole water column and the partitioning into sub-basins will be performed by DHI, it seems sufficient to presently report an overview of the results.

3.1 Simulation result of 6500 BC

The first simulation was performed for the 6500 BC period. Since the both the Sound and the channel through the contemporary equivalent to the Danish Belt are maximally narrow (i.e. one grid cell wide) the buildup of increasing sea level during the spin-up month did not suffice to impede a few instances of salt water inflow during the first three months. This is due to a combination of wind and elevated sea level on the Kattegat boundary, Figure B-6. After these three initial months the Baltic sea level is sufficiently elevated to inhibit further inflows. The surface saline water is subsequently flushed out again except for a minor parcel that by the end of year is has penetrated to the deep basin east of Gotland.

Table B-2. The freshwater discharge of the Baltic Sea as derived by /Gustafsson and Westman 2002/.

	Baltic Sea freshwater discharge			Change relative 2000 AD mean		
Year	min	mean	max	min	mean	max
	(10^3 m3)	(10^3 m3)	(10^3 m3)	%	%	%
6500 BC	14.0	18.0	22.0	90	116	142
3000 BC	8.0	10.8	13.5	52	69	87
1000 BC	11.0	13.0	15.0	71	84	97
2000 AD	14.5	15.5	16.5	94	100	106

The most pertinent parameters for judging the water transport of possible released nuclides in the Öregrundsgrepen area are the bottom currents. This 2D-field is averaged with hourly temporal resolution and saved each month. In order not to present an excessive number of diagrams, the result in Figure B-7 has been subdivided into groups of two months: winter, spring, early summer, late summer, early fall and late fall. The plotting order of the current roses has been performed as to minimize the risk of overwriting of smaller vectors by those of greater magnitude. The resolution of the directions is 10°. In only few instances were velocities exceeding 6 cm/s recorded.

3.2 Simulation result of 3000 BC

The second run for the bathymetry of 3000 BC, the Danish straits are widely open but the Sound between contemporary Sweden and Denmark needed to be connected by adding a few missing grid cells to the otherwise blocked channel. The current roses are shown in Figure B-8 from which it is evident that SW corner of the covered area touches land. The current speeds within the Öregrundsgrepen area seem to be limited to 6 cm/s but outside this area stronger currents can be noted.

3.3 Simulation result of 1000 BC

The third run for the bathymetry of 1000 BC, the Danish straits and the Sound are somewhat deeper than for 3000 BC. The current roses in Figure B-9 show that a few more grid cells near the SW corner have become land. The maximal current speeds within the Öregrundsgrepen area seem to be limited to 6 cm/s but outside this area, stronger currents can be noted again as for the 3000 BC run. The velocities in the SE-corner are now on considerably more shallow areas which results in noticeably increased speeds most likely wind-induced.

4 Discussion

The present results are to an unknown extent sensitive to the made assumptions foremost by allowing the atmospheric forcing be from the year 2004 – a relatively mild winter year. All three years are subjected to the same forcing so the main model feature that can be compared is the varying bathymetry.

The general outcome of the presented 2D-current roses (Figures B-7–B-9) of the bottom-most layers seems consistent with the present time general circulation in the Baltic.

It has recently been revealed by comparing the effect of two different wind data sets (Mueller and Mesan) that the local manifestation of Baltic circulation is surprisingly sensitive to the Baltic wind forcing. It is further known that the existence of an ice cover has a strong impact of the wind interaction with the sea. For both these factors there does not exist any hard data for the actual time periods of the present study. The way to mitigate this lack of hard evidence would be to perform sensitivity analysis in analogy of that performed for the local Forsmark area /Engqvist and Andrejev 2000/.

The average salinity and its correspondingly inferred total freshwater discharge to the all Baltic basins were computed employing a barotropic discrete basin model with which a steady-state was attained /Gustafsson and Westman 2002/. These results have been adopted to the presently deployed 3D-model. It would be interesting to verify that such steady-state is attainable also for this 3D-model approach, but this would take considerably longer computing time than has been alotted in this project.

It has been pointed out that for the assumed freshwater Baltic period (6500 BC) there were some inflows of saline Kattegat water. For the sufficiently far north located Forsmark area this is deemed not risking to influence the water circulation at this location. For a study of the Laxemar-Simpevarp area for 6500 BC, this problem must be addressed either by a sufficiently elevated initial sea level, or by data assimilation.

It is assumed that radionuclides are released within the area marked by the squares with broken lines in Figures B-7 through B-9, and that the maximum length scale of the largest sub-basin (into which the Öregrundsgrepen area has been partitioned) is about three nautical miles. To obtain a relevant appreciation of the residence time from the saved arrays of average speeds with regard to directions (deci-degree resolution) and month, the maximum speed with regard to direction is selected each

month and the monthly average value is computed for the 7x7-array of the northeast corner (see Figures B-7, B-8 and B-9). The minimum of these 49 values is then found to be 3.0, 2.9 and 3.9 cm/s for the years 6500, 3000 and 1000 BC respectively.

Dividing the length-scale with these velocities gives the sought estimates of residence times: 2.1, 2.2 and 1.6 days, *i.e.* significantly greater than the hourly sampling rate and of the same order of magnitude but somewhat higher than earlier estimates pertaining to residence time estimates of present times /Lindborg 2005/. If the vertical exchange had also been taken into the consideration, this would most likely substantially lower these estimates.

5 Conclusions

The present analysis is straightforward. The inferred altered bathymetry of previous stages (6500, 3000 and 1000 BC) of the Baltic Sea makes the site of possible release points of radionuclides from the Öregrundsgrepen area to be submerged on a more or less sloping bottom in contrast to the present case of being semi-landlocked in a funnel-like bay with its major opening toward the north. These alterations and altered salinity distribution and freshwater discharge – all other forcing being the same as for 2004 – result in slightly increased residence times for the 2D-bottommost layers compared to the earlier estimated present corresponding residence times.

6 References

Engqvist A, Andrejev O, 1999. Water exchange of Öregrundsgrepen. A baroclinic 3D-model study. SKB report TR-99-11. ISSN 1404-0344. 59 pp.

Engqvist A, Andrejev O, 2000. Sensitivity analysis with regard to variations of physical forcing including two possible future hydrographic regimes for the Öregrundsgrepen. A follow-up baroclinic 3D-model study. SKB report TR-00-01. ISSN 1404-0344. 44 pp.

Engqvist A, Andrejev O, 2008. Validation of coastal oceanographic models at Forsmark. Site descriptive modelling SDM-Site Forsmark. TR-08-01. ISSN 1404-0344. 64 pp.

Gustafsson B, 2004. Millenial changes of the Baltic Sea salinity. Studies of the sensitivity of the salinity to climate change. SKB TR-04-12, Svensk Kärnbränslehantering AB.

Gustafsson B, Westman P, 2002. On the causes for salinity variations in the Baltic during the last 8500 years. Paleooceanography, 15(3), 1–12.

Lindborg T (ed), 2005. Description of surface systems. SKB report R-05-03. ISSN 1402-3091. p. 146.

Sjöberg B (ed), 1992. Sea and coast. Almqvist & Wiksell Int., Stockholm. ISBN 91-87760-16-9.

Svensk Kärnbränslehantering AB, 2006. The biosphere at Forsmark. Data, assumptions and models used in the SR-Can assessment. SKB, R-06-82.

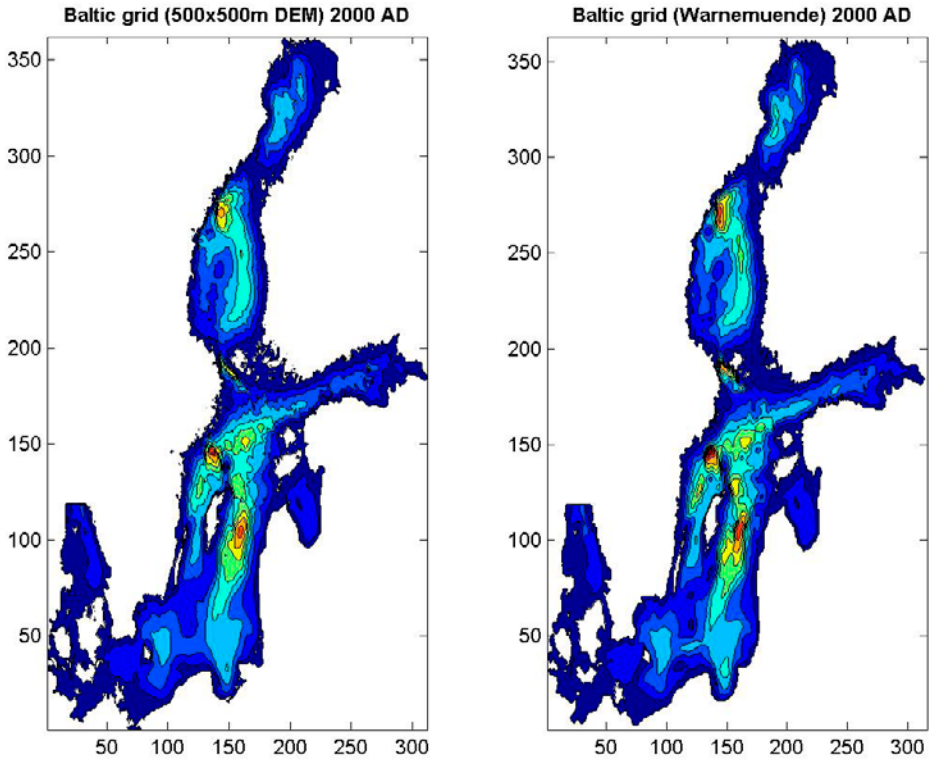

Figure B-1 . *Comparison of two 2′ × 2′ grids of the contemporary Baltic Sea depicted with bathymetry in the same depth scale. The left pane is derived from the 500 x 500 m DEM, the right panel from the Warnemuende data set used for earlier Baltic model runs of the present time /e.g. Engqvist and Andrejev 1999/.*

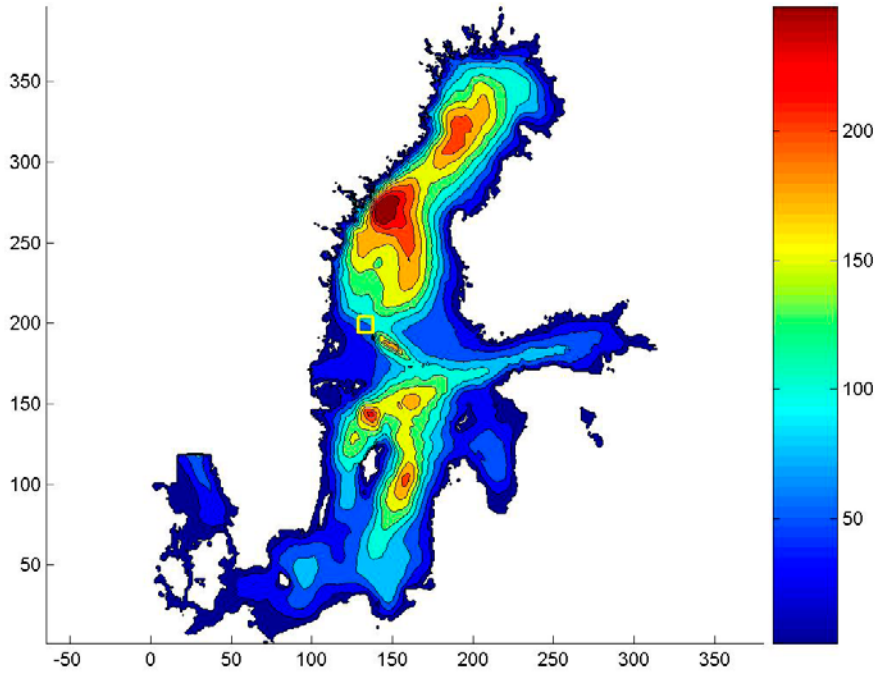

Figure B-2. *Bathymetry of the Baltic Sea 6500 BC transformed to the grid coordinates of the numerical model according to the specified procedure. Only the lakes that cause numerical inconveniences (as the disconnected Ladoga) have been edited away. The Forsmark area depicted in Figure B-5 is marked with a yellow rectangle near the center of the picture.*

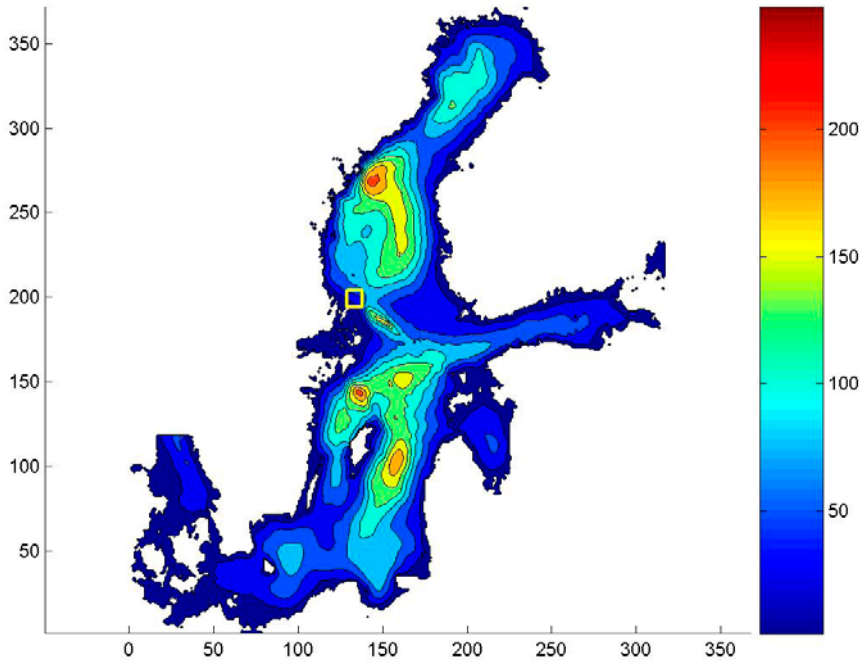

Figure B-3. *Bathymetry of the Baltic Sea 3000 BC transformed to the grid coordinates of the numerical model according to the specified procedure. The Forsmark area depicted in Figure B-5 is marked with a yellow rectangle near the center of the picture.*

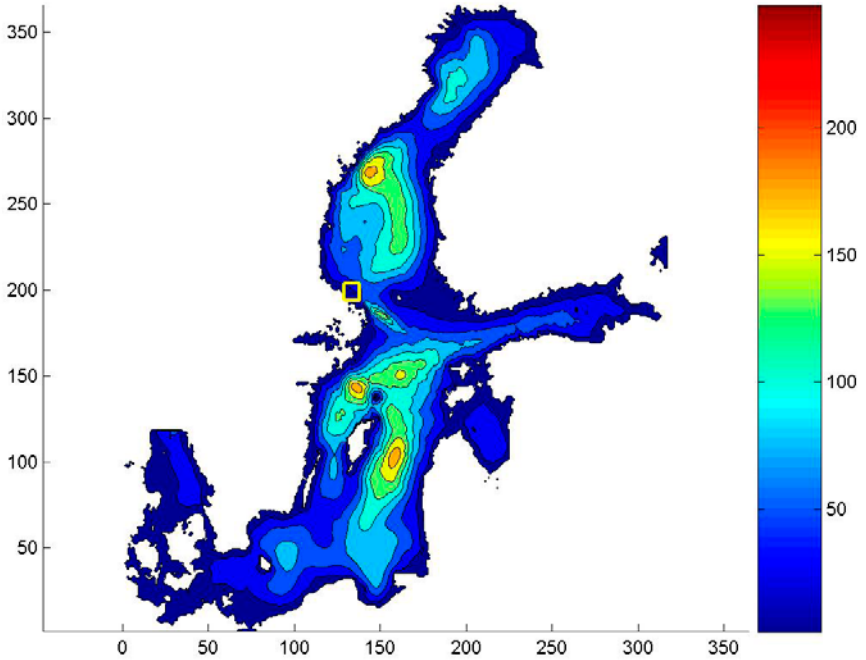

Figure B-4. *Bathymetry of the Baltic Sea 1000 BC transformed to the grid coordinates of the numerical model according to the specified procedure. The Forsmark area depicted in Figure B-5 is marked with a yellow rectangle near the center of the picture.*

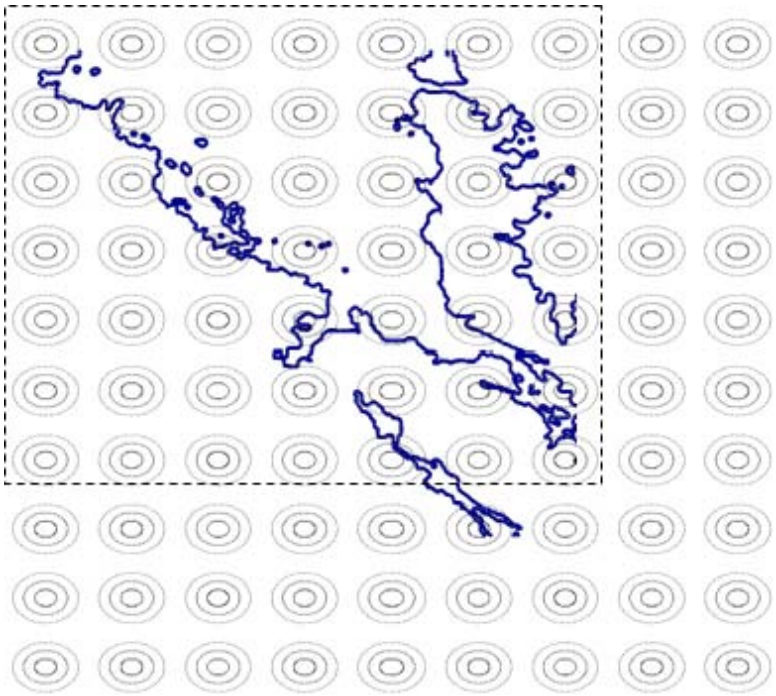

Figure B-5. *The location of the outputted current roses in relationship to the present time outline of the Forsmark coastal area. The concentric circles mark the location of saved current roses representing the velocities 2, 4 and 6 cm/s. The square outlined with a broken line constrains the grid points to the proper Öregrundsgrepen area.*

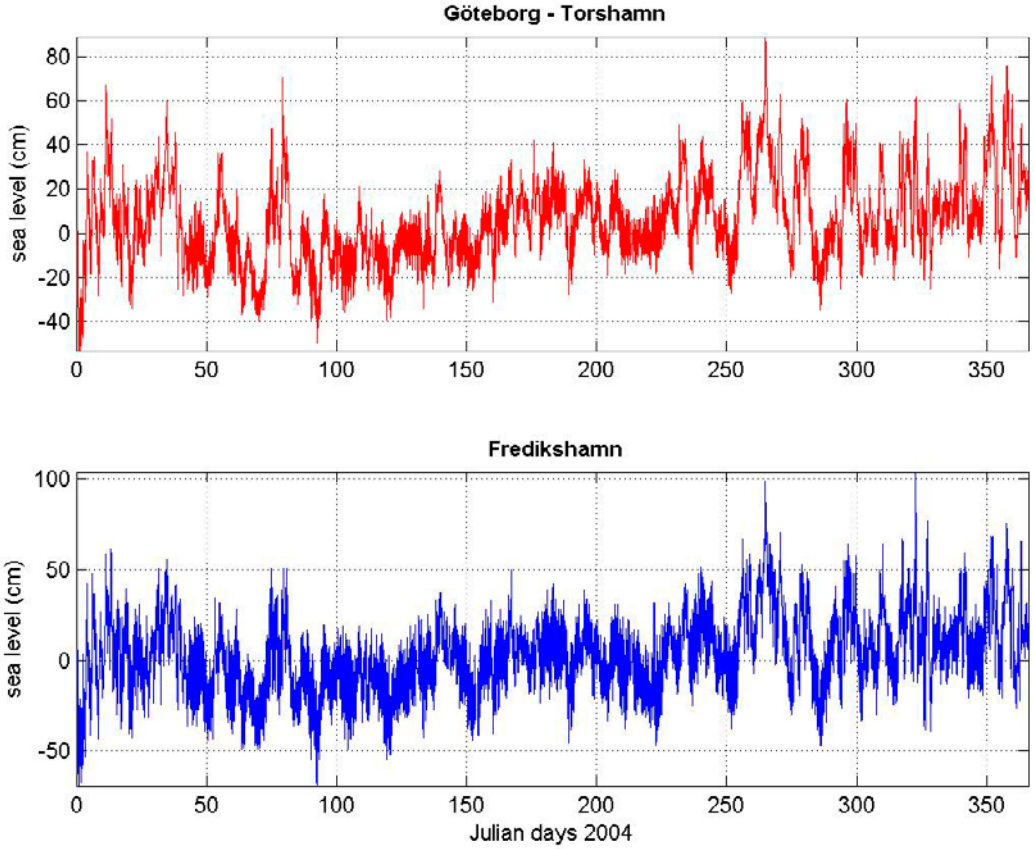

Figure B-6. *The sea level fluctuation on either side of the Kattegat boundary. The instances of elevated sea level during the first three months suffice to enter a few blotches of salt water that during the rest of the year end up in the deep basin east of Gotland.*

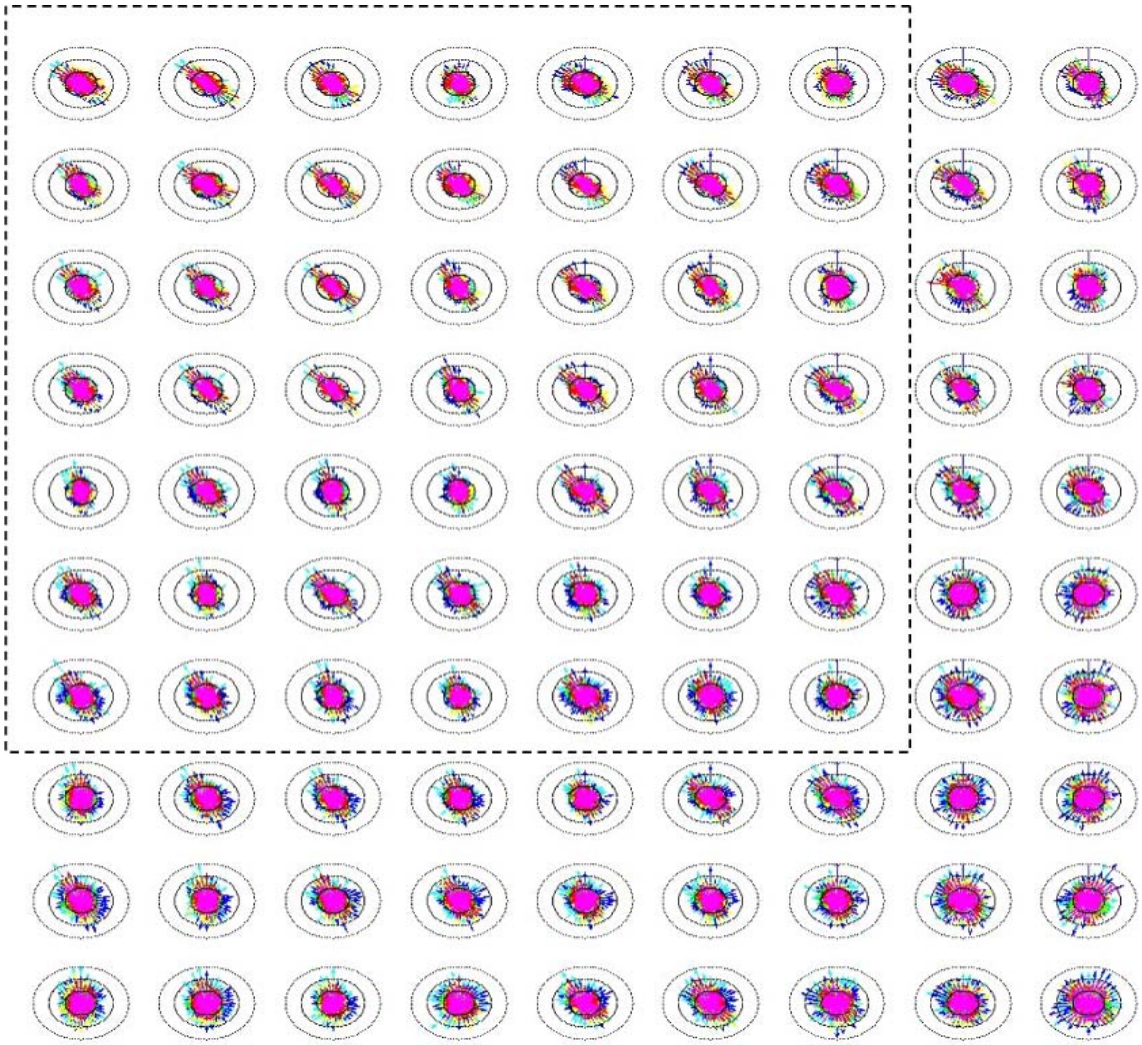

Figure B-7. *Current roses geographically aligned as in Figure B-5 but presenting all hourly currents during one (leap-)year cycle* ***6500 BC****. The three concentric circles denote current speed ranging from 2 cm/s to 6 cm/s. It seems that roses within the corresponding area of the Öregrundsgrepen show a tendency to be in the NW/SE-direction, i.e. aligned to the isobaths, while most of the other current roses display a more even distribution around the compass. The plotting order (and color legend) is: late fall (light blue), winter (dark blue), early fall (yellow), spring (green), early summer (red), late summer (magenta), i.e. in descending order of current amplitudes, in order to avoid overwriting of previously depicted vectors. The broken line square marks the 7 × 7 grid points for which the minimum of the maximal velocities is calculated.*

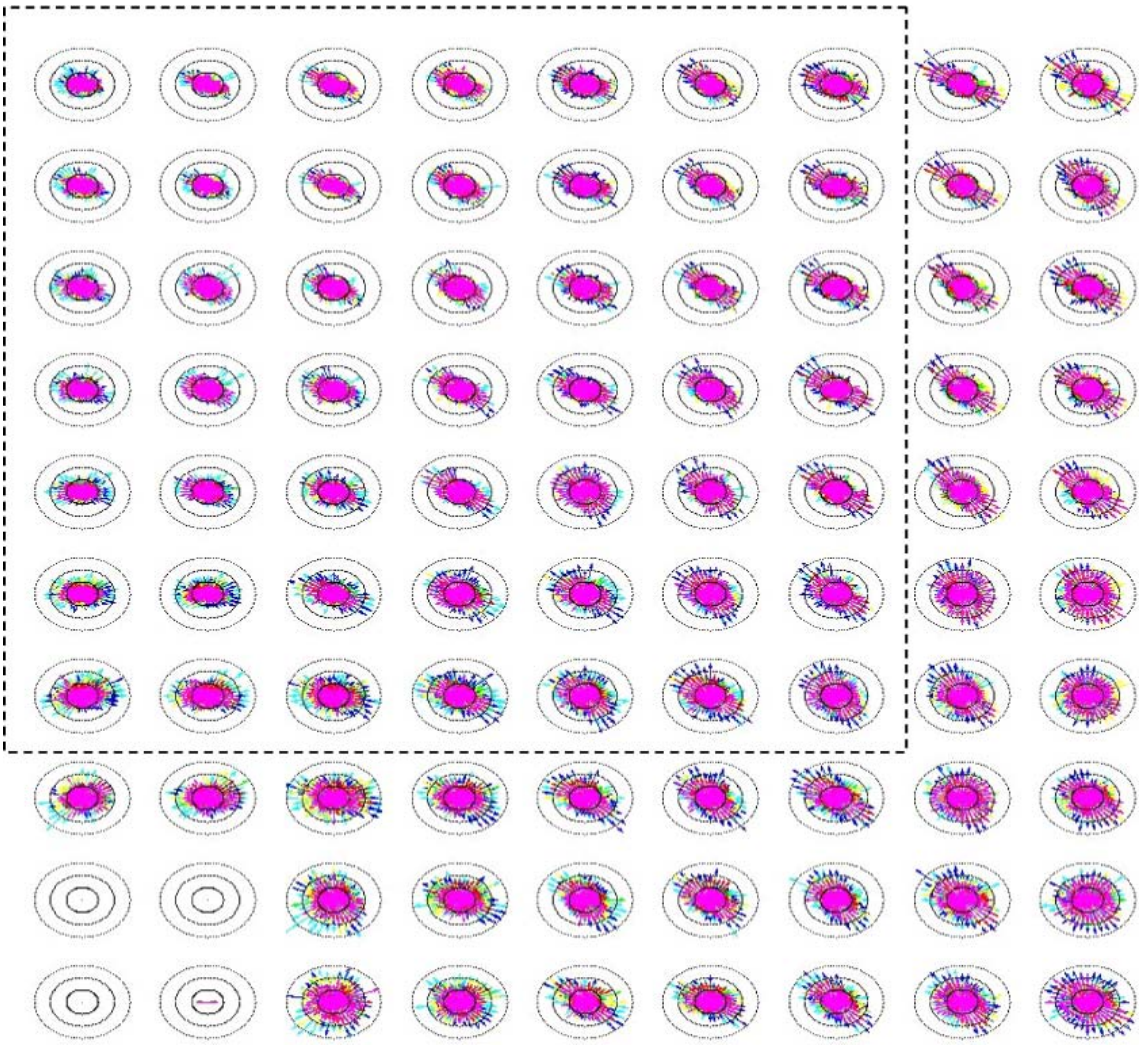

Figure B-8. *Current roses geographically aligned as in Figure B-5 but presenting all hourly currents during one (leap-)year cycle* ***3000 BC****. The three concentric circles denote current speed ranging from 2 cm/s to 6 cm/s. It seems that roses within the corresponding area of the Öregrundsgrepen show a tendency to be in the NW/SE-direction, i.e. aligned to the isobaths, while most of the other current roses display a more even distribution around the compass. The plotting order and color legend is the same as for Figure B-7, i.e. in descending order of anticipated current amplitudes, in order to avoid overwriting of previously depicted vectors. For the farther off-shore grid cells the current velocities are generally more elevated compared to the year 6500 BC. The flow of four grid cells near the SE-corner during this period one is land-formed and the others fall on newly formed land. The broken line square marks the 7 × 7 grid points for which the minimum of the maximal velocities is calculated.*

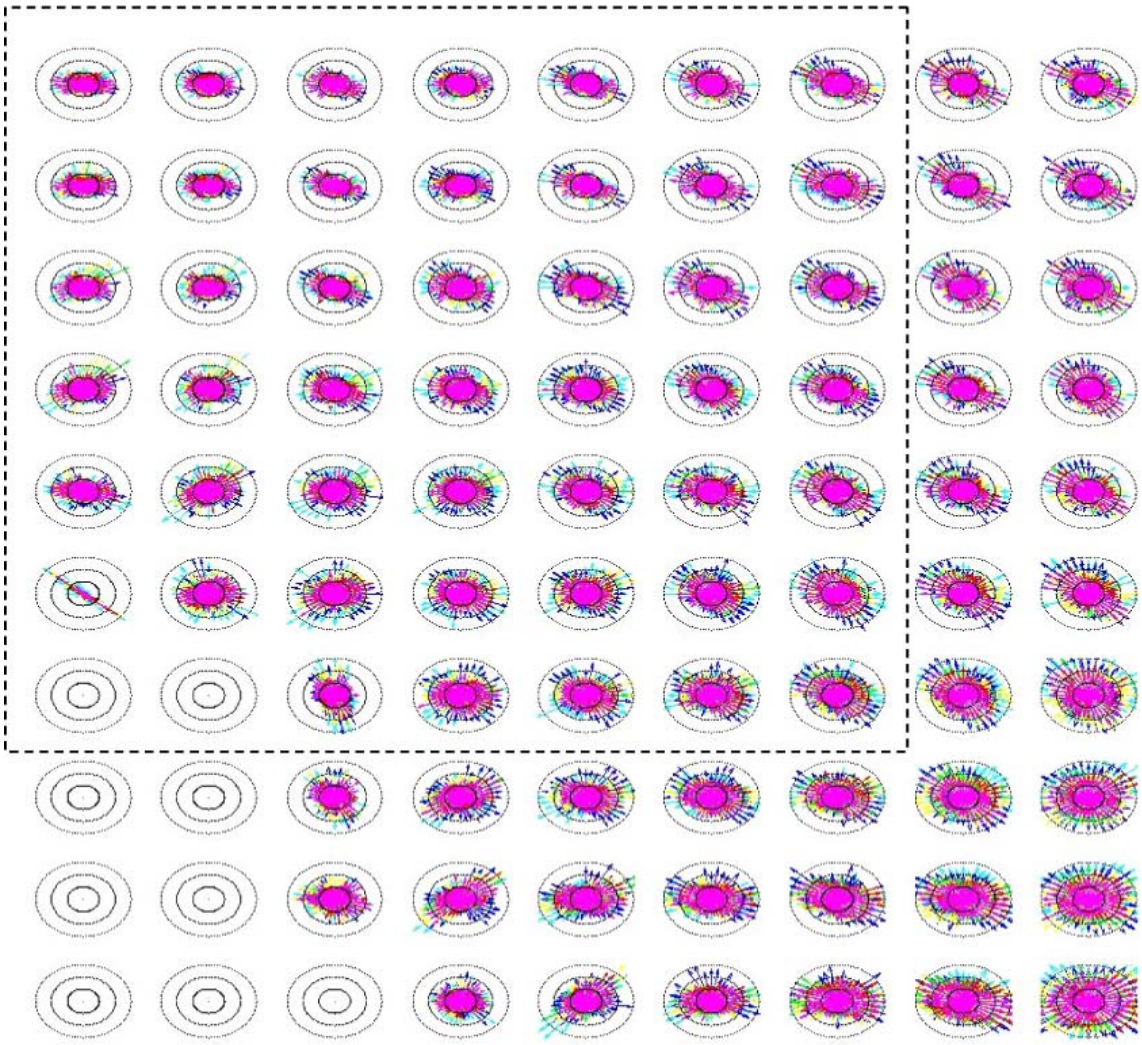

Figure B-9. *Current roses geographically aligned as in Figure B-5 but presenting all hourly currents during one (leap-)year cycle* **1000 BC**. *The three concentric circles denote current speed ranging from 2 cm/s to 6 cm/s. It seems that roses within the corresponding area of the Öregrundsgrepen show a tendency to be in the NW/SE-direction i.e. aligned to the isobaths, while most of the other current roses display a more evenly distribution around the compass. The plotting order and color legend is the same as for Figure B-7, i.e. in descending order of current amplitudes, in order to avoid overwriting of previously depicted vectors. For the farther off-shore grid cells the current velocities are generally more elevated compared to the year 6500 BC, but in parity with the speeds of the year 3000 BC. The grid cells near the SW-corner during this period fall on yet more newly formed islands compared to the year 3000 BC. The broken line square marks the 7 × 7 grid points for which the minimum of the maximal velocities is calculated. The current roses of the SE grid cells are closer to the surface and their increased velocities are most likely a reflection of the wind-induced current.*